

# Evaluation of blue carbon sequestration in salt marsh habitats, Tauranga Harbour

*Prepared for Bay of Plenty Regional Council*

*June 2024*

Prepared by:

Andrew Swales  
Greg Olsen  
Rae Jung  
Barry Greenfield  
Mike Crump  
Margaret McMonagle  
Alice Broadhead

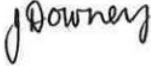
For any information regarding this report please contact:

Andrew Swales  
Principal Scientist/Programme Leader  
Coastal and Estuarine Physical Processes Group  
Andrew.Swales@niwa.co.nz

National Institute of Water & Atmospheric Research Ltd  
PO Box 11115  
Hamilton 3251

Phone +64 7 856 7026

NIWA CLIENT REPORT No: 2024197HN  
Report date: June 2024  
NIWA Project: BOP23203

| Quality Assurance Statement   |                          |                         |
|---|--------------------------|-------------------------|
|  | Reviewed by:             | Phoebe Stewart-Sinclair |
|  | Formatting checked by:   | Jo Downey               |
|  | Approved for release by: | Scott Stephens          |

---

© All rights reserved. This publication may not be reproduced or copied in any form without the permission of the copyright owner(s). Such permission is only to be given in accordance with the terms of the client's contract with NIWA. This copyright extends to all forms of copying and any storage of material in any kind of information retrieval system.

Whilst NIWA has used all reasonable endeavours to ensure that the information contained in this document is accurate, NIWA does not give any express or implied warranty as to the completeness of the information contained herein, or that it will be suitable for any purpose(s) other than those specifically contemplated during the project or agreed by NIWA and the client.

# Contents

- Executive summary .....6**
  
- 1 Introduction .....8**
  - 1.1 Coastal blue carbon.....8
  - 1.2 Study purpose and tasks .....9
  - 1.3 Study area.....11
  
- 2 Methods.....22**
  - 2.1 Sediment core collection.....22
  - 2.2 Sediment composition .....23
  - 2.3 Organic carbon in salt marsh sediment.....24
  - 2.4 Sediment accumulation rates.....25
  - 2.5 Organic carbon stock.....27
  - 2.6 Organic carbon sequestration rate .....27
  
- 3 Results.....28**
  - 3.1 Sediment accumulation rates and sediment properties.....28
  - 3.2 Organic Carbon .....46
  
- 4 Discussion.....55**
  - 4.1 Sediment accumulation rates.....55
  - 4.2 Organic carbon sequestration .....57
  
- 5 Acknowledgements.....59**
  
- 6 References.....60**
  
- Appendix A Sediment core sites .....64**
  
- Appendix B Sediment dating .....67**

## Tables

- Table 1-1: Summary of New Zealand coastal blue carbon habitats compared to terrestrial native forests. 9
- Table 1-2: Summary of long-term annual average catchment flows and sediment loads to study estuaries. 13
- Table 3-1: Summary of AMS <sup>14</sup>C dating results for Oikimoke Estuary. 42
- Table 3-2: Organic carbon inventory in mega-grams per hectare (MgC ha<sup>-1</sup>) in salt marsh sediment cores. 52

|            |   |    |
|------------|---|----|
| Table 3-3: | Salt marsh organic carbon sequestration rates, mega-grams per hectare per year ( $\text{MgC ha}^{-1} \text{ yr}^{-1}$ ) over the 100 years prior to 2023. | 53 |
| Table 4-1: | Summary of $^{210}\text{Pb}$ SAR ( $\text{mm yr}^{-1}$ ) for Tauranga Harbour salt marshes and comparison with unvegetated intertidal flats.              | 57 |
| Table B-1: | Summary of cockle shell samples submitted for AMS radiocarbon dating.   | 70 |

## Figures

|              |   |    |
|--------------|---|----|
| Figure 1-1:  | Tauranga harbour - location of estuaries included in the study.   | 10 |
| Figure 1-2:  | Salt marsh and mangrove habitats, Katikati Estuary, 24 August 2023.   | 13 |
| Figure 1-3:  | Katikati Estuary - historical changes in the extent of salt marsh and mangrove habitats, 1948 to 2022.                | 15 |
| Figure 1-4:  | Salt marsh and mangrove habitats, Rereatukahia Estuary, 24 August 2023.   | 16 |
| Figure 1-5:  | Rereatukahia Estuary - historical changes in the extent of salt marsh and mangrove habitats, 1948 to 2022.            | 17 |
| Figure 1-6:  | Oikimoke salt marsh and mangrove habitats, Wairoa Estuary, 13 November 2023.  | 18 |
| Figure 1-7:  | Oikimoke Estuary - historical changes in the extent of salt marsh and mangrove habitats, 1943 to 2022.                | 20 |
| Figure 1-8:  | Oikimoke salt marsh (1943) in the paddock where sediment cores O1–O3 were collected for this study in 2023.           | 21 |
| Figure 2-1:  | Location of core sites in salt marsh habitats in the three Tauranga Harbour estuaries.                                | 22 |
| Figure 2-2:  | Scatterplot of loss on ignition (LOI%) and total organic carbon (TOC%) data and fitted linear regression.             | 25 |
| Figure 2-3:  | Cockle shell valves from an articulated specimen (sample O1-B, 64-cm depth) preserved in core O1, Oikimoke Estuary.   | 26 |
| Figure 3-1:  | Core K1, Katikati Estuary. X-radiograph of salt marsh core (0-61 cm).   | 28 |
| Figure 3-2:  | Core K1 (Katikati Estuary) - ages of sediment layers, sediment accumulation rates (SAR), and sediment properties.     | 29 |
| Figure 3-3:  | Core K2, Katikati Estuary. X-radiograph of salt marsh core (0-65 cm).   | 30 |
| Figure 3-4:  | Core K2 (Katikati Estuary) - ages of sediment layers, sediment accumulation rates (SAR), and sediment properties.     | 31 |
| Figure 3-5:  | Core K3, Katikati Estuary. X-radiograph of salt marsh core (0-60.5 cm).   | 32 |
| Figure 3-6:  | Core K3 (Katikati Estuary) - ages of sediment layers, sediment accumulation rates (SAR), and sediment properties.     | 33 |
| Figure 3-7:  | Core R1, Reretukahia Estuary. X-radiograph of salt marsh core (0-68 cm).  | 34 |
| Figure 3-8:  | Core R1 (Rereatukahia Estuary) - ages of sediment layers, sediment accumulation rates (SAR), and sediment properties. | 35 |
| Figure 3-9:  | Core R2, Reretukahia Estuary. X-radiograph of salt marsh core (0-62 cm).  | 36 |
| Figure 3-10: | Core R2 (Rereatukahia Estuary) - ages of sediment layers, sediment accumulation rates (SAR), and sediment properties. | 37 |
| Figure 3-11: | Core R3, Reretukahia Estuary. X-radiograph of salt marsh core (0-64 cm).  | 38 |
| Figure 3-12: | Core R3 (Rereatukahia Estuary) - ages of sediment layers, sediment accumulation rates (SAR), and sediment properties. | 39 |

|              |  |    |
|--------------|--|----|
| Figure 3-13: | Core O1, Oikimoke Estuary. X-radiograph of salt marsh core (0-66.5 cm).  | 40 |
| Figure 3-14: | Core O1 (Oikimoke Estuary) - ages of sediment layers, sediment accumulation rates (SAR), and sediment properties.            | 41 |
| Figure 3-15: | Core O2, Oikimoke Estuary. X-radiograph of salt marsh core (0-60 cm).  | 43 |
| Figure 3-16: | Core O2 (Oikimoke Estuary) - ages of sediment layers, sediment accumulation rates (SAR), and sediment properties.            | 44 |
| Figure 3-17: | Core O3, Oikimoke Estuary. X-radiograph of salt marsh core (0-62 cm).  | 45 |
| Figure 3-18: | Core O3 (Oikimoke Estuary) - ages of sediment layers, sediment accumulation rates (SAR), and sediment properties.            | 46 |
| Figure 3-19: | Katikati estuary salt marsh cores K1 –K3. Total organic carbon (TOC%) profiles to 100 cm depth.                              | 47 |
| Figure 3-20: | Rereatukahia estuary salt marsh cores R1 –R3. Total organic carbon (TOC%) profiles to 100 cm depth.                          | 48 |
| Figure 3-21: | Oikimoke estuary salt marsh cores O1 –O3. Total organic carbon (TOC%) profiles to 100 cm depth.                              | 49 |
| Figure 3-22: | Cumulative organic carbon ( $\text{g cm}^{-2}$ ) with depth from sediment surface.   | 50 |
| Figure 3-23: | Cumulative organic carbon (%) with depth from sediment surface.  | 51 |
| Figure 4-1:  | Location of Tauranga Harbour estuaries in earlier study where sediment accumulation rates quantified (Huirama et al., 2021). | 56 |
| Figure B-1:  | $^{210}\text{Pb}$ pathways to estuarine sediments.   | 68 |

## Executive summary

Bay of Plenty Regional Council (BoPRC) commissioned a study to evaluate the carbon storage potential of intact salt marsh wetlands. As well as contributing to knowledge of carbon storage and sequestration rates in NZ salt marsh systems, the study's results will inform the development of incentives to encourage salt marsh restoration on private property. The study focuses on three estuaries fringing the western shore of Tauranga Harbour: Katikati, Rereatukahia and Oikimoke. This blue carbon evaluation is undertaken, where appropriate, in accordance with blue carbon methods described by Howard et al. (2014).

Organic carbon inventories (Mega-gram C per hectare, MgC ha<sup>-1</sup>) and sequestration rates (MgC ha<sup>-1</sup> yr<sup>-1</sup>) were calculated from organic carbon abundance in salt marsh sediment and sediment accumulation rates (SAR). Replicate cores were collected at low tide along salt marsh transects (three sites per transect) during 15–17 May 2023. The cores were analysed to determine downcore profiles of total organic carbon (TOC%), dry bulk sediment density, particle size distributions using image analysis and excess lead-210 (<sup>210</sup>Pb) and caesium-137 (<sup>137</sup>Cs) activities for dating and determination of sediment accumulation rates (SAR). The <sup>210</sup>Pb dating was used to determine organic carbon sequestration rates over the last 100 years across all nine core sites. In the Oikimoke cores, cockle shells (*Austrovenus stutchburyi*, 3 replicates/core) were collected from a shell layer at 60–70-cm depth for radiocarbon (<sup>14</sup>C) dating. The calibrated <sup>14</sup>C ages were used to determine background SAR and organic carbon sequestration rates over 6,500–7,000 years prior to the mid-1800s. The cores were also x-ray imaged to provide information about the fine-scale stratigraphy of the sediment deposits and to inform the analysis and interpretation of the <sup>210</sup>Pb profiles for sediment dating. Training has also been provided to BoPRC staff in blue carbon coring methods through participation in field work.

The key findings of the study are:

- <sup>210</sup>Pb SAR in the Katikati, Rereatukahia and Oikimoke salt marshes have averaged 1.1–2.6 mm yr<sup>-1</sup> since the mid-1800s. These rates are substantially lower than <sup>210</sup>Pb SAR (post-1940s) on unvegetated intertidal flats (averages: 4–9.7 mm yr<sup>-1</sup>) in the Taupiro, Waikareo and Waimapu estuaries (Tauranga Harbour, Huirama et al., 2021). These differences are consistent with differences in hydroperiod and wave exposure between the two habitat types. Salt marshes are inundated for short periods during spring-tide and storm tides when the potential for suspended mineral sediment to be delivered to the marsh exists. However, salt marsh sediment deposits are unlikely to be disturbed by waves or tidal currents and hence preserve a more complete and longer sedimentation record.
- Background <sup>14</sup>C SAR in the Oikimoke salt marsh has averaged 0.04 mm yr<sup>-1</sup> over the ~6,500 years prior to the mid-1800s, when SAR increased 20- to 50-fold (i.e., last 130–170 years). These findings are consistent with Huirama et al., (2021) who found that background SAR averaged 0.05 mm yr<sup>-1</sup> over the last ~7,000 years.
- Organic carbon inventories over the last 100 years (~1923–2023) were in the range 20 to 62 MgC ha<sup>-1</sup> and 76–162 MgC ha<sup>-1</sup> for the entire sediment column to 100-cm depth. These 100-cm values are substantially higher than the organic carbon inventories for New Zealand salt marshes cited by Ross et al. (2023, 38–57 MgC ha<sup>-1</sup>) from previous studies.
- Organic carbon sequestration rates over the last 100 years displayed substantial variability (range: 0.19–0.59 MgC ha<sup>-1</sup> yr<sup>-1</sup>) that largely reflected between-site variations in SAR. The

organic carbon sequestration rate cited by Ross et al, (2023) of  $0.46 \text{ MgC ha}^{-1} \text{ yr}^{-1}$  (i.e., converting from  $\text{CO}_2/3.67 = \text{C}$ ) is within the range of values calculated here for Tauranga Harbour salt marshes.

- Background organic carbon sequestration rates were calculated for the ~6,300–6,700-years prior to the mid-1800s (Oikimoke cores). We found that background sequestration rates ( $0.0061$  and  $0.0013 \text{ MgC ha}^{-1} \text{ yr}^{-1}$ ) are no more than 1% of sequestration rates over the last 100 years. These relatively low values largely reflect low background SAR that are less than 2% of modern values, and to a lesser extent low TOC values (i.e., < 1%). It is also possible that background sequestration rates are over-estimated due to salt marsh roots penetrating older sediment below the excess  $^{210}\text{Pb}$  layer.
- The key objective of this study was to evaluate the carbon storage potential of intact salt marsh wetlands. Historical aerial photographs show that the salt marshes sampled in this study pre-date the 1940s. The Oikimoke salt marsh appears to be the most recent, with a 1943 image (Figure 1-8) indicating that this former farm paddock was in the process of being colonised by saltmarsh and thus the Katikati and Rereatukahia salt marshes pre-date Oikimoke. Organic carbon inventories and sequestration rates do not however reflect this. In particular, the 100-year inventories and sequestration rates for Oikimoke ( $40 \pm 19 \text{ MgC ha}^{-1}$ ,  $0.19\text{--}0.59 \text{ MgC ha}^{-1} \text{ yr}^{-1}$ ) are within the range of values for Katikati ( $58 \pm 2(\text{SD}) \text{ MgC ha}^{-1}$ ,  $0.51\text{--}0.55 \text{ MgC ha}^{-1} \text{ yr}^{-1}$ ) and Rereatukahia ( $28 \pm 11 \text{ MgC ha}^{-1}$ ,  $0.16\text{--}0.41 \text{ MgC ha}^{-1} \text{ yr}^{-1}$ ). The influence of salt marsh age on organic carbon sequestration will be more fully explored further in the second phase of this study.

# 1 Introduction

## 1.1 Coastal blue carbon

Research interest in the function of coastal wetlands for capture and sequestration of atmospheric carbon dioxide (i.e., coastal blue carbon) and application has grown rapidly over the last decades or so. Lovelock and Duarte (2019) provide an overview of the development of blue carbon science and its emerging application to climate mitigation strategies. Mangrove, tidal marshes (salt marshes) and seagrass ecosystems align with multiple criteria for blue Carbon ecosystems (table 1, Lovelock and Duarte (2019)). *Critical for the development of actionable projects, these ecosystems fall within the IPCC definition of wetlands and mangroves are often classified as 'forests' (and therefore included in national forest inventories), enabling their inclusion within greenhouse gas accounting guidance of the International Panel on Climate Change (IPCC).* These coastal wetland habitats are also important ecosystems for climate change adaptation (Duarte et al., 2013). As a result, several nations have included coastal wetlands in their mitigation activities within their National Determined Contributions (Paris Agreement, 2016).

The Coastal Blue Carbon manual (Howard, Hoyt, Isensee, Pidgeon, Telszewski, (eds.), 2014) published by The BLUE CARBON initiative provides a comprehensive description of standardized methods for field measurements and analysis of blue carbon stocks and flux in coastal ecosystems. Howard *et al.* (2014) define coastal blue carbon as *the carbon stored in mangroves, salt tidal marshes, and seagrass meadows within the soil, the living biomass aboveground (leaves, branches, stems), the living biomass belowground (roots), and the non-living biomass (e.g., litter and dead wood).* In contrast to terrestrial ecosystems where carbon storage is limited by high availability of oxygen (enabling aerobic microbial carbon oxidation) and relatively rapidly turned over, carbon sequestered in coastal systems can remain trapped for centuries to millennia, due to anaerobic (low-no oxygen) conditions in water-saturated marine sediment. Sediment and carbon accumulates in estuarine and marine receiving environments, resulting in continuous build-up of carbon over time. Examples cited by Howard *et al.* (2014) include the *Posidonia oceanica* seagrass meadows in Portlligat Bay (Spain, Lo Iacono *et al.* 2008; Serrano *et al.* 2014) and the mangroves of Twin Cay (Belize), that have accreted more than 10 metres of carbon-rich soil over the last 6000 years old (McKee *et al.* 2007;). The tidal salt marshes of northern New England have accumulated 3–5 metres of carbon-rich sediment over the last 3000–4000 years (Johnson *et al.* 2007).

In New Zealand, interest in coastal blue carbon has grown over the last five years or so. Several studies of blue carbon stocks have been conducted and provide some information to evaluate the prospects of blue carbon for future offsetting, and to quantify the value of blue carbon as another ecosystem service provided by coastal wetlands. Ross *et al.* (2023) provides a preliminary estimates of coastal blue carbon stocks for New Zealand (Table 11) based on a small number of published and unpublished studies. These data suggest that mangrove and salt marsh habitats presently contribute the bulk of organic carbon to New Zealand's coastal blue carbon stock. Although salt marshes occur in both the North and South Islands, mangrove forest habitat only occur in the upper North Island. While salt marsh habitat is restricted to a relatively narrow band in the upper intertidal zone, by contrast mangrove can occupy the entire upper to mid-intertidal zone down to mean sea level (MSL). Mangrove forests have also rapidly expanded their distribution in estuaries since the 1930s, averaging 4.1% yr<sup>-1</sup> (range -0.2 to 20.2% yr<sup>-1</sup>, Morrissey *et al.*, 2010). These data are based on aerial photographic surveys that began in the 1930s, so that our understanding of earlier changes in the distribution of mangrove forest and salt marshes is poor.

**Table 1-1: Summary of New Zealand coastal blue carbon habitats compared to terrestrial native forests.**  
Source: reproduced from Ross et al. (2023).

| Habitat                   | Current extent (ha) | Carbon stock (t C <sup>-1</sup> ha <sup>-1</sup> ) | National Carbon Stock (Mt C) | Carbon sequestration (t CO <sub>2</sub> ha <sup>-1</sup> yr <sup>-1</sup> ) |
|---------------------------|---------------------|--|------------------------------|---|
| Salt marshes              | 18 580              | 38–57  | 0.71–1.06                    | 1.69 ± 0.37   |
| Mangroves                 | 28 172              | 62 ± 6.9   | 1.74 ± 0.19                  | 3.3 (0.77–7.78)   |
| Seagrass                  | 29 499              | 14–27  | 0.41–0.80                    | –   |
| Terrestrial Native Forest | 7 800 000           | 144  | 1 800                        | 2.88  |

**Notes:** (1) National carbon stock is calculated by multiplying the carbon stock per hectare and the habitat extent. (2) Estimate of current carbon sink size is calculated by multiplying current habitat extent and the carbon sequestration rate. (3) **Published data sources:** Berthelsen et al. (2023) Bulmer et al. (2020), DOC Sea Sketch (2018), Ministry for the Environment (2022, 2023); (4) C sequestration rate (column 5) can be calculated by conversion CO<sub>2</sub>/3.67 (Ross et al., 2023).

## 1.2 Study purpose and tasks

Bay of Plenty Regional Council (BoPRC) is undertaking this study to evaluate the carbon storage potential of intact salt marsh wetlands, based on analysis of dated sediment cores.

It should be noted that the extent to which the coring locations were in pasture prior to colonisation by salt marsh is unknown because at most sites this process was initiated prior to the aerial photographic record (i.e., post-1943). This colonisation process has coincided with sea level rise (SLR) during the historical era and likely represents a recolonisation process following earlier reclamation of earlier saltmarsh habitat for farming.

As well as contributing to knowledge carbon storage and sequestration rates in NZ salt marsh systems, the study's results will inform the development of incentives to encourage salt marsh restoration on private property.

The study focuses on three estuaries fringing the western shore of Tauranga Harbour (Figure 1-1):

- Katikati Estuary
- Rereatukahia Estuary
- Oikimoke Estuary

This blue carbon evaluation is undertaken, where appropriate, in accordance with blue carbon methods described by Howard et al. (2014). Training is also to be provided to BoPRC staff in blue carbon coring methods through participation in field work.



**Figure 1-1: Tauranga harbour - location of estuaries included in the study.**

The key tasks are to:

- Provide training to BOPRC staff in blue carbon coring methods during field work.
- Collect cores for sediment dating and blue carbon evaluations from at least 3 sites in each estuary. Sites selected in consultation with BOPRC.
- Duplicate sediment cores with be collected at each of the three sites selected in each salt marsh for sediment dating and archiving. Cores to be collected in 500-600 mm lengths of 100mm diameter PVC pipe.

- A 500-600mm long Perspex tray core will be collected for X-ray imaging to determine the stratigraphy of each core and thereby inform selection of samples for radioisotope dating. Minimum of three Perspex tray cores per salt marsh.
- Subsample the blue carbon cores in 5-cm depth increments to 100 cm depth for sediment total organic carbon (TOC%) content and dry bulk density (DBD,  $\text{g cm}^{-3}$ ).
- Analyse all samples (18-20 per core) for DBD and Loss on Ignition LOI% and select a third of the samples from each core for elemental analyser (C, N) analyses of TOC% and thereby determine TOC% for all samples using a LOI–TOC calibration.
- Analyse selected samples for lead-210 ( $^{210}\text{Pb}$ ) and caesium-137 ( $^{137}\text{Cs}$ ) dating of sediment cores to determine time-averaged sediment accumulation rates (SAR) over the last ~100 years.
- Analyse selected samples for particle size using an image analysis method.
- Data analysis and reporting including objectives, site descriptions, methods, results.

## 1.3 Study area

### 1.3.1 Tauranga Moana

Tauranga Moana is located in the western Bay of Plenty, with the City of Tauranga fringing its southern shoreline. The harbour is indented on its western shore by numerous estuaries, typically with high-tide areas less than several  $\text{km}^2$ . The harbour is sheltered from the open coast to the east by Matakana Island, a 25-km long sand barrier (Briggs et al. 1996). Tauranga Moana has a total high tide area of ~200  $\text{km}^2$ , and receives runoff from a 1,300  $\text{km}^2$  catchment, which consists of 27 major rivers and 46 minor streams (Lawton and Conroy 2019). The Harbour is generally shallow with extensive intertidal sandflats and mudflats (total intertidal: 154  $\text{km}^2$ , NZ estuaries classification database [NZECD], NIWA) in sheltered areas with short wave fetch and/or near sub-catchment outlets (Briggs et al. 1996). The spring tidal-prism volume is some 211 million  $\text{m}^3$  (0.211  $\text{km}^3$ ) with a mean water depth is 2.1 m (NZECD, Hicks and Hume 1997; Lawton and Conroy 2019). The Port of Tauranga, located near Tauranga City, is the largest commercial port in New Zealand (Lawton and Conroy, 2019). Although the harbour is generally shallow, tidal scour and artificial dredging at the port maintains the southern harbour entrance (Briggs et al. 1996).

The BoPRC Coastal Environment Plan has identified Tauranga Moana as an outstanding natural feature and landscape, and an area of significant conservation value (excludes Port of Tauranga) (Lawton and Conroy 2019). The BoPRC measures sedimentation rates in Tauranga Moana at 69 intertidal sites, as part of the Estuarine Benthic Health Monitoring programme. Sediment accretion rates at these sites are measured seasonally using buried plates.

Several previous studies have obtained sediment accumulation rates (SAR) for Tauranga Harbour. Burggraaf et al. (1994) calculated a SAR of ~1  $\text{mm yr}^{-1}$  (1950–1991) in the Waikareao, based on DDT contaminant profiles. Hancock et al. (2009) calculated SAR from the naturally occurring radionuclide  $^{210}\text{Pb}$  in sediment cores for intertidal flats located in several estuaries in the vicinity of Tauranga City. The  $^{210}\text{Pb}$  SAR varied from 1.3–7.2  $\text{mm yr}^{-1}$  over the previous 70–90 years. Stokes (2010) also calculated a  $^{210}\text{Pb}$  SAR of 2.3  $\text{mm yr}^{-1}$  (1950–1990) for Waikaraka Estuary.

### 1.3.2 Climate, Geology, and Landuse

Tauranga Harbour is largely sheltered from the prevailing south-west winds by the Kaimai and Mamaku ranges, so that a large proportion of rainfall is received during periods of north to north-east (i.e., onshore) winds. When pressure gradients associated with weather systems are weak on fine summer days, northerly sea breezes of 20–30 km hr<sup>-1</sup> develop and penetrate inland (Chappell, 2013). Mean annual wind speeds in Tauranga Moana are 14 km hr<sup>-1</sup>. Median annual rainfall varies from 1,200–1,600 mm yr<sup>-1</sup> (Tauranga Harbour) and can reach up to 2,200 mm yr<sup>-1</sup> in the coastal ranges. The median annual temperature for Tauranga Moana is 9.6°C (Chappell, 2013).

The geology of the harbour and catchment is composed of late Pliocene to Pleistocene volcanic rocks and volcanogenic sediment. The Tauranga Basin is one of the six principle physiographic units within Tauranga Moana. Basement rocks are composed of Waiteariki Ignimbrite (average 2.2 m thick) at 50 – 100 m depth below the seafloor. The sediment that has subsequently infilled the basin is composed of unconsolidated or weakly consolidated mud, sand and gravel of terrigenous, estuarine and shallow marine origin (Briggs et al. 1996; MacPherson et al. 2017).

Catchment land cover is mainly comprised of mature bush (i.e., indigenous forest has 41% coverage and exotic forest 12%) and agricultural land (just over 40% coverage, comprising sheep, beef and dairy). Urban areas accounts for 9% of the total catchment area, although the proportion of urban land use has increased since 2012 (Lawton and Conroy, 2019). Recent historical events that may have impacted on sedimentation in the study estuaries are the 1981 failure of the Ruahihi Power Station dam and Cyclone Bola (1988). An estimated 1.5 million cubic metres of mud was discharged to the harbour by the dam failure. Cyclone Bola resulted in severe hillslope failure and soil erosion that would likely have delivered large quantities of fine sediment to the harbour and its fringing estuaries (Crawshaw 2020a).

### 1.3.3 Salt marshes

The relevant features of each salt marsh and its upstream catchment are summarised in this section.

#### **Katikati Estuary**

Estimates of long-term annual average suspended sediment loads for sub-catchments draining to each of the study estuaries are provided by NIWA's NZ River Maps (NZRM, Booker and Whitehead, 2017, <https://shiny.niwa.co.nz/nzrivermaps/>). The NZRM tool is a national-scale multi-variate statistical model based on data provided by the River Environment Classification (REC-1). Sediment yield data incorporated in NZRM is derived from measured suspended sediment yields from 233 New Zealand catchments (Hicks et al. 2011). Estimates of annual average flows and suspended sediment loads are summarised in Table 1-2. The specific sediment load from the Katikati Catchment and its tributaries, of 49–52 t km<sup>-2</sup> yr<sup>-1</sup> are typical values for North Island lowland catchments.



**Figure 1-2: Salt marsh and mangrove habitats, Katikati Estuary, 24 August 2023.**

Source: Bay of Plenty Regional Council.

**Table 1-2: Summary of long-term annual average catchment flows and sediment loads to study estuaries.** Sub-catchment suspended sediment loads and mean annual flow (Source: NZ River Maps, Booker and Whitehead, 2017).

| Sub-catchment                  | Area (km <sup>2</sup> ) | Mean flow (m <sup>3</sup> s <sup>-1</sup> ) | SS Load (t yr <sup>-1</sup> ) | Specific SS Load (t km <sup>-2</sup> yr <sup>-1</sup> ) |
|--------------------------------|-------------------------|---|-------------------------------|---|
| <b>Katikati Estuary</b>        | <b>28.4</b>             | <b>0.68</b>                                 | <b>1 396</b>                  | <b>49.2</b>   |
| Uretara Stream                 | 18.0                    | 0.42  | 856                           | 47.6  |
| Tahawai Stream                 | 10.4                    | 0.26  | 540                           | 51.9  |
| <b>Te Rereatakahia Estuary</b> | <b>45.7</b>             | <b>1.55</b>                                 | <b>2 240</b>                  | <b>49.0</b>   |
| Te Rereatakahia Stream         | 33.5                    | 1.27  | 1 600                         | 47.8  |
| Te Mania Stream                | 12.2                    | 0.28  | 640                           | 52.5  |
| <b>Oikimoke Estuary</b>        |                         |   |                               |   |
| Wairoa River                   | 457                     | 14.9  | 30 200                        | 66.1  |

The present-day salt marsh community varies between core sites in the relative proportions of Sea Rush (*Juncus Kraussii* subsp. *Australiensis*) with some Oioi (*Apodasmia similis*) (Pers Comm., Heather MacKenzie BoPRC).

Sea Rush dominates in the immediate vicinity of site K1, whereas Oioi dominates at K2 and K3 that are closer to the main tidal channel and also likely to be at a lower elevation (i.e., with higher hydroperiod).

Historical aerial photography for the Katikati Estuary shows that salt marsh was established on the intertidal flats where the sediment cores were collected since at least 1948 (Figure 1-3). This record also indicates that mangrove have colonised areas of unvegetated intertidal flat and replaced a substantial area (i.e., ~one third) of salt marsh since 1960 at its previous northern extent. The mangroves are likely to have colonised intertidal flat along the seaward edge of the salt marsh habitat then penetrating the marsh using the tidal creek network as a conduit for propagules. The 2022 image clearly shows that mangrove are colonising the salt marsh along the tidal creeks. The K1–K3 core sites are presently occupied entirely by salt marsh, although mangrove have colonised salt marsh with ~5 m of these sites via a tidal creek.



**Figure 1-3: Katikati Estuary - historical changes in the extent of salt marsh and mangrove habitats, 1948 to 2022.** Aerial photographs supplied by Bay of Plenty Regional Council.

## Rereatukahia Estuary

The Rereatukahia Estuary is located five kilometres south-west of Katikati and receives runoff from a 18.6 km<sup>2</sup> catchment that flows east from the Kaimai-Mamaku Forest Park to Tauranga Harbour (BoPRC Sub-catchment Action Plan [SAP], 2012). Indigenous vegetation accounts for 62% of the catchment landcover, with pasture (20%), horticulture (13%) and exotic forest (5%) in the mid-lower reaches of the catchment. Soils are vulnerable to erosion under poor vegetation cover or intensive land-use (BoPRC-SAP, 2012). The specific sediment load from the Rereatukahia Catchment and its tributaries, of 48–53 t km<sup>-2</sup> yr<sup>-1</sup> (Table 1-2) are typical values for North Island lowland catchments.



**Figure 1-4: Salt marsh and mangrove habitats, Rereatukahia Estuary, 24 August 2023.** Source: Bay of Plenty Regional Council.

The present-day salt marsh community is dominated by Oioi at all three cores sites, with a small proportion of Sea Rush (*Pers Comm.*, Heather MacKenzie BoPRC). These core sites are located on the upper intertidal zone and several hundred metres from a major tidal channel (Figure 1-5).

Historical aerial photography for the Rereatukahia Estuary shows that salt marsh was established on the intertidal flats where the sediment cores were collected since at least 1948 (Figure 1-5). This record also indicates that mangrove have colonised areas of former salt marsh that fringed the upper-intertidal zone along the shoreline and have replaced a substantial area (i.e., ~one third) of salt marsh since 1960. As noted in the Katikati Estuary, mangroves are likely to have colonised intertidal flat along the seaward edge of the salt marsh habitat then penetrating the marsh using the tidal creek network as a conduit for propagules. The 2022 image clearly shows that mangrove are colonising the salt marsh along the tidal creeks. The R1–R3 core sites are presently occupied entirely by salt marsh, although mangroves are colonising salt marsh along the banks of tidal creeks that drain this marsh area.

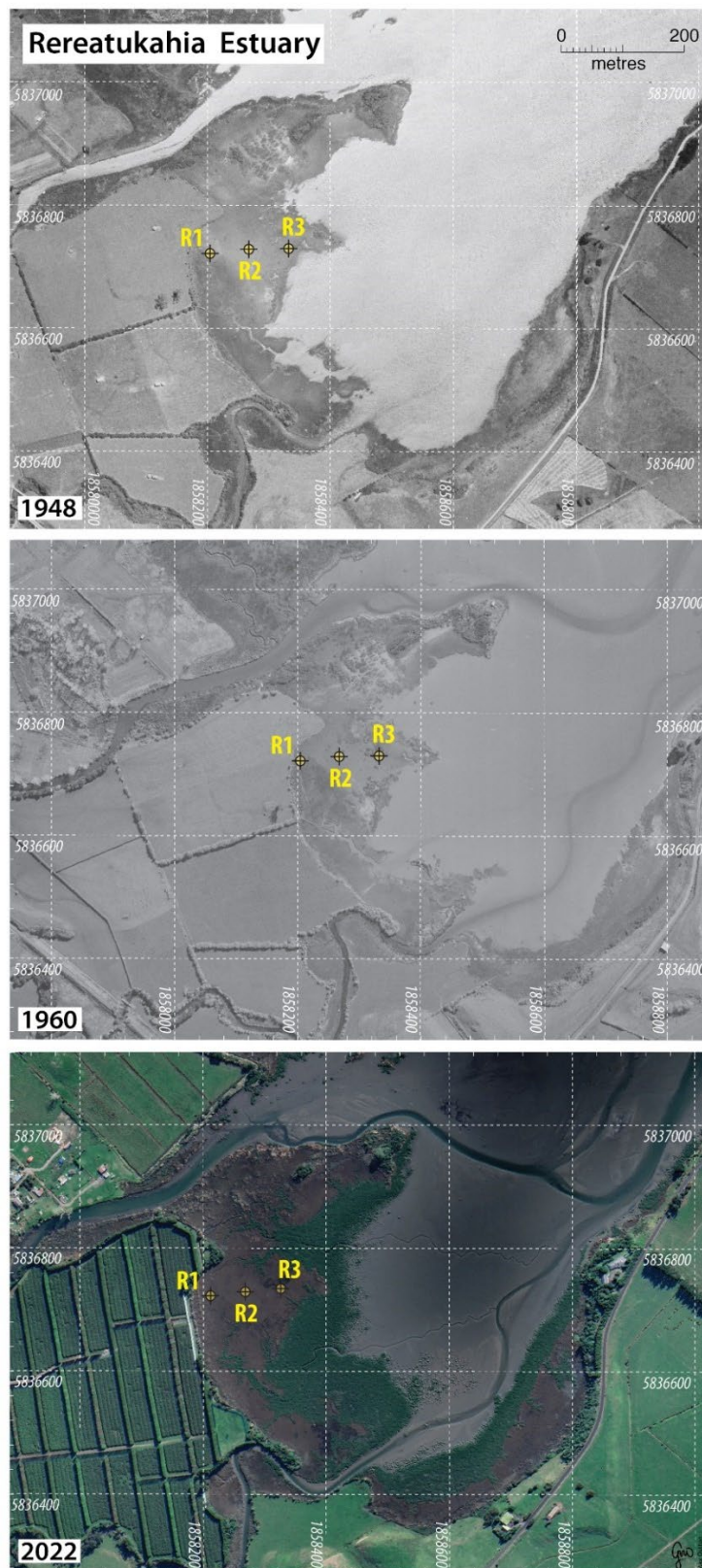


**Figure 1-5: Rereatukahia Estuary - historical changes in the extent of salt marsh and mangrove habitats, 1948 to 2022.** Aerial photographs supplied by Bay of Plenty Regional Council.

## Oikimoke salt marsh

The Oikimoke salt marsh fringes the upper intertidal flats along the inner-harbour shoreline immediately north of the Wairoa River mouth (Figure 1-6). The Wairoa is the largest discharging to Tauranga Harbour, receiving runoff from a 463 km<sup>2</sup> catchment (BoPRC Wairoa SAP, 2012). Land use is dominated by pastoral agriculture (47%) and Indigenous vegetation (41%). Horticultural land use (9%) occurs in the lower catchment. Soils are derived from air-fall rhyolitic tephra overlying loess and weathered rhyolitic tephra. The soils have a high clay content and are vulnerable to erosion where vegetation is removed or under intensive land-use. Soils on the floodplains and lower flats are formed from a mixture of peat and alluvial rhyolitic ash with wetness limitations to production (BoPRC Wairoa SAP, 2012). The specific sediment load from the Wairoa Catchment is 66 t km<sup>-2</sup> yr<sup>-1</sup> (Table 1-2) are typical values for North Island lowland catchments. The relatively large size of this catchment, however, means that the Wairoa River has the largest annual suspended load (30,000 t yr<sup>-1</sup>) of any catchment discharging to Tauranga Harbour. The 1981 failure of the Ruahihi Power Station dam, located in the middle reaches of the catchment, is also estimated to have discharged 1.5 million cubic metres of mud to the harbour.

The Oikimoke O1–O3 core sites are located on private land fringing the harbour shoreline and are located landward of a stop bank constructed sometime before 1943 (Figure 1-7). The area where cores were collected may have been converted or partially converted to pasture for a time before being recolonised by saltmarsh before 1943.



**Figure 1-6: Oikimoke salt marsh and mangrove habitats, Wairoa Estuary, 13 November 2023.**

Wairoa River mouth in the top right of the image with Tauranga City to the south. Aerial photographs supplied by Bay of Plenty Regional Council.

The present-day salt marsh community at the core sites is dominated by Oioi with a small proportion of Sea Rush being present.

Historical aerial photography for the Oikimoke Estuary suggest that salt marsh had re-established on the low-lying paddock where the sediment cores were collected prior to 1943 (Figure 1-7 and Figure 1-8). The presence of cockle shell at 60–70-cm depth in the Oikimoke cores show that this area had been reclaimed from intertidal flats at an earlier time (Section 3.1.3). This historical record also indicates that mangrove have colonised areas of unvegetated intertidal flat and salt marsh along the shoreline since 1959, albeit to a lesser extent than at the Katikati and Rereatukahia site. As previously noted, mangroves are penetrating the salt marsh habitat by using the tidal creek network as a conduit for propagules. The 2022 image clearly shows that mangrove are colonising the salt marsh along the tidal creeks. The O1–O3 core sites are presently occupied by salt marsh, although mangroves are now with ~10 m of the core site locations.

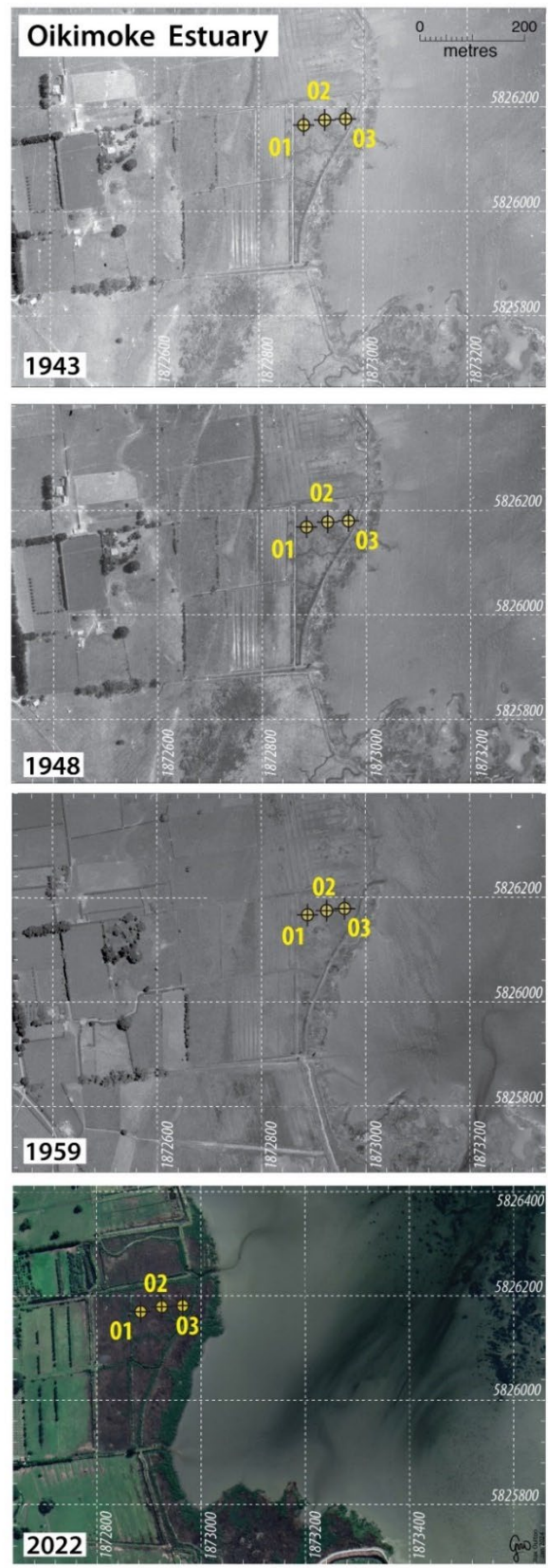


**Figure 1-7: Oikimoke Estuary - historical changes in the extent of salt marsh and mangrove habitats, 1943 to 2022.** Aerial photographs supplied by Bay of Plenty Regional Council.



**Figure 1-8: Oikimoke salt marsh (1943) in the paddock where sediment cores O1–O3 were collected for this study in 2023.** Cadastral boundaries are indicated by the yellow lines, with cores collected from the largest paddock. Aerial photographs supplied by Bay of Plenty Regional Council.

## 2 Methods

### 2.1 Sediment core collection

Sediment cores were collected along transects established in salt marsh habitat in each of the study estuaries at low tide  $\pm 3$  hours during the period 15 to 17 May 2023. Figure 2-1 shows the location of the core sampling sites in each of the three estuaries.

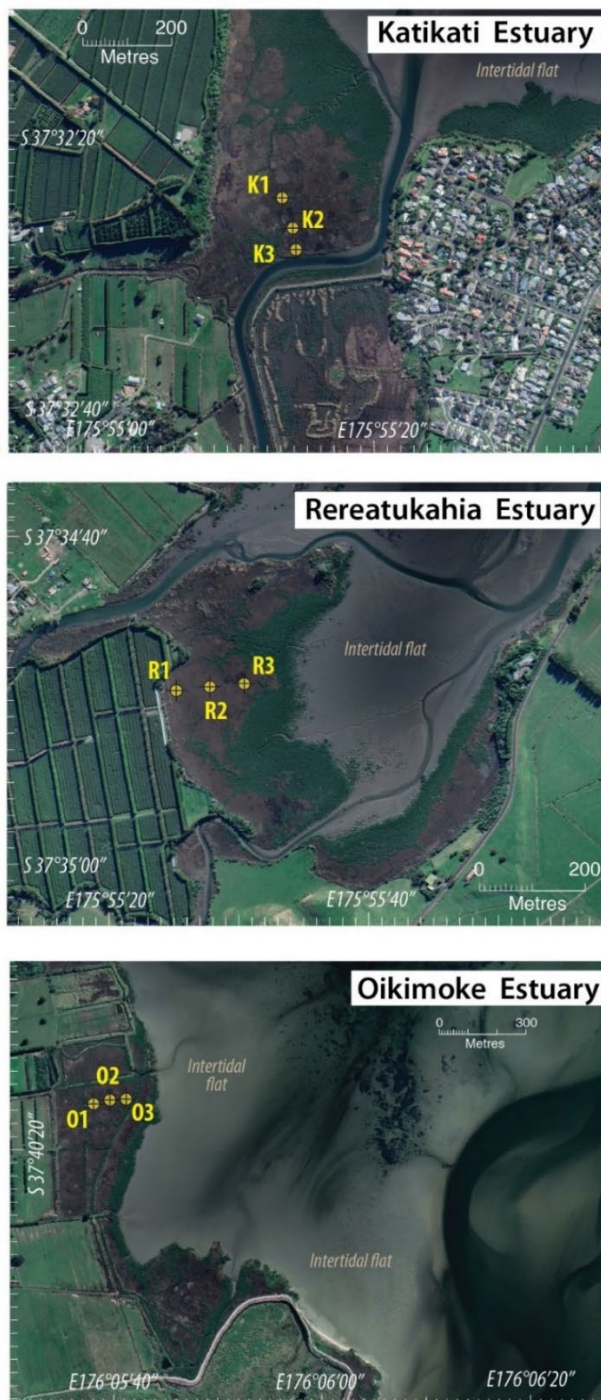


**Figure 2-1:** Location of core sites in salt marsh habitats in the three Tauranga Harbour estuaries. Katikati (K1–K3), Rereatukahia (R1–R3) and Oikimoke (O1–O3) Estuaries.

Replicate sediment cores were collected at each site using three methods:

- Perspex-tray corers 27 cm x 3 cm cross-section x 80 cm long. This method provides slabs of sediment of uniform thickness for x-ray imaging that capture the fine detail of preserved sedimentary structures. This information also informs the interpretation of the fallout radioisotope profiles of lead-210 ( $^{210}\text{Pb}$ ) and caesium-137 ( $^{137}\text{Cs}$ ) for sediment dating and determination of sediment accumulation rates (SAR).
- Gauge-Augur (90 mm diameter x 100-cm length. These sediment cores are sectioned into 5-cm length in the field and subsequently analysed to determine total organic carbon (TOC %) content by loss on ignition (LOI %) and Elemental Analyser.
- PVC pipe -10 cm diameter x 100 cm lengths. Archive cores for additional analyses as maybe required in the future.

## 2.2 Sediment composition

Sediment composition and stratigraphy preserved in the cores were determined by x-ray imaging and analyses of selected samples. X-radiographs reveal material density contrasts (due to particle size and composition, porosity) and provides information on fine-scale sedimentary fabric (i.e., structures and sediment textures formed by physical processes and animals living in the sediment) preserved in the cores. Density differences between layers of silt and sand or mud-infilled animal burrows are easily recognised the x-radiographs even though they may not be visible to the naked eye. These x-radiographs are negative images so that relatively high-density objects appear white (e.g., shell valves) and low-density materials such as muds or organic material appear as darker areas.

As well as documenting changes in sediment composition with depth, the x-radiographs are used to inform selection of samples for dating. Fine-scale (mm) differences in sediment density due to particle size, composition and/or water content are readily identified. For ground-truthing sediment properties, dry-bulk sediment density ( $\rho_d$ ,  $\text{g cm}^{-3}$ ) profiles were also determined for each core from the net dry weight of samples of a known volume.

The sediment cores were x-ray imaged using a Varian PaxScan 4030E digital detector panel and an Ecotron EPX-F2800 portable x-ray generator. X-ray energy and exposure settings were typically 63–71 keV and 25 mAs (milli-Amp seconds).

Particle size distributions (PSD) were measured using an Eye-Tech image-analysis system that captured, two-dimensional silhouettes of suspended particles. Samples were analysed in a core collected at each site in six depth increments: 0–2, 5–6, 10–11, 20–21, 30–31, 39–40 cm. A major benefit of the image-analysis method is that the size and shape of particles are directly measured rather than inferred (e.g., Laser diffraction, particle size distribution based on back-scattered light pattern). Particle imaging was conducted using a DW lens (detector pixel size  $1.95 \mu\text{m}$ ) that captured particles in the range 4 – 966  $\mu\text{m}$  diameter. Sub-samples of 1–2  $\text{cm}^3$  were analysed in suspension, following ultrasonic dispersion for four minutes prior to, and during, analysis. The typical run time of 400 seconds with 100–200 thousand particles analysed per sample.

These data were used to calculate size distributions based on particle volume, number, and surface area. PSD based on particle spherical volume are reported (i.e.,  $V = 4/3\pi r^3$ ), with particle volume being closely related to sediment mass and sedimentation. Although the clay fraction was not measured, the contribution of these finest particles will generally be negligible.

For example, a 100 µm diameter sphere has a volume one thousand times greater than a 10 µm sphere and one million times greater than the volume of a 1 µm sphere. Standard statistical measures of PSD are reported (i.e., mean, median/D50, mode, D10, D90). Size and shape data for each particle analysed was saved to a spreadsheet. In-depth analysis of these datasets is beyond the scope of the present study, however, further analysis of the size and shape (e.g., aspect ratio) information will likely provide insights on the proportions of mineral sediment particles and organic matter.

## 2.3 Organic carbon in salt marsh sediment

### 2.3.1 Laboratory analyses

The organic carbon content of the sediment cores was estimated indirectly by loss on ignition (LOI) and by direct measurement of Total Organic Carbon (TOC %) by Elemental Analyser. All of the samples were analysed by LOI and a subset of the samples (~30%) were also analysed for TOC% by Elemental Analyser. TOC% values for the remaining 70% of samples were estimated by linear regression of TOC% with LOI% ( $\text{TOC\%} = (0.36 * \text{LOI\%}) - 0.45$ ,  $r^2 = 0.87$ ,  $n = 52$ ). An advantage of this dual approach is that the dry weights of LOI sub-samples are substantially larger (i.e., 10-20 g) than for TOC (10-30 mg). Thus, LOI samples are less likely to be affected by errors caused by sub-sampling from incompletely mixed (i.e., heterogenous) sediment samples.

LOI analysis was undertaken by first sub-sampling a known volume of sediment (i.e., typically 40 cm<sup>3</sup>) from each 5-cm depth increment core sample. The samples were dried at 103°C to yield the sample dry weight then heated in a furnace to 400°C for 6 hours. This treatment is designed to avoid loss of water bound strongly in layer clay minerals so that weight loss primarily reflects ignition of organic matter. As an index of organic content, LOI should be done at temperatures *lower* than the clay dehydroxylation endotherm, with 400°C (c.f. 550°C) being a good compromise (Mook and Hoskin, 1982). The weight of each ashed sample was then measured to four decimal places and LOI% calculated from the dried and ashed weights and sample volume.

TOC% was determined using an Elementar Unicube (C/N) High temperature combustion technique (detection limit 0.05, method MAM, 01-1090). The sediment samples are acidified with 0.1M H<sub>2</sub>SO<sub>4</sub> to remove inorganic carbon, rinsed thoroughly with pure water, dried at 60°C and then analysed on the Elementar Unicube. A weighed amount of sample is combusted at 900°C in the presence of catalyst to convert Carbon to Carbon dioxide. Separation of the gases occurs using a chromatographic column and they are determined in succession with a Thermal Conductivity Detector (TNLET, 1994).

Figure 2-2 presents the LOI%-TOC% data and the fitted linear regression relationship. The slope of the relationship (0.36) is close to the 0.4 ratio expected for the TOC/LOI ratio in young salt marshes and salt marshes with strong contributions of carbon from terrigenous and/or estuarine sources (e.g., Craft et al., 1991).

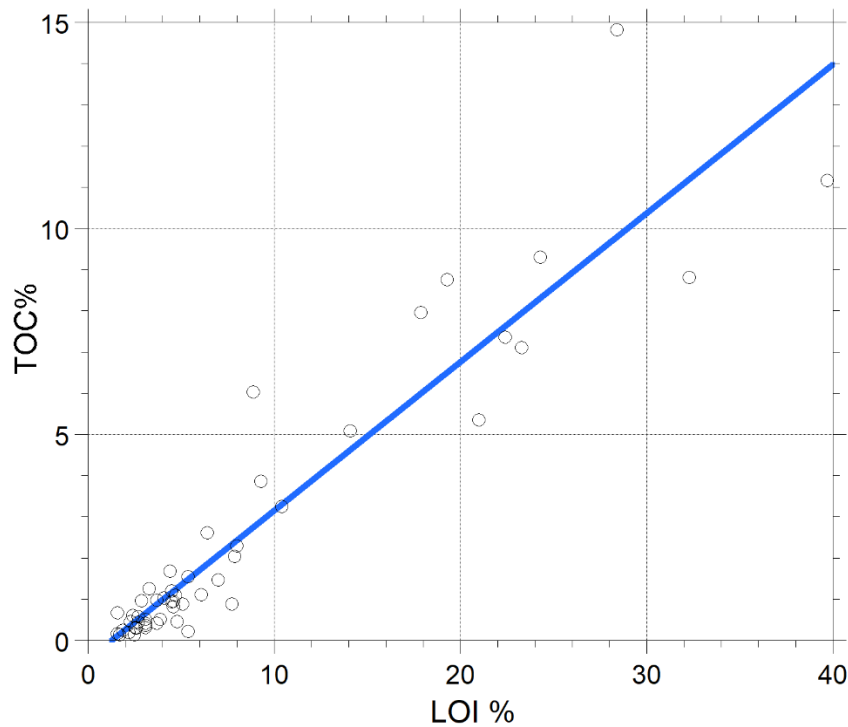


**Figure 2-2: Scatterplot of loss on ignition (LOI%) and total organic carbon (TOC%) data and fitted linear regression.** Regression relationship:  $\text{TOC}\% = (0.36 \cdot \text{LOI}\%) - 0.45$ ,  $r^2 = 0.87$ ,  $n = 52$ ,  $P < 0.001$

## 2.4 Sediment accumulation rates

Sediment accumulation rates (SAR) were determined from radionuclide profiling of the sediment cores. The calculated SAR are time-averaged values expressed as millimetres per year ( $\text{mm yr}^{-1}$ ). Radionuclides are strongly attracted to the surfaces of clay and silt particles, characteristic of fine-grained sediment deposits, which makes them particularly useful as “mud meters” to determine sediment accumulation rates (Sommerfield et al. 1999). In the present study, sediment accumulation rates over the last several decades to century were quantified using the depth profiles of naturally occurring excess lead-210 ( $^{210}\text{Pb}_{\text{ex}}$ , half-life 22 years). The basic principles of  $^{210}\text{Pb}$  dating are described in Appendix B (Sediment dating). Caesium-137 ( $^{137}\text{Cs}$ , half-life 30 years) dating has also commonly used to determine SAR in aquatic receiving environments for sediment deposited since the early-1950s (Robbins and Edgington 1975; Wise 1977; Ritchie and McHenry 1990), when atmospheric deposition of nuclear bomb-produced  $^{137}\text{Cs}$  was first detected in New Zealand.

Sediment dating using two or more independent methods offsets the limitations of any one approach. This is important when interpreting sediment profiles from estuaries because of the potential confounding effects of sediment mixing by physical and biological processes (Smith, 2001). In the present study,  $^{137}\text{Cs}$  was not consistently detected in each sample downcore and across the sampled estuaries and is now at the limits of its usefulness due its 30-year half-life and time elapsed since the historical deposition 1963/64 peak in the southern hemisphere (Matthews, 1989; Miller and Kuehl, 2010). The 1963/64 peak in atmospheric deposition cannot reliably be identified in estuarine sediment cores because  $^{137}\text{Cs}$  is also delivered to estuaries indirectly via catchment soil erosion. Consequently, the maximum depth of  $^{137}\text{Cs}$  in a core can potentially be used to identify initial introduction in the early-1950s or the 1963/64 peak, given the limitations described above.

The activity of excess  $^{210}\text{Pb}$  in each core was determined by gamma spectrometry of 40–60 g dry samples (1-cm slices) of sediment taken at increasing depths from each core. The radionuclide activity of a sediment sample is expressed as Becquerel (number of disintegrations per second) per kilogram ( $\text{Bq kg}^{-1}$ ). The radioactivity of samples was counted at the ESR National Radiation Laboratory for 23 hours using a Canberra Model BE5030 hyper-pure germanium detector. Surface-mixed layers (SML), where they occur, can be identified from the vertical profile of radionuclide activity. Mixing occurs due to the burrowing and feeding activities of benthic animals and/or physical disturbance by processes such as sediment resuspension/deposition by wind waves. These radionuclide dating techniques and calculation of SAR are described in detail in Appendix B.

Estimates of pre-historic SAR were determined for two salt marsh core sites located in Oikimoke Estuary (cores O1 and O3) using atomic mass spectrometry (AMS) radiocarbon ( $^{14}\text{C}$ ) dating. Replicate shell valves of the common suspension-feeding bivalve *Austrovenus stutchburyi* (cockle) were selected for dating. The New Zealand cockle is particularly suitable for radiocarbon dating as they have  $^{14}\text{C}$  concentrations in their carbonate that are similar to those found in marine shellfish (Hogg et al. 1998). This means that marine reservoir effects (i.e., “old” carbon in ocean waters mixing with coastal waters) can, in part, be modelled for using the marine  $^{14}\text{C}$  calibration curve (Petchey et al. 2008). However, the reservoir age in New Zealand is relatively poorly constrained (Clark et al., 2019). All radiocarbon ages reported in the current study are in calibrated years before present (cal. yr BP) following laboratory calibration using OxCal 4.4.4 (Bronk Ramsey, 2021) r5, using marine data from Heaton et al. (2020) and a reservoir correction ( $\Delta R -154 \pm 38$ ).

Cockle shell valves, both articulated and individually were identified in the cores at 64–66 cm (core O1) and 60–68 cm (core O3) well below the depth profile of excess  $^{210}\text{Pb}$ . Samples from articulated valves with intact surface ornamentation were favoured for dating. This indicates that the animals died in situ in the upper-most sediment column or were not transported far from their place of origin. In life, cockles typically occur in the upper several cm of the substrate. In the Tuapiro P55 core, three shell valves were taken from a shell layer at 63–65 cm depth. Three samples from a shell bed (59–64 cm) were selected from the Waimapu P16 core, with two of these samples from individual shellfish with articulated valves. Details of the dated samples are included in Appendix B.



**Figure 2-3:** Cockle shell valves from an articulated specimen (sample O1-B, 64-cm depth) preserved in core O1, Oikimoke Estuary.

## 2.5 Organic carbon stock

Organic carbon stocks in the 100 cm sediment cores were estimated using standard methods described in the Coastal Blue Carbon: Methods Manual (Howard et al., 2014). Rates of organic carbon sequestration were also calculated using the carbon stock estimates and lead-210 ( $^{210}\text{Pb}$ ) SAR data.

Total organic carbon stock in each core was determined as follows:

- TOC% and DBD determined for each 5-cm depth increment samples in each core, as described above in the laboratory method section.
- The soil carbon density (SCD) was calculated as the product of  $\text{DBD} \times (\text{TOC}\% / 100)$  to yield organic carbon content in units of  $\text{g cm}^{-3}$ .
- The soil organic carbon content in each 5-cm depth increment samples per unit area ( $\text{gC cm}^{-2}$ ) is given by the product  $\text{SCD} \times 5$ .
- The total organic carbon stock to any depth horizon ( $\text{OC}_{\text{horizon}}$ ,  $\text{gC cm}^{-2}$ ) is calculated by summing the soil organic carbon content of each 5-cm increment in the range to depth horizon. In the present study, the total organic carbon stock was calculated for three intervals: (1) to 100-cm depth; (2) to the base of the  $^{210}\text{Pb}$  dated sediment (~90–160 yr); and (3) for the last 100 years (~1923–2023).
- These  $\text{OC}_{\text{horizon}}$  quantities ( $\text{gC cm}^{-2}$ ) were transformed to mega-grams of organic carbon per hectare ( $\text{MgC ha}^{-1}$ ,  $\text{Mg} = 1 \text{ tonne}$ ,  $\text{ha} = 10,000 \text{ m}^2$ ) as the product  $(\text{OC}_{\text{stock}} / 10^6) \times 10^8$ .

## 2.6 Organic carbon sequestration rate

Time-averaged organic carbon sequestration rates for each depth horizon were calculated by combining organic carbon stock estimates with SAR determined from  $^{210}\text{Pb}$  dating of sediment cores from each site. AMS radiocarbon dating of samples from core sites O1 and O3 also enabled time-averaged organic carbon sequestration rates over several thousand years prior to the mid-1800s when large-scale catchment deforestation commenced. Time-averaged OC sequestration rates were calculated as follows:

- Calculate the OC accumulation rate from the organic carbon content per 5-cm core increment ( $\text{g cm}^{-2}$ ) using the time-averaged  $^{210}\text{Pb}$  SAR ( $\text{mm yr}^{-1}$ ) as  $\text{OC} / (5 / (^{210}\text{Pb SAR} / 10))$ . The /10 division converts SAR to  $\text{cm}^{-2}$  such that the OC accumulation rate per 5-cm increment has units of  $\text{g cm}^{-2} \text{ yr}^{-1}$  and converted to  $\text{Mg ha}^2 \text{ yr}^{-1}$  as described in the previous section.
- Basic statistical measures of the time-averaged OC accumulation rate for the 5-cm increment values were calculated: mean, median, standard deviation.

### 3 Results

The following sections present the results of the x-ray imaging,  $^{210}\text{Pb}$  and  $^{14}\text{C}$  dating, sediment composition and organic carbon sequestration for each salt marsh.

#### 3.1 Sediment accumulation rates and sediment properties

##### 3.1.1 Katikati Estuary

###### Core K1

The x-radiographs for core K1 show that sediment deposits are composed of a low-density/organic-rich (dark hue) surface layer (0–12 cm depth) overlaying a higher density sand-rich sediment (light hue) to the base of the core. This layer represents the main root mass of the salt marsh plants. There is negligible preservation of stratification in this muddy sand, suggest a degree of mixing and/or winnowing of mud. Numerous vertically orientated mm-diameter tubes of low-density material are evident to the base of the core (61 cm depth). These features are also consistent with the root structures of the overlying salt marsh plant community (Figure 3-1).

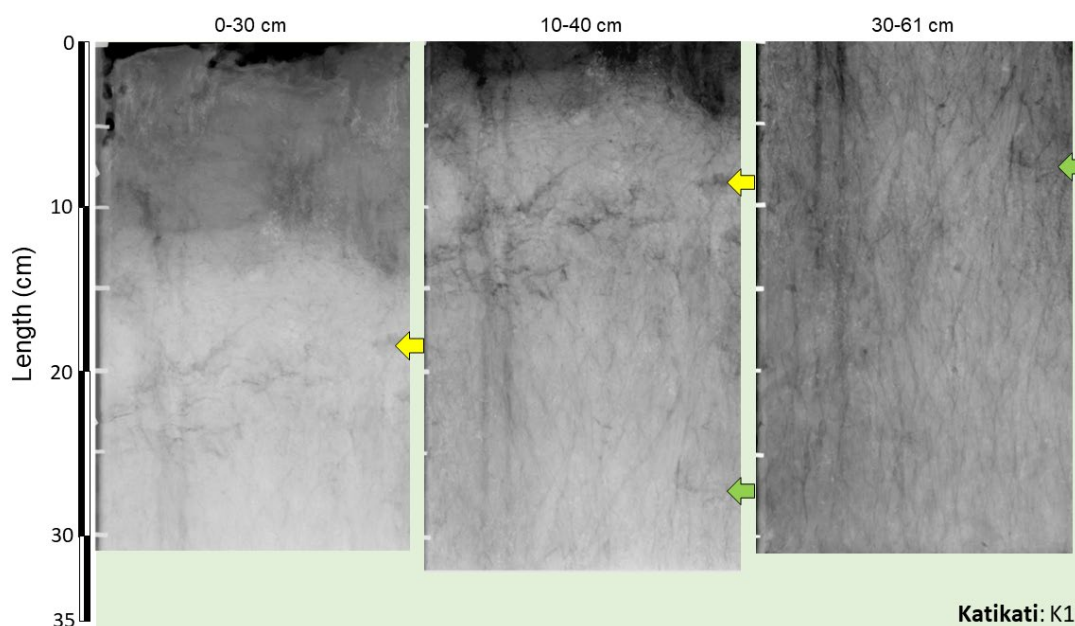


**Figure 3-1: Core K1, Katikati Estuary. X-radiograph of salt marsh core (0-61 cm).** These x-radiographs have been inverted so that relatively high-density objects appear white (e.g., shell valves) and low-density materials such as muds or organic material appear as darker areas. The x-radiographs represent core sections up to 35-cm long, with the depth intervals indicated the top of each image. The coloured arrows indicate matching positions (i.e., depth in core) in each x-radiograph.

Excess  $^{210}\text{Pb}$  occurs in the upper 32-cm of the sediment column, with a time-averaged  $^{210}\text{Pb}$  SAR of  $2.8 \text{ mm yr}^{-1}$  (fit:  $r^2 = 0.88$ ), with the earliest sediment in this layer deposited in the early 1900s (Figure 3-2). Caesium-137 was detected in only two samples (7–8, 10-11 cm depth) that may coincide with the 1963/64  $^{137}\text{Cs}$  atmospheric fallout peak, although this uncertain. Assuming this chronology yields a time-averaged SAR of  $1.8 \text{ mm yr}^{-1}$ . This is substantially less than the  $^{210}\text{Pb}$  SAR value. Dry bulk densities ( $\rho_d$ ) in core K1 vary from  $0.2\text{--}1.1 \text{ g cm}^{-3}$  with a peak  $\rho_d$  occurring at 17–18-cm depth ( $^{210}\text{Pb}$  year: 1962) and declining to  $0.4 \text{ g cm}^{-3}$  at 10-cm depth, near the base of the salt marsh root mass (Figure 3-2). The low dry-bulk densities are consistent with mud- and/or mud-rich sediment.

For comparison, the unconsolidated estuarine mud of the southern Firth of Thames has typical  $\rho_d$  values  $\sim 0.5 \text{ g cm}^{-3}$  (Swales et al., 2015). The reduction in dry-bulk density in the early-1960s coincides with a marked increase in sediment mud content from  $\sim 15\%$  to  $30\text{--}50\%$  in the mud-/organic-rich surface layer (Figure 3-2). Likewise, mean particle size reduces from  $220\text{--}235 \mu\text{m}$  below the 1962 horizon to  $220\text{--}235 \mu\text{m}$  in the mud-rich layer above.

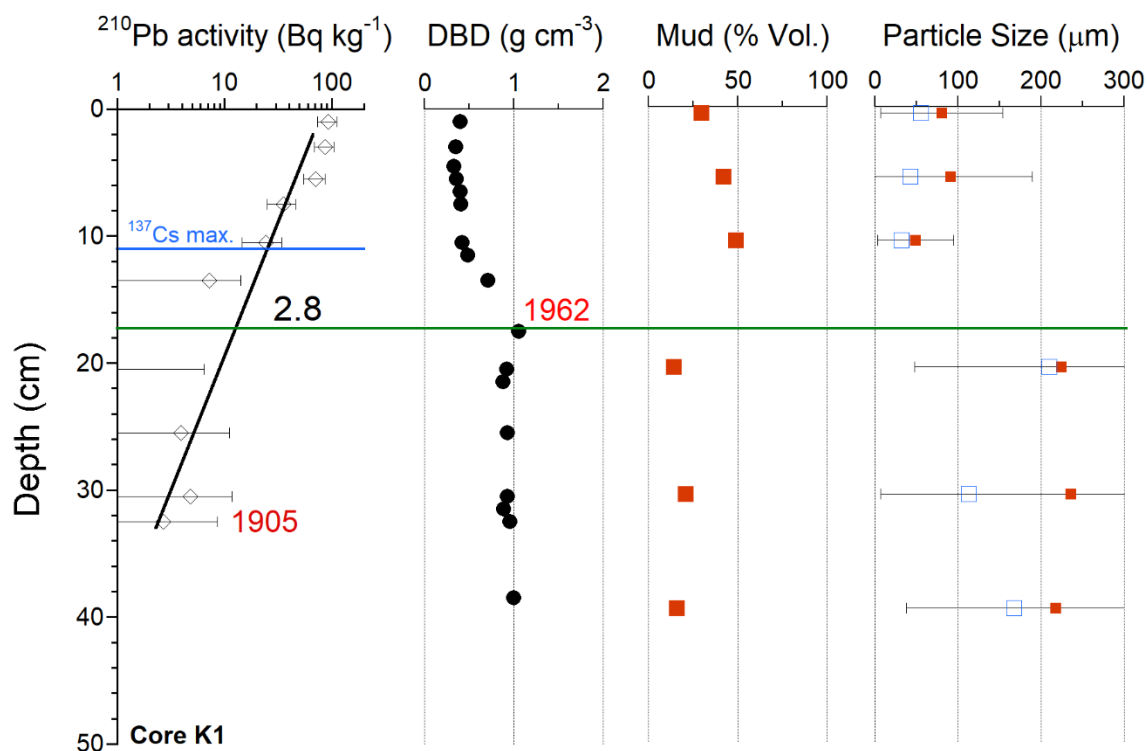


**Figure 3-2: Core K1 (Katikati Estuary) - ages of sediment layers, sediment accumulation rates (SAR), and sediment properties.** Left to right: Excess  $^{210}\text{Pb}$  activity profiles with 95% confidence intervals shown. Time-averaged SAR ( $\text{mm yr}^{-1}$ , black text) derived from regression fit ( $r^2 = 0.88$ ) to natural log-transformed excess  $^{210}\text{Pb}$  data. Calculated age at the base of activity profile is shown in red text. Sediment dry bulk density profile (DBD,  $\text{g cm}^{-3}$ ). Mud % by particle volume. Mean (closed square) with standard deviation and median particle size (microns,  $\mu\text{m}$ ).

## Core K2

The x-radiographs for core K2 indicate a more complex sedimentary structure than observed in core K1. Three layers of low-density/organic-rich (dark hue) sediment interlayered with higher density sand-rich sediment (light hue) occur in the upper 32-cm of the core:  $0\text{--}7$ ,  $10\text{--}25$ ,  $28\text{--}32 \text{ cm}$  (Figure 3-3). These layers represent the main root mass of the salt marsh. This organic-rich sediment overlays higher density, heterogeneous, sand-rich sediment (light hue) to the base of the core at  $65\text{-cm}$  depth. There is negligible preservation of stratification in this muddy-sand layer, suggest a degree of mixing and/or winnowing of mud. As observed in core K1, numerous mm-diameter root structures of the overlying salt marsh plant community penetrate the sand layer to the base of the core (Figure 3-3).

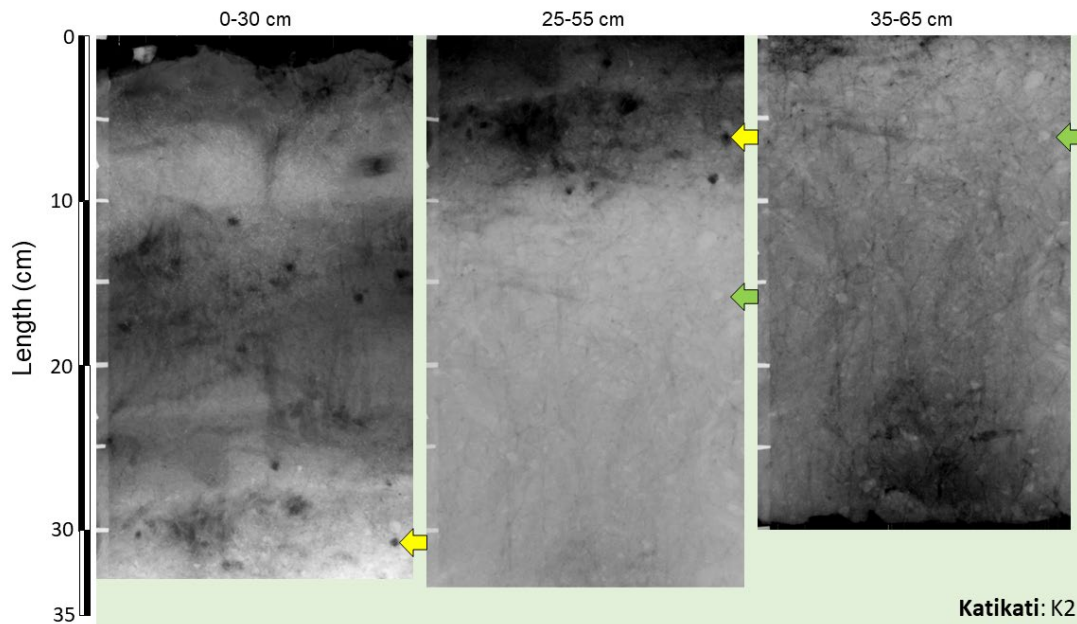


**Figure 3-3: Core K2, Katikati Estuary. X-radiograph of salt marsh core (0-65 cm).** These x-radiographs have been inverted so that relatively high-density objects appear white (e.g., shell valves) and low-density materials such as muds or organic material appear as darker areas. The x-radiographs represent core sections up to 35-cm long, with the depth intervals indicated the top of each image. The coloured arrows indicate matching positions (i.e., depth in core) in each x-radiograph.

Excess  $^{210}\text{Pb}$  occurs in the upper 33-cm of the sediment column, with a time-averaged  $^{210}\text{Pb}$  SAR of  $2.7 \text{ mm yr}^{-1}$  (fit:  $r^2 = 0.85$ ), with the earliest sediment in this layer deposited in the early 1900s (Figure 3-4, Figure 3-2). As observed in core K1,  $^{137}\text{Cs}$  was detected in only two samples (10–11, 14–15 cm depth), with the highest activity at 14–15-cm ( $4.1 \text{ Bq kg}^{-1}$ ) that may coincide with the 1963/64  $^{137}\text{Cs}$  atmospheric fallout peak, although this is uncertain. Assuming this chronology yields a time-averaged SAR of  $2.5 \text{ mm yr}^{-1}$  that is consistent with the  $^{210}\text{Pb}$  SAR value. Dry bulk densities ( $\rho_d$ ) in core K2 vary from  $0.3\text{--}1.3 \text{ g cm}^{-3}$  with a peak  $\rho_d$  occurring at 7–8-cm depth ( $^{210}\text{Pb}$  year: 1993) and declining to  $0.3\text{--}0.5 \text{ g cm}^{-3}$  in the near-surface salt marsh root mass (Figure 3-4). A second  $\rho_d$  peak occurs at 38–39 cm depth, near the top of the sand layer. The low dry-bulk densities are consistent with mud- and/or mud-rich sediment. The depth profile of the sediment mud content progressively increases towards the surface, from 4% (38–39-cm) to 50% in the top 10-cm of the core. Likewise, mean particle size progressively reduces from  $235 \mu\text{m}$  (fine sand, 40 cm) to  $\sim 50 \mu\text{m}$  in the top 10-cm of the core.

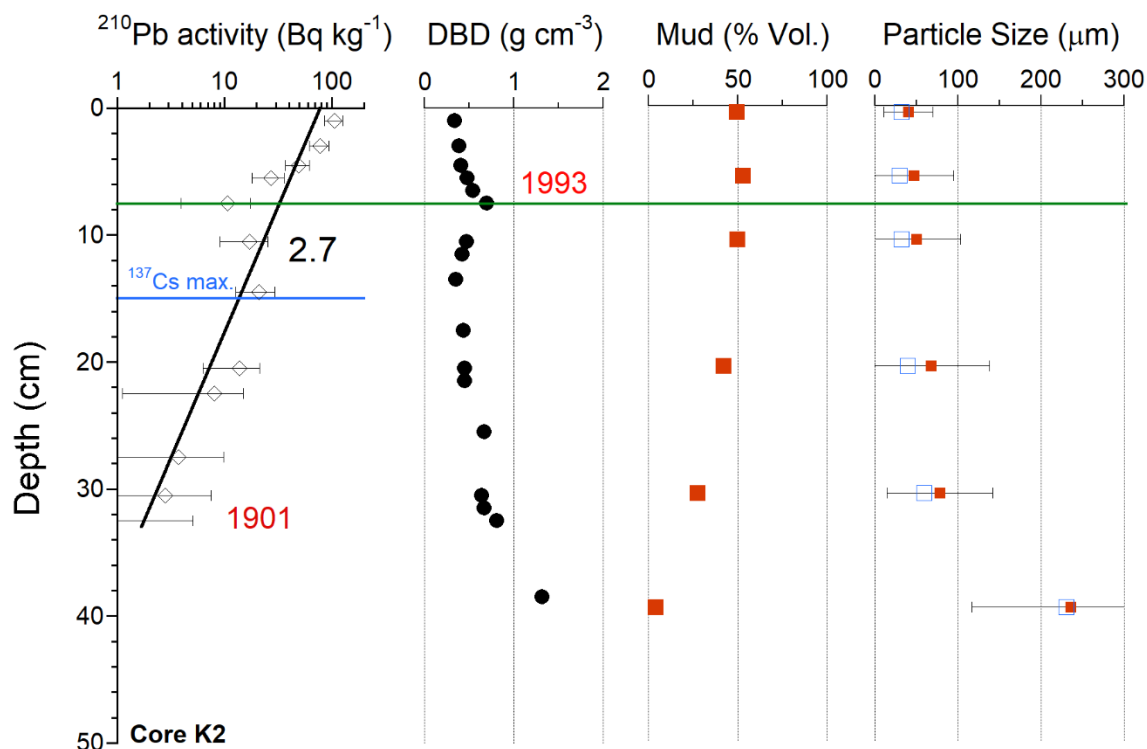


**Figure 3-4: Core K2 (Katikati Estuary) - ages of sediment layers, sediment accumulation rates (SAR), and sediment properties.** Left to right: Excess  $^{210}\text{Pb}$  activity profiles with 95% confidence intervals shown. Time-averaged SAR ( $\text{mm yr}^{-1}$ , black text) derived from regression fit ( $r^2 = 0.85$ ) to natural log-transformed excess  $^{210}\text{Pb}$  data. Calculated age at the base of activity profile is shown in red text. Sediment dry bulk density profile (DBD,  $\text{g cm}^{-3}$ ). Mud % by particle volume. Mean (closed square) with standard deviation and median particle size (microns,  $\mu\text{m}$ ).

### Core K3

The x-radiographs for core K3 are similar to K2 and exhibit alternating layers of low-density/organic-rich (dark hue) sediment and higher density sand-rich sediment (light hue) occur in the upper ~40-cm of the core: 0–7, 10–22 cm (Figure 3-5). These layers represent the main root mass of the salt marsh. This organic-rich sediment overlays higher density, heterogenous, muddy-sand sediment (light hue) to the base of the core at 60-cm depth. There is negligible preservation of stratification in this muddy-sand layer, suggest a degree of mixing and/or winnowing of mud. As observed at the other Katikati salt marsh cores sites, numerous mm-diameter root structures of the overlying salt marsh plant community penetrate the sand layer to the base of the core (Figure 3-3).

Excess  $^{210}\text{Pb}$  occurs in the upper 28-cm of the sediment column, with a time-averaged  $^{210}\text{Pb}$  SAR of  $2.3 \text{ mm yr}^{-1}$  (fit:  $r^2 = 0.79$ ), with the earliest sediment in this layer deposited in the early 1900s (Figure 3-6, Figure 3-2). As observed in cores K1 and K2,  $^{137}\text{Cs}$  was not consistently detected in samples down-core, albeit in three samples (7–8, 10–11, 14–15 cm depth), with the highest activity at 14–15-cm ( $2 \text{ Bq kg}^{-1}$ ) that may coincide with the 1963/64  $^{137}\text{Cs}$  deposition peak, although this is uncertain. Assuming this chronology yields a time-averaged SAR of  $2.5 \text{ mm yr}^{-1}$  that is consistent with the  $^{210}\text{Pb}$  SAR value.

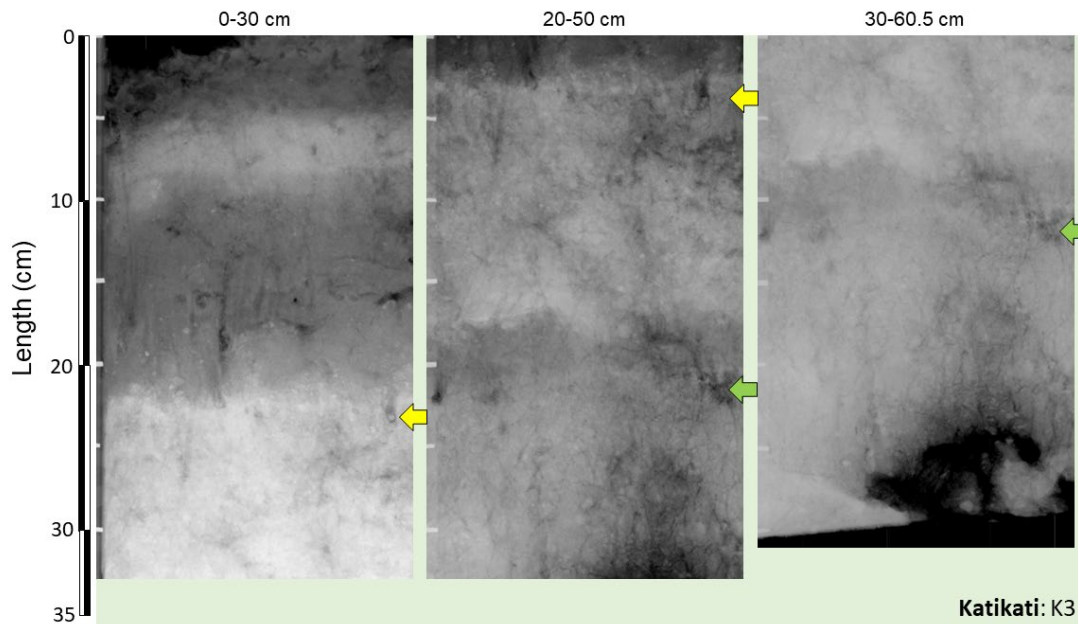


**Figure 3-5: Core K3, Katikati Estuary. X-radiograph of salt marsh core (0-60.5 cm).** These x-radiographs have been inverted so that relatively high-density objects appear white (e.g., shell valves) and low-density materials such as muds or organic material appear as darker areas. The x-radiographs represent core sections up to 35-cm long, with the depth intervals indicated the top of each image. The coloured arrows indicate matching positions (i.e., depth in core) in each x-radiograph.

Dry bulk densities ( $\rho_d$ ) in core K3 vary from 0.3–1.0 g cm<sup>-3</sup> with a peak  $\rho_d$  occurring at 22–23-cm depth (<sup>210</sup>Pb year: 1923) and gradually declining to 0.3 g cm<sup>-3</sup> at 10-cm depth (Figure 3-6, Figure 3-2). A second  $\rho_d$  peak occurs at 7–8 cm depth in the top-most sand layer. The depth profile of the sediment mud content mirrors the dry-bulk density profile, being less than 10% below 25-cm depth (<sup>210</sup>Pb year: 1923) and, as observed in core K2, increasing to 50% in the top 10-cm of the core. Likewise, mean particle size progressively reduces from ~250  $\mu$ m (fine/medium sand, 40 cm) to 50–100  $\mu$ m in the top 10-cm of the core.

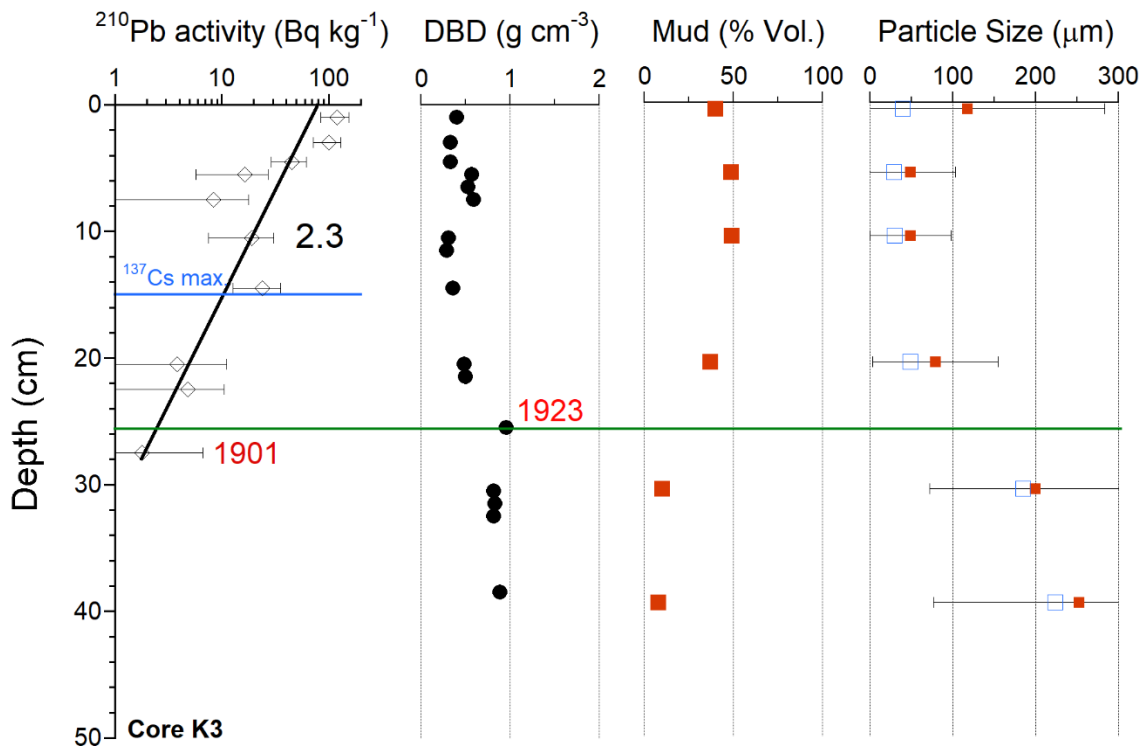


**Figure 3-6: Core K3 (Katikati Estuary) - ages of sediment layers, sediment accumulation rates (SAR), and sediment properties.** Left to right: Excess  $^{210}\text{Pb}$  activity profiles with 95% confidence intervals shown. Time-averaged SAR ( $\text{mm yr}^{-1}$ , black text) derived from regression fit ( $r^2 = 0.79$ ) to natural log-transformed excess  $^{210}\text{Pb}$  data. Calculated age at the base of activity profile is shown in red text. Sediment dry bulk density profile (DBD,  $\text{g cm}^{-3}$ ). Mud % by particle volume. Mean (closed square) with standard deviation and median particle size (microns,  $\mu\text{m}$ ).

### 3.1.2 Rereatukahia Estuary

#### Core R1

The x-radiographs for core R1 display similar sedimentary structures to those observed in the Katikati salt marsh cores, with alternating, decimetre-thick, layers of low-density/organic-rich (dark hue) sediment with higher density sediment (light hue). This layering extends to 43-cm depth (Figure 3-7) where this organic/mud-rich upper layer contacts the underlying muddy-sand body. The muddy sand is heterogenous with negligible preservation of stratification in this sand layer, suggest a degree of mixing and/or winnowing of mud. As observed at the Katikati salt marsh core sites, mm-diameter root structures penetrate the sand layer to the base of the core (Figure 3-7).

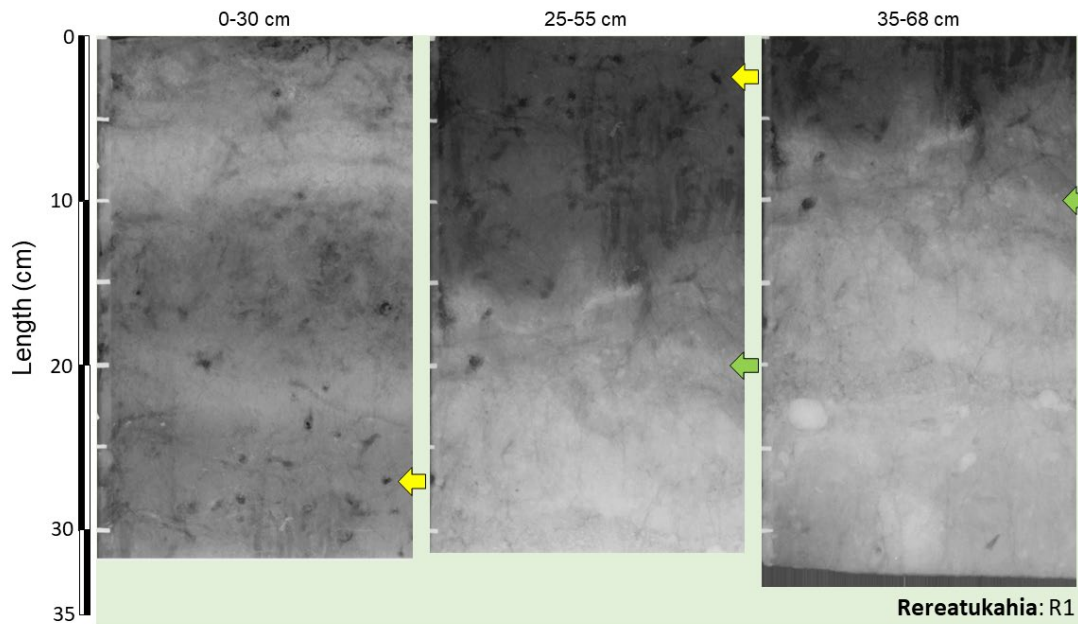


**Figure 3-7: Core R1, Reretukahia Estuary. X-radiograph of salt marsh core (0-68 cm).** These x-radiographs have been inverted so that relatively high-density objects appear white (e.g., shell valves) and low-density materials such as muds or organic material appear as darker areas. The x-radiographs represent core sections up to 35-cm long, with the depth intervals indicated the top of each image. The coloured arrows indicate matching positions (i.e., depth in core) in each x-radiograph.

Excess  $^{210}\text{Pb}$  extends to 44-cm depth in core R1, although the activity is highly variable and lacks a coherent pattern of exponential decay down-core. A log-linear regression was fitted to the top 10-cm of the core where the excess  $^{210}\text{Pb}$  profile displayed consistent exponential decay. This yielded a time-averaged  $^{210}\text{Pb}$  SAR of  $1.3 \text{ mm yr}^{-1}$  (fit:  $r^2 = 0.89$ ), with the sediment at 10-cm dated to  $^{210}\text{Pb}$  year 1938 (Figure 3-8, Figure 3-2). As observed in cores K1 and K2,  $^{137}\text{Cs}$  was not consistently detected in samples down-core (10–11, 13–14 cm depth), with the highest activity at 13–14-cm ( $3.5 \text{ Bq kg}^{-1}$ ) that may coincide with the 1963/64  $^{137}\text{Cs}$  deposition peak, although this is uncertain. Assuming this chronology yields a time-averaged SAR of  $2.3 \text{ mm yr}^{-1}$  that is not consistent with the  $^{210}\text{Pb}$  SAR value.

Dry bulk densities ( $\rho_d$ ) in core R1 vary from  $0.3\text{--}0.69 \text{ g cm}^{-3}$  with a peak  $\rho_d$  occurring at 7–8-cm depth ( $^{210}\text{Pb}$  year: 1969) and being relatively uniform in the organic-sediment rich top layer (to  $0.4\text{--}0.5 \text{ g cm}^{-3}$  (Figure 3-8, Figure 3-2). A second  $\rho_d$  peak occurs at the base of the core 43–44 cm depth. Sediment mud content progressively increases from the base of the core (18%) and being relatively uniform above 10-cm depth (46–50%). Likewise, mean particle size progressively reduces from  $\sim 130 \mu\text{m}$  (fine sand, 40 cm) to  $46\text{--}50 \mu\text{m}$  in the top 10-cm of the core.

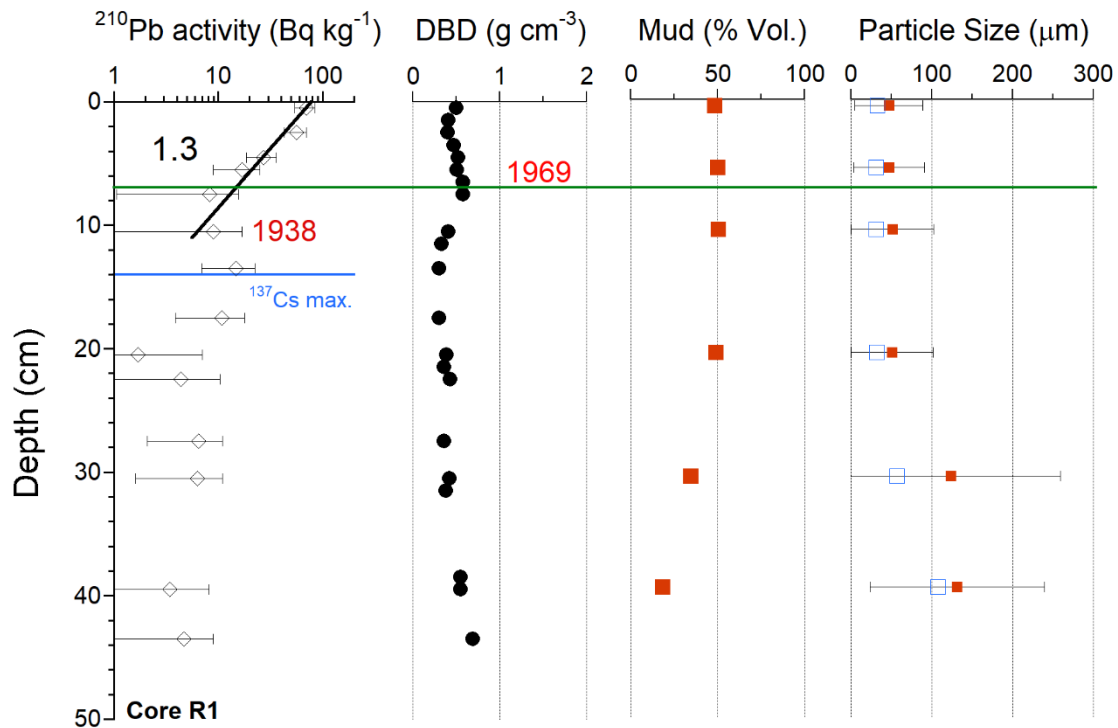


**Figure 3-8: Core R1 (Rereatukahia Estuary) - ages of sediment layers, sediment accumulation rates (SAR), and sediment properties.** Left to right: Excess  $^{210}\text{Pb}$  activity profiles with 95% confidence intervals shown. Time-averaged SAR ( $\text{mm yr}^{-1}$ , black text) derived from regression fit ( $r^2 = 0.89$ ) to natural log-transformed excess  $^{210}\text{Pb}$  data. Calculated age at the base of activity profile is shown in red text. Sediment dry bulk density profile (DBD,  $\text{g cm}^{-3}$ ). Mud % by particle volume. Mean (closed square) with standard deviation and median particle size (microns,  $\mu\text{m}$ ).

## Core R2

The x-radiographs for core R2 display a similar range of sedimentary structures to those described for the Katikati salt marsh cores. A low density low-density/organic-rich (dark hue) sediment occurs in the top 5-cm of the core with a sediment layer (5–0 cm depth) of intermediate density to the organic rich layer overlying muddy-sand at 10–62-cm depth (Figure 3-9). The muddy sand is heterogenous with negligible preservation of stratification in this sand layer, suggest a degree of mixing and/or winnowing of mud. As previously observed, mm-diameter root structures penetrate the sand layer to the base of the core.

Excess  $^{210}\text{Pb}$  extends to 40-cm depth in core R2, although the activity is highly variable and, like core R1, lacks a coherent pattern of exponential decay down-core. A log-linear regression was fitted to the top 11-cm of the core where the excess  $^{210}\text{Pb}$  profile displayed consistent exponential decay. This yielded a time-averaged  $^{210}\text{Pb}$  SAR of  $0.8 \text{ mm yr}^{-1}$  (fit:  $r^2 = 0.80$ ), with the sediment at 11-cm dated to  $^{210}\text{Pb}$  year 1885 (Figure 3-10, Figure 3-2). Notably,  $^{137}\text{Cs}$  was consistently detected in samples down-core to 6-cm depth (5 samples), with the highest activity at 1–2-cm ( $1.85 \text{ Bq kg}^{-1}$ ) that may coincide with the 1963/64  $^{137}\text{Cs}$  deposition peak, although this is uncertain. Assuming this chronology yields a time-averaged SAR of  $0.3 \text{ mm yr}^{-1}$  that is not consistent with the  $^{210}\text{Pb}$  SAR value.

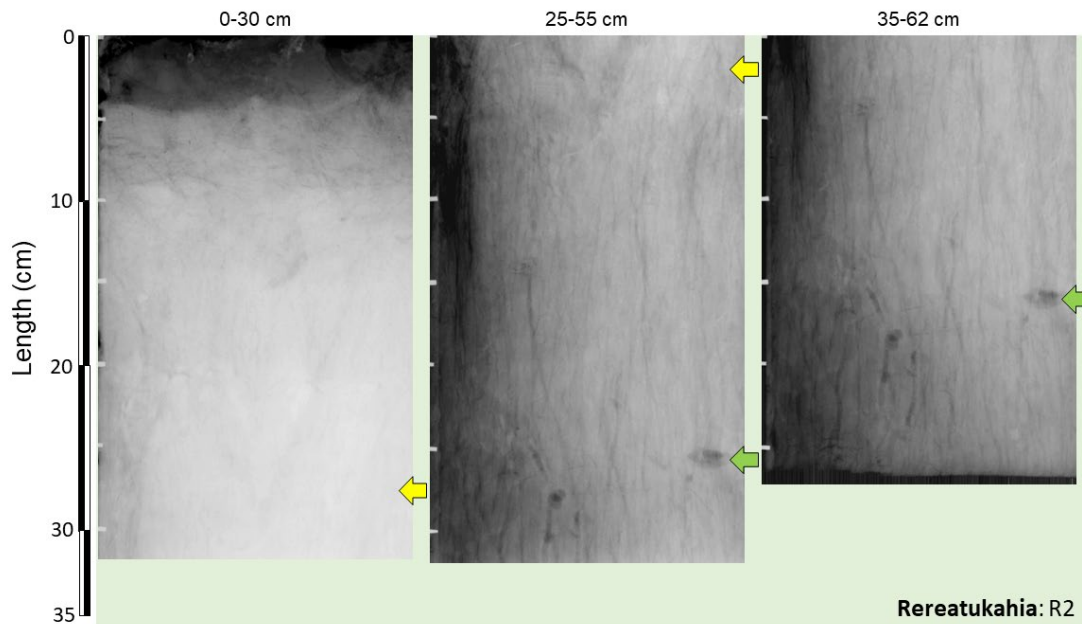


**Figure 3-9: Core R2, Reretukahia Estuary. X-radiograph of salt marsh core (0-62 cm).** These x-radiographs have been inverted so that relatively high-density objects appear white (e.g., shell valves) and low-density materials such as muds or organic material appear as darker areas. The x-radiographs represent core sections up to 35-cm long, with the depth intervals indicated the top of each image. The coloured arrows indicate matching positions (i.e., depth in core) in each x-radiograph.

Dry bulk densities ( $\rho_d$ ) in core R2 vary from 0.3–1.1 g cm<sup>-3</sup>. The  $\rho_d$  is highly uniform in the muddy-fine sand underlying the organic-rich surface layers (0–10 cm), with  $\rho_d$  of 0.93–1.1 g cm<sup>-3</sup>. Sediment dry-bulk density progressively decreases above 10-cm depth (1880s) from 1 to 0.3 g cm<sup>-3</sup> at the substrate surface. Sediment mud content below 10-cm depth varies in the range 16–35% and abruptly increases to 42–45% in the upper mud- and organic-rich surface layers. Mean particle size in the muddy-sand varies from 144–167  $\mu\text{m}$  (fine sand, 40 cm) and reduces to 45  $\mu\text{m}$  (medium silt) in the top 10-cm of the core.

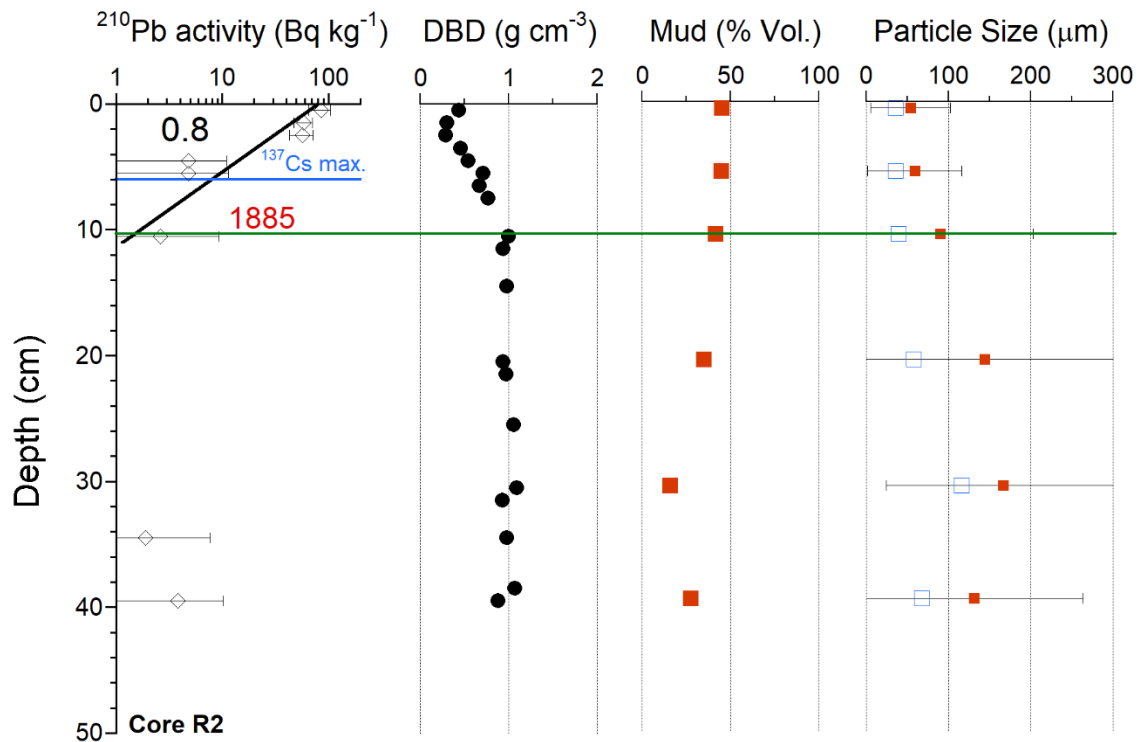


**Figure 3-10: Core R2 (Rereatukahia Estuary) - ages of sediment layers, sediment accumulation rates (SAR), and sediment properties.**

Left to right: Excess  $^{210}\text{Pb}$  activity profiles with 95% confidence intervals shown. Time-averaged SAR ( $\text{mm yr}^{-1}$ , black text) derived from regression fit ( $r^2 = 0.80$ ) to natural log-transformed excess  $^{210}\text{Pb}$  data. Calculated age at the base of activity profile is shown in red text. Sediment dry bulk density profile (DBD,  $\text{g cm}^{-3}$ ). Mud % by particle volume. Mean (closed square) with standard deviation and median particle size (microns,  $\mu\text{m}$ ).

### Core R3

X-radiographs for core R3 are similar to R2, with a low density low-density/organic-rich (dark hue) sediment occurring in the top 10-cm of the core, overlaying a muddy-sand from 10–64-cm depth (Figure 3-11). The muddy sand is heterogenous with negligible preservation of stratification in this sand layer, suggest a degree of mixing and/or winnowing of mud. Numerous mm-diameter root structures penetrate the muddy-sand layer to the base of the core.

Excess  $^{210}\text{Pb}$  extends to 40-cm depth, although the activity is again highly variable and, like cores R1 and R2, lacks a coherent pattern of exponential decay down-core (Figure 3-12). A log-linear regression was fitted to the top 21-cm of the core where the excess  $^{210}\text{Pb}$  profile displayed consistent exponential decay. This yielded a time-averaged  $^{210}\text{Pb}$  SAR of  $1.3 \text{ mm yr}^{-1}$  (fit:  $r^2 = 0.99$ ), with the sediment at 21-cm dated to  $^{210}\text{Pb}$  year 1862 (Figure 3-12).  $^{137}\text{Cs}$  was detected in samples between 5 and 11-cm depth (5–6, 7–8, 10–11 cm), with the highest activity at 7–8-cm ( $3.7 \text{ Bq kg}^{-1}$ ) that may coincide with the 1963/64  $^{137}\text{Cs}$  deposition peak, although this is uncertain. Assuming this chronology yields a time-averaged SAR of  $1.3 \text{ mm yr}^{-1}$  that is the same as  $^{210}\text{Pb}$  SAR value.

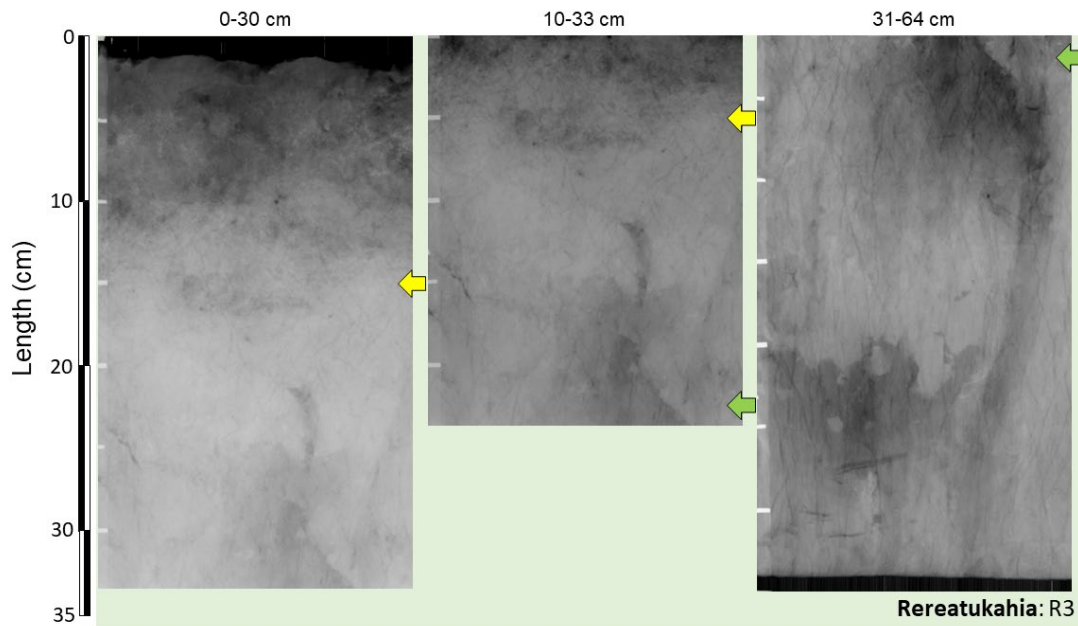


**Figure 3-11: Core R3, Reretukahia Estuary. X-radiograph of salt marsh core (0-64 cm).** These x-radiographs have been inverted so that relatively high-density objects appear white (e.g., shell valves) and low-density materials such as muds or organic material appear as darker areas. The x-radiographs represent core sections up to 35-cm long, with the depth intervals indicated the top of each image. The coloured arrows indicate matching positions (i.e., depth in core) in each x-radiograph.

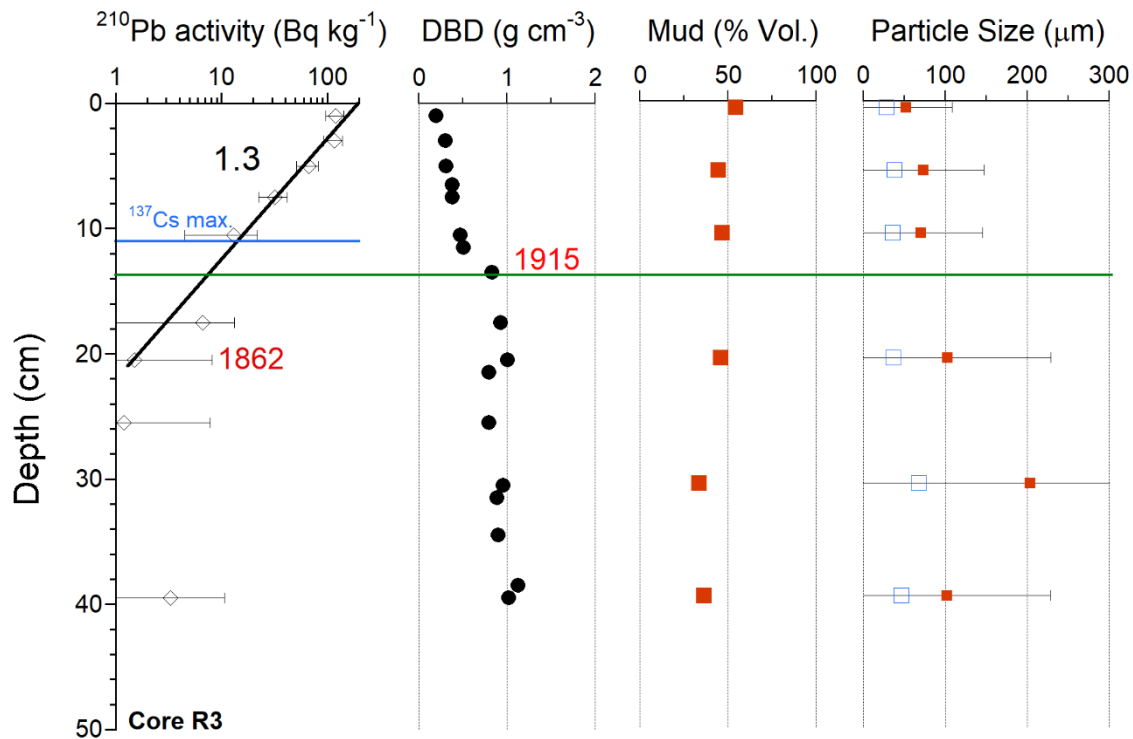


**Figure 3-12: Core R3 (Rereatukahia Estuary) - ages of sediment layers, sediment accumulation rates (SAR), and sediment properties.** Left to right: Excess  $^{210}\text{Pb}$  activity profiles with 95% confidence intervals shown. Time-averaged SAR ( $\text{mm yr}^{-1}$ , black text) derived from regression fit ( $r^2 = 0.99$ ) to natural log-transformed excess  $^{210}\text{Pb}$  data. Calculated age at the base of activity profile is shown in red text. Sediment dry bulk density

Dry bulk densities ( $\rho_d$ ) in core R3 vary from 0.2–1.1  $\text{g cm}^{-3}$ . The  $\rho_d$  in the muddy-fine sand below 14-cm depth (1915) is relatively uniform (0.80–1.1  $\text{g cm}^{-3}$ , Figure 3-12). Sediment dry-bulk density progressively decreases above 14-cm depth (1880s) from 0.8 to  $\sim 0.3 \text{ g cm}^{-3}$  at the substrate surface. Sediment mud content in the underlying muddy-sand varies from 33–46% and gradually increases to 54% in the upper mud- and organic-rich surface layers. Mean particle size in the muddy-sand varies from 100–200  $\mu\text{m}$  (fine sand) and reduces to 50–70  $\mu\text{m}$  (coarse silt–very-fine sand) in the top 11-cm of the core.

### 3.1.3 Oikimoke Estuary

#### Core O1

X-radiographs for Oikimoke core O1 display sedimentary fabrics to those described for cores collected from the Katikati and Rereatukahia salt marshes. A low density low-density/organic-rich (dark hue) sediment occupies the top 10-cm of the core, overlaying a muddy-sand from 10–67-cm depth (Figure 3-13). The muddy sand is heterogenous with negligible preservation of stratification in this sand layer, suggest a degree of mixing and/or winnowing of mud. Numerous mm-diameter root structures penetrate the muddy-sand layer to the base of the core. A layer of cockle shell (*Austrovenus stutchburyi*) occurs in core basal sediment at 60–66 cm depth.

Excess  $^{210}\text{Pb}$  extends to 40-cm depth, with a coherent pattern of exponential decay down-core (Figure 3-14). A log-linear regression was fitted to the entire excess  $^{210}\text{Pb}$  profile, which yielded a time-averaged  $^{210}\text{Pb}$  SAR of 2.2  $\text{mm yr}^{-1}$  (fit:  $r^2 = 0.94$ ), with the sediment at 40-cm dated to  $^{210}\text{Pb}$  year 1842.

$^{137}\text{Cs}$  was detected in two samples (7–8, 10–11 cm), with the highest activity at 7–8-cm ( $1.7 \text{ Bq kg}^{-1}$ ) that may coincide with the 1963/64  $^{137}\text{Cs}$  deposition peak, although this is uncertain. Assuming this chronology yields a time-averaged SAR of  $1.3 \text{ mm yr}^{-1}$  that is not consistent with the  $^{210}\text{Pb}$  SAR value.

Dry bulk densities ( $\rho_d$ ) in core O1 vary from  $0.3\text{--}1.3 \text{ g cm}^{-3}$ . The  $\rho_d$  in the muddy-fine sand below 13-cm depth (1915) is relatively uniform ( $1.1\text{--}1.3 \text{ g cm}^{-3}$ , Figure 3-14). Sediment dry-bulk density progressively decreases above this depth (1959) from 1.1 to  $\sim 0.3 \text{ g cm}^{-3}$  and is highly uniform in the top 5-cm of the core. Sediment mud content in the underlying muddy-sand is relatively low (2–10%) and gradually increases to 10–20% in the mud-/organic-rich surface layer. Mean particle size in the muddy-sand varies from  $170\text{--}208 \mu\text{m}$  (fine sand) and reduces to  $130\text{--}168 \mu\text{m}$  (fine sand) in the top 11-cm of the core (Figure 3-14).

Core O1 does not preserve any evidence of a mud-rich event layer that could be attributed to high fluxes of fine sediment associated with the failure of the Ruahihi dam in 1981.

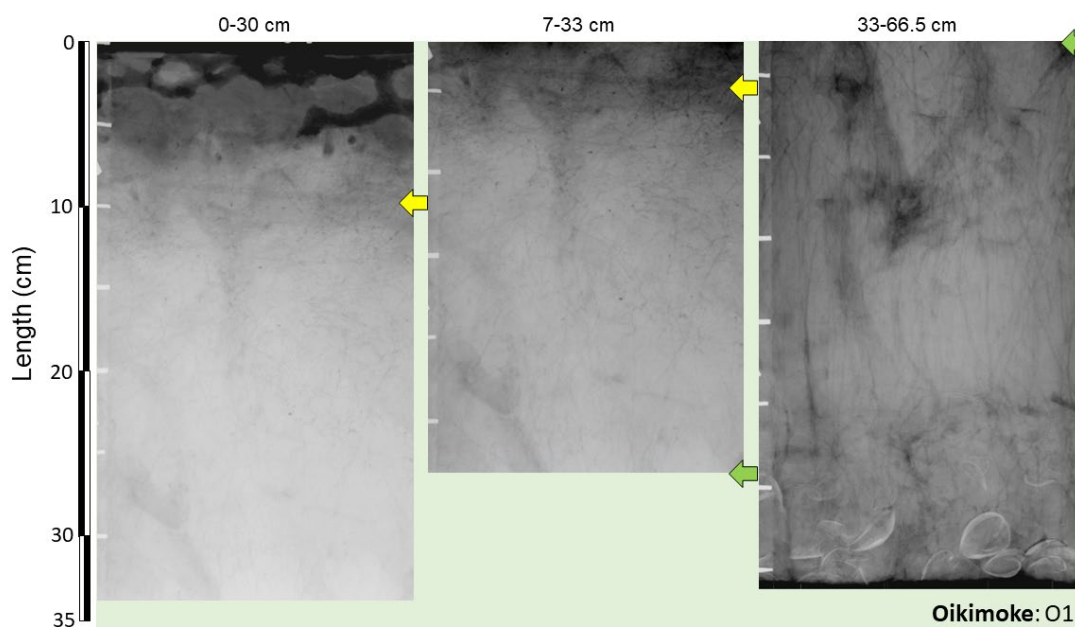


**Figure 3-13: Core O1, Oikimoke Estuary. X-radiograph of salt marsh core (0-66.5 cm).** These x-radiographs have been inverted so that relatively high-density objects appear white (e.g., shell valves) and low-density materials such as muds or organic material appear as darker areas. The x-radiographs represent core sections up to 35-cm long, with the depth intervals indicated the top of each image. The coloured arrows indicate matching positions (i.e., depth in core) in each x-radiograph.

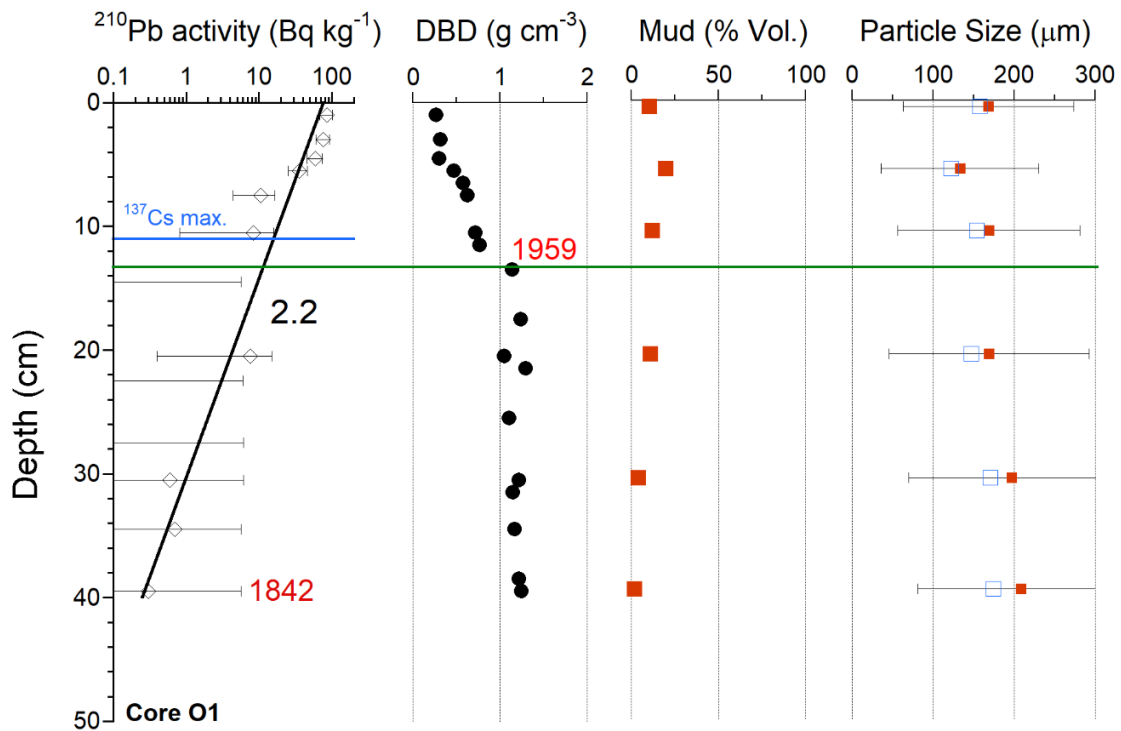


**Figure 3-14: Core O1 (Oikimoke Estuary) - ages of sediment layers, sediment accumulation rates (SAR), and sediment properties.** Left to right: Excess  $^{210}\text{Pb}$  activity profiles with 95% confidence intervals shown. Time-averaged SAR ( $\text{mm yr}^{-1}$ , black text) derived from regression fit ( $r^2 = 0.94$ ) to natural log-transformed excess  $^{210}\text{Pb}$  data. Calculated age at the base of activity profile is shown in red text. Sediment dry bulk density profile (DBD,  $\text{g cm}^{-3}$ ). Mud % by particle volume. Mean (closed square) with standard deviation and median particle size (microns,  $\mu\text{m}$ ).

Radiocarbon dating of three cockle shell valves (*Austrovenus stutchburyi*) from three different individuals collected from core basal sediment (64–66 cm depth range) provided consistent ages (Table 3-1) with 95% probability range of calibrated  $^{14}\text{C}$  ages in the range 6,410–6,840 cal. yr BP. These  $^{14}\text{C}$  ages yielded a time-average SAR of  $0.04 \text{ mm yr}^{-1}$ , below the excess  $^{210}\text{Pb}$  layer (i.e., pre-1840s).

**Table 3-1: Summary of AMS <sup>14</sup>C dating results for Oikimoke Estuary.** Radiocarbon dating results for cockle shell (*Austrovenus stutchburyi*) sampled from cores O1 and O3 (Oikimoke Estuary). The <sup>14</sup>C age ± 1 standard deviation (Before Present, BP = 1950) is based on the Libby half-life (5,568 yr) with correction for isotopic fractionation. The laboratory calibration used OxCal 4.4.4 (Bronk and Ramsey, 2021) r5, using marine data from Heaton et al. (2020) and a reservoir correction (ΔR -154 ± 38). The 95% probability age range is used to calculate the time-average SAR value.

| Core/sample      | Sample ID        | Depth increment (cm) | <sup>14</sup> C (radiocarbon) age (Years Before Present) | Calibrated <sup>14</sup> C age range (cal. yr BP, 95% Probability) |
|------------------|------------------|----------------------|--|--|
| <b>Core O1/A</b> | <i>Wk-57779</i>  | 65–66 (sample A)     | 6 202 ± 20   | 6 780–6 410  |
| /B               | <i>Wk-57780</i>  | 64–65 (sample B)     | 6 206 ± 20   | 6 790–6 430  |
| /D               | <i>Wk-57781</i>  | 65–66 (sample D)     | 6 245 ± 23   | 6 840–6 470  |
| <b>Core O3/B</b> | <i>Wk- 57782</i> | 64–65 (sample B)     | 6 226 ± 18   | 6 820–6 440  |
| /D               | <i>Wk- 57783</i> | 67–68 (sample D)     | 6 172 ± 23   | 6 750–6 390  |
| /E               | <i>Wk-57784</i>  | 60–61 (sample E)     | 6 144 ± 17   | 6 730–6 370  |

## Core O2

The sedimentary fabrics observed in core O2 are similar to those described in the salt marsh cores collected for this study. A low density low-density/organic-rich (dark hue) sediment occupies the top 10-cm of the core, overlaying a muddy-sand from 10–60-cm depth (Figure 3-15). The muddy sand is heterogenous with negligible preservation of stratification in this sand layer, suggest a degree of mixing and/or winnowing of mud. Numerous mm-diameter root structures penetrate the muddy-sand layer to the base of the core. There are also traces of larger diameter (~ 1-cm) 10-cm long tubes at 15–33-cm depth that likely represent infilled burrows.

Excess <sup>210</sup>Pb extends to 40-cm depth, with a coherent pattern of exponential decay down-core (Figure 3-16). A log-linear regression was fitted to the entire excess <sup>210</sup>Pb profile, which yielded a time-averaged <sup>210</sup>Pb SAR of 2.7 mm yr<sup>-1</sup> (fit:  $r^2 = 0.79$ ), with the sediment at 40-cm dated to <sup>210</sup>Pb year 1875. <sup>137</sup>Cs was detected in one sample (2–4 cm, 1.4 Bq kg<sup>-1</sup>).

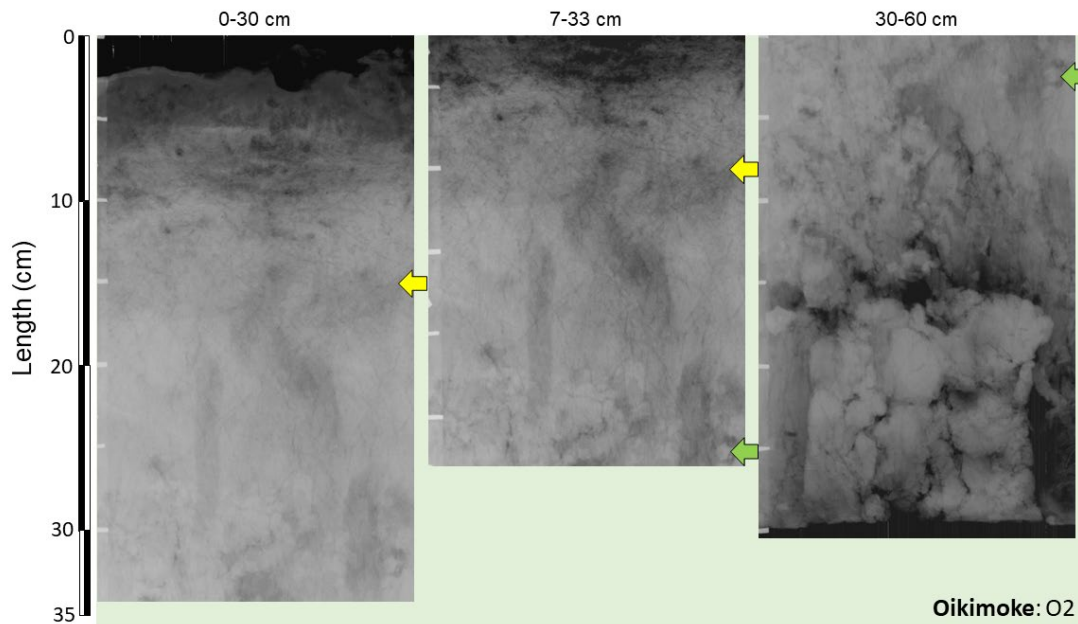


**Figure 3-15: Core O2, Oikimoke Estuary. X-radiograph of salt marsh core (0-60 cm).** These x-radiographs have been inverted so that relatively high-density objects appear white (e.g., shell valves) and low-density materials such as muds or organic material appear as darker areas. The x-radiographs represent core sections up to 35-cm long, with the depth intervals indicated the top of each image. The coloured arrows indicate matching positions (i.e., depth in core) in each x-radiograph.

Dry bulk densities ( $\rho_d$ ) in core O1 vary from 0.3–1.2 g cm<sup>-3</sup>. The  $\rho_d$  in the muddy-fine sand below 12-cm depth (1982) is relatively uniform (0.9–1.2 g cm<sup>-3</sup>, Figure 3-16). Sediment dry-bulk density progressively decreases above this depth, from 0.9 to ~0.3 g cm<sup>-3</sup>. Sediment mud content in the underlying sand is low (2–4%) then increases exponentially in the mud-/organic-rich surface layer, from 5% (11-cm depth) to 49% at the surface. Mean particle size in the underlying sand layer is highly uniform (217–220  $\mu$ m, fine sand) and reduces to 50  $\mu$ m (coarse silt) at the surface (0–1 cm, Figure 3-16). Core O2 does not preserve any evidence of a mud-rich event layer that could be attributed to high fluxes of fine sediment associated with the failure of the Ruahihi dam in 1981.

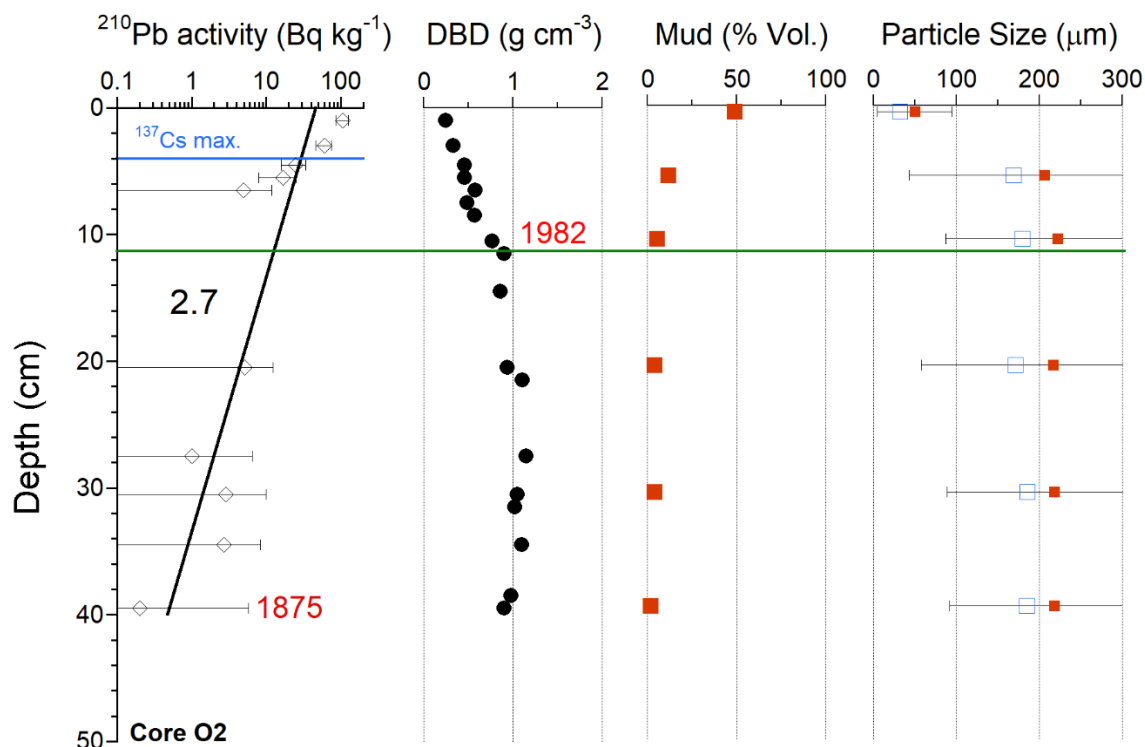


**Figure 3-16: Core O2 (Oikimoke Estuary) - ages of sediment layers, sediment accumulation rates (SAR), and sediment properties.** Left to right: Excess  $^{210}\text{Pb}$  activity profiles with 95% confidence intervals shown. Time-averaged SAR ( $\text{mm yr}^{-1}$ , black text) derived from regression fit ( $r^2 = 0.79$ ) to natural log-transformed excess  $^{210}\text{Pb}$  data. Calculated age at the base of activity profile is shown in red text. Sediment dry bulk density profile (DBD,  $\text{g cm}^{-3}$ ). Mud % by particle volume. Mean (closed square) with standard deviation and median particle size (microns,  $\mu\text{m}$ ).

### Core O3

The x-radiograph for core O3 is very similar to core O2 and have general features in common with salt marsh cores collected for the study estuaries. A low density low-density/organic-rich (dark hue) sediment occupies the top 10-cm of the core, overlaying a muddy-sand from 10–62-cm depth (Figure 3-17). The muddy sand is heterogenous with negligible preservation of stratification in this sand layer, suggest a degree of mixing and/or winnowing of mud. Numerous mm-diameter root structures penetrate the muddy-sand layer to the base of the core. As observed in core O2, there are also traces of larger diameter ( $\sim 1\text{-cm}$ ) 10-cm long tubes at 10–52-cm depth that likely represent infilled burrows (Figure 3-17).

Excess  $^{210}\text{Pb}$  extends to 44-cm depth, with a coherent albeit more complex pattern of exponential decay down-core (Figure 3-18) than observed at other core sites. The excess  $^{210}\text{Pb}$  profile exhibited an apparent change in sediment accumulation rate, as indicated by an inflection in the profile at 10–11-cm depth. The excess  $^{210}\text{Pb}$  profile was modelled as a high-SAR (lower) and low-SAR upper layer, with two log-linear regression relationships fitted. These yielded time-averaged  $^{210}\text{Pb}$  SAR of  $10.6 \text{ mm yr}^{-1}$  (lower layer fit:  $r^2 = 0.12$ ) and  $0.8 \text{ mm yr}^{-1}$  (upper layer fit:  $r^2 = 0.79$ ), with the reduction SAR occurring in the late-1800s ( $^{210}\text{Pb}$  year: 1885). The beginning of the high-SAR period dates to  $^{210}\text{Pb}$  year 1854.  $^{137}\text{Cs}$  was detected in a single sample (2–4 cm,  $1.7 \text{ Bq kg}^{-1}$ ).

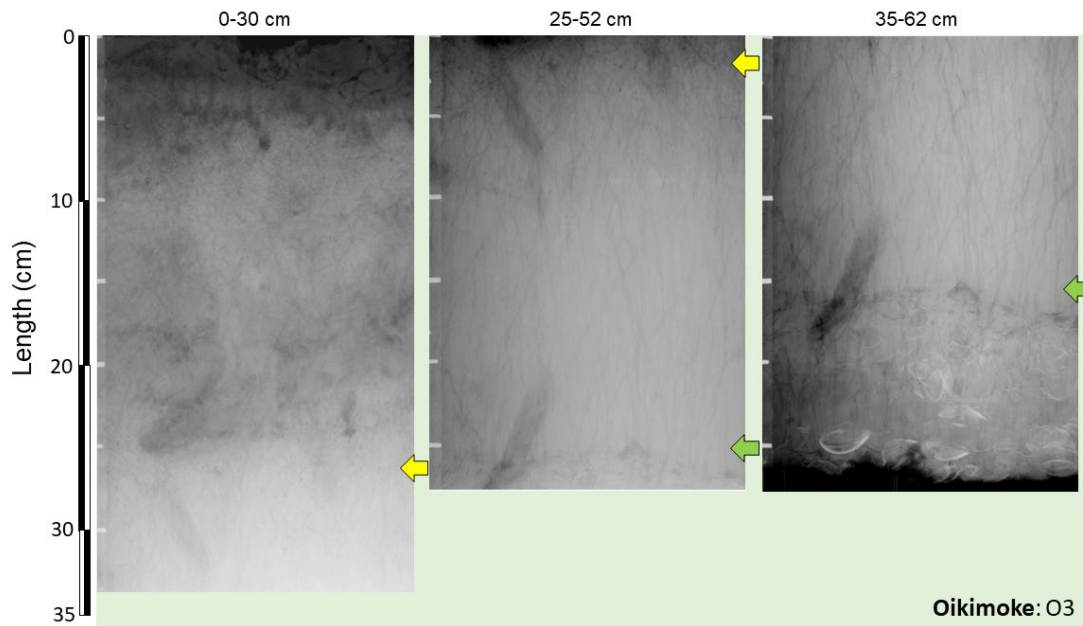


**Figure 3-17: Core O3, Oikimoke Estuary. X-radiograph of salt marsh core (0-62 cm).** These x-radiographs have been inverted so that relatively high-density objects appear white (e.g., shell valves) and low-density materials such as muds or organic material appear as darker areas. The x-radiographs represent core sections up to 35-cm long, with the depth intervals indicated the top of each image. The coloured arrows indicate matching positions (i.e., depth in core) in each x-radiograph.

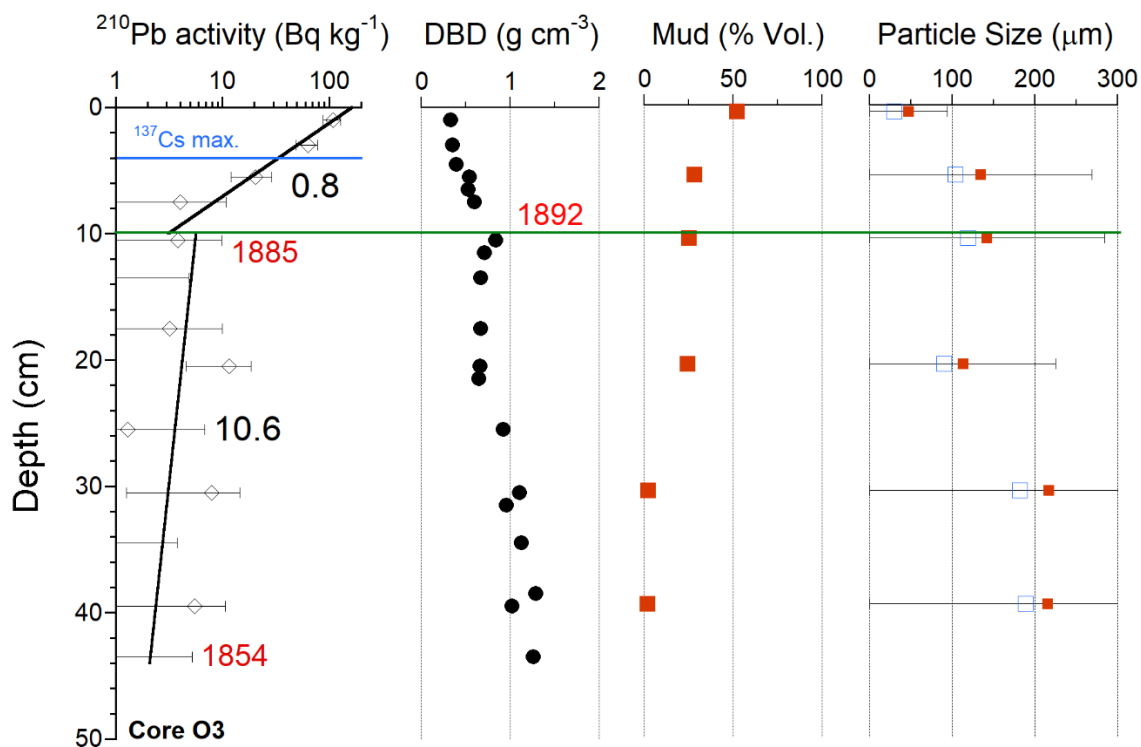


**Figure 3-18: Core O3 (Oikimoke Estuary) - ages of sediment layers, sediment accumulation rates (SAR), and sediment properties.** Left to right: Excess  $^{210}\text{Pb}$  activity profiles with 95% confidence intervals shown. Time-averaged SAR ( $\text{mm yr}^{-1}$ , black text) derived from regression fit ( $r^2 = 0.93$  [0–10 cm],  $r^2 = 0.12$  [10–44 cm]) to natural log-transformed excess  $^{210}\text{Pb}$  data. Calculated age at the base of activity profile is shown in red text. Sediment dry bulk density profile (DBD,  $\text{g cm}^{-3}$ ). Mud % by particle volume. Mean (closed square) with standard deviation and median particle size (microns,  $\mu\text{m}$ ).

Radiocarbon dating of three cockle shell valves (*Austrovenus stutchburyi*) from three different individuals preserved in sediment near the base of the site O3 Perspex-tray core (61–68 cm depth range) provided consistent ages (Table 3-1) with 95% probability range of calibrated  $^{14}\text{C}$  ages are 6,370-6,820 cal. yr BP and yielded a time-average SAR of 0.03–0.04  $\text{mm yr}^{-1}$  below the excess  $^{210}\text{Pb}$  layer (i.e., pre-1850s).

## 3.2 Organic Carbon

### 3.2.1 TOC Profiles

Total organic carbon (%) profiles for the Katikati, Rereatukahia and Oikimoke salt marshes are presented in Figure 3-19, Figure 3-20 and Figure 3-21 respectively. The figures include results for the sub-set of samples (one-third of ~180 total) where both LOI% and TOC% were measured to develop a regression relationship to estimate TOC% from LOI% in all the remaining samples. In general, there was very good agreement between the measured and estimated TOC% values that reflects the strong correlation of determination of the LOI-TOC regression ( $r^2 = 0.87$ ,  $P < 0.001$ ).

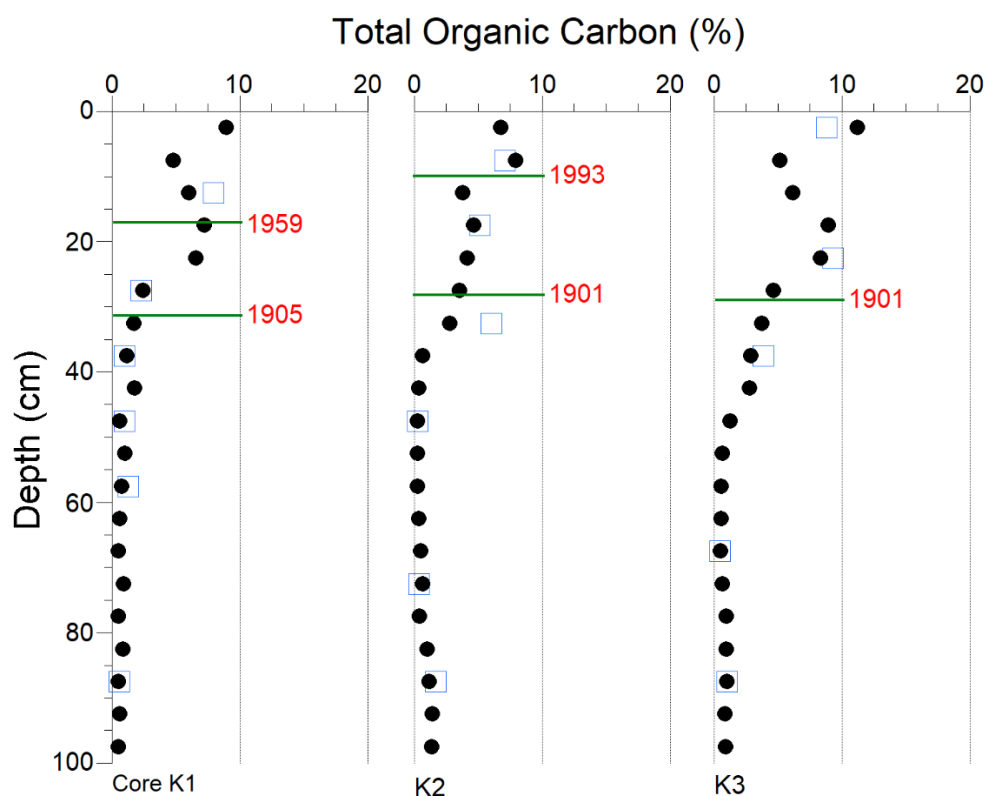


**Figure 3-19: Katikati estuary salt marsh cores K1 –K3. Total organic carbon (TOC%) profiles to 100 cm depth.** Sediment samples analysed in 5-cm depth increments. TOC% estimated from the LOI-TOC regression relationship (circles) (Figure 2-2) and measured TOC% values for selected samples (squares). Estimated  $^{210}\text{Pb}$  sediment ages (years Common Era [CE]) at base of excess  $^{210}\text{Pb}$  profile (bottom value) and at peak sediment dry bulk density (top value).

In the Katikati salt marsh, the TOC% profiles to 100-cm depth show that TOC values are typically < 1% prior the early-1900s. Organic carbon content in core K1 begins in  $^{210}\text{Pb}$  year 1905 and earlier and 10-cm further downcore in K2 and K3 (Figure 3-19). The timing of the shift from low-TOC (<1 %) to high-TOC in the Rerearukahia salt marsh is well constrained by  $^{210}\text{Pb}$  dating, occurring in the 1860–1880s in cores R2 and R3 (Figure 3-20). In the Oikimoke salt marsh the increase in TOC also occurs in the mid–late-1800s (Figure 3-21). Radiocarbon dating of cockle shell at ~65-cm depth (cores O1 and O3, 6,400–6,800 years B.P.) and  $^{14}\text{C}$  SAR ( $0.04 \text{ mm yr}^{-1}$ ) shows that sediment and organic carbon accumulated at a vanishingly small rate in this estuary prior to the mid-1800s. Organic carbon at the base of these cores was likely deposited several thousand years earlier.

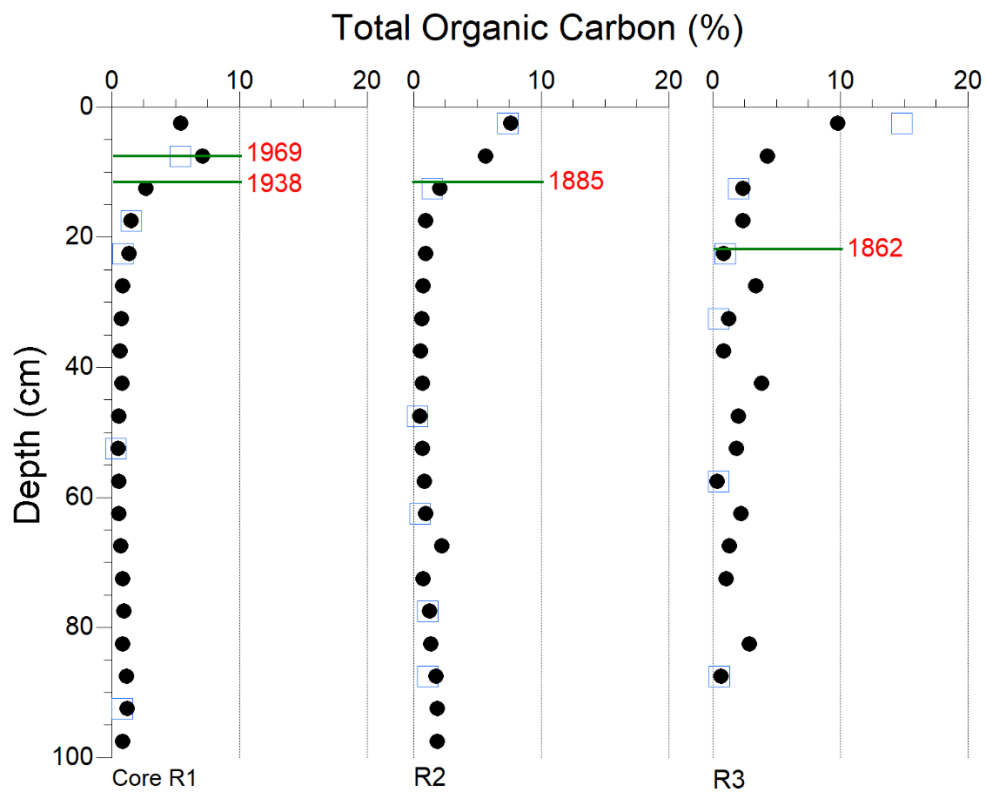


**Figure 3-20: Rereatukahia estuary salt marsh cores R1–R3. Total organic carbon (TOC%) profiles to 100 cm depth.** Sediment samples analysed in 5-cm depth increments. TOC% estimated from the LOI-TOC regression relationship (circles) (Figure 2-2) and measured TOC% values for selected samples (squares). Estimated  $^{210}\text{Pb}$  sediment ages (years Common Era [CE]) at base of excess  $^{210}\text{Pb}$  profile (bottom value) and at peak sediment dry bulk density (top value).

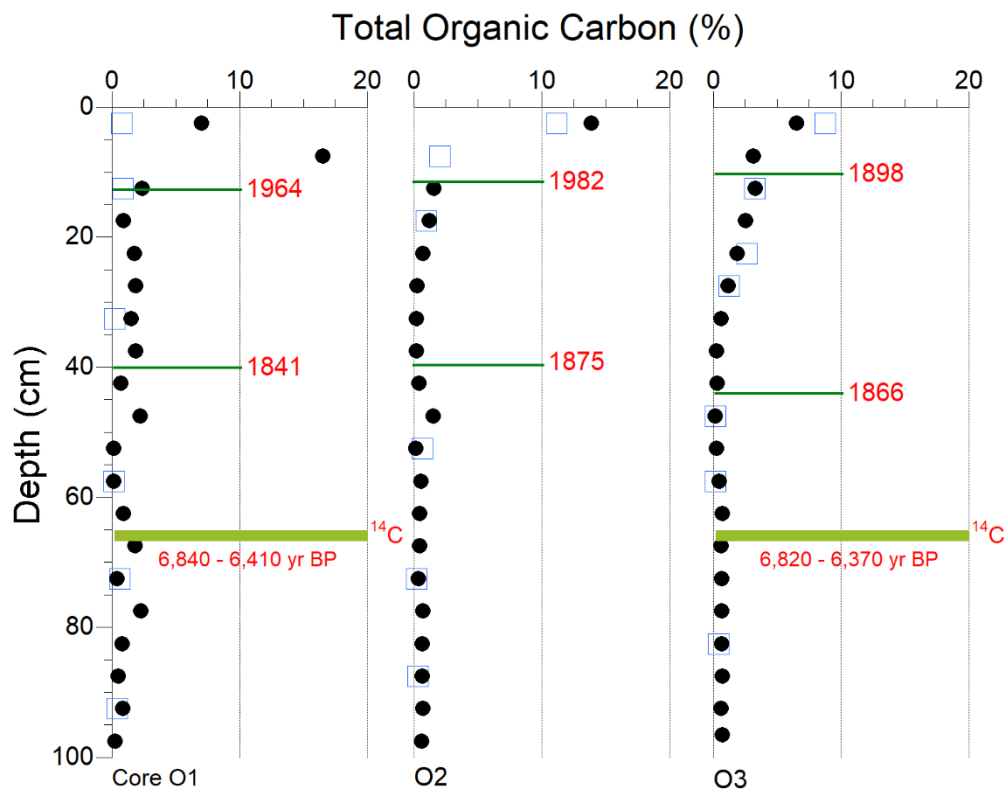


**Figure 3-21: Oikimoke estuary salt marsh cores O1 –O3. Total organic carbon (TOC%) profiles to 100 cm depth.** Sediment samples analysed in 5-cm depth increments. TOC% estimated from the LOI-TOC regression relationship (circles) (Figure 2-2) and measured TOC% values for selected samples (squares). Estimated  $^{210}\text{Pb}$  sediment ages (years Common Era [CE]) at base of excess  $^{210}\text{Pb}$  profile (bottom value) and at peak sediment dry-bulk density (top value). AMS  $^{14}\text{C}$  age ranges (95% probability) for cockle shell sampled from cores O1 and O3.

Figure 3-22 and Figure 3-23 present cumulative organic carbon (Cum-OC, downcore) curves ( $\text{g cm}^{-2}$  and % of total a 100-cm depth) for each of the three salt marshes. The Katikati salt marsh Cum-OC curves are most uniform in terms of rate of accumulation and total areal organic carbon content, although core K3 (most seaward site) has a slightly higher rate of accumulation ( $1.2\text{--}1.4 \text{ g cm}^{-2}$ ). The Rereatakahia and Oikimoke salt marshes display high variability, largely due to substantially higher rates of organic carbon accumulation at the most seaward core sites (i.e., R3, O3) (Figure 2-1). The Cum-OC% profiles show that 50% of the total organic carbon is sequestered in top 20–37-cm of sediment column, except for core R2 (50%, 50-cm) (Figure 3-23).

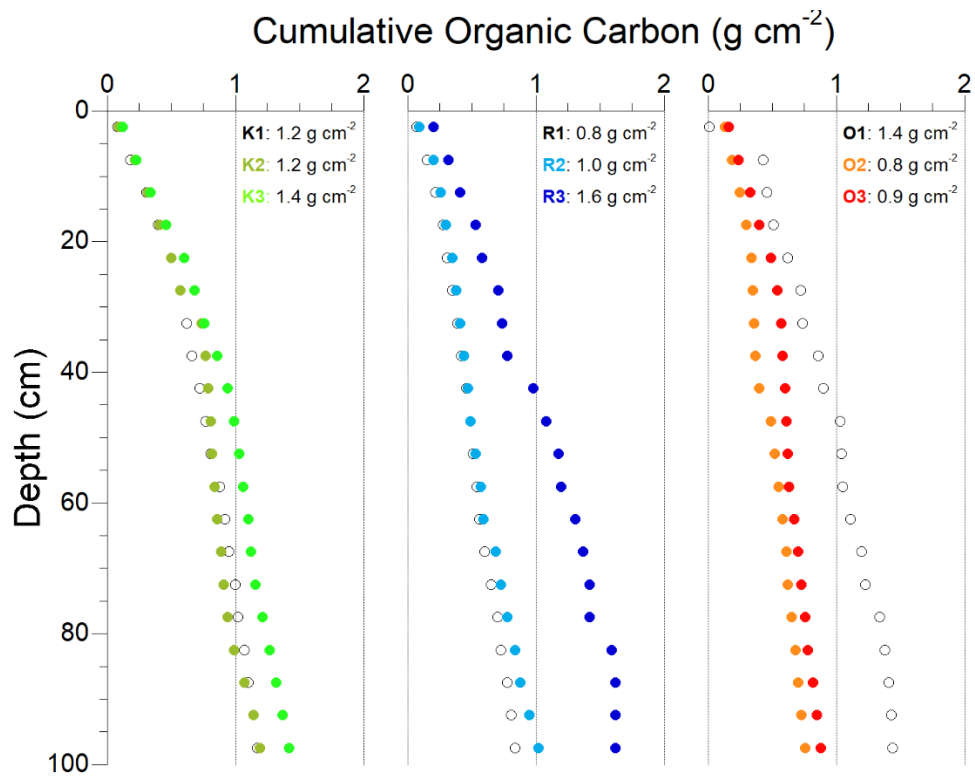


**Figure 3-22: Cumulative organic carbon (g cm<sup>-2</sup>) with depth from sediment surface.** Left to right: Katikati, Rereatukahia and Oikimoke Estuary core sites. Values are total organic carbon in 95 to 100 cm depth increment.

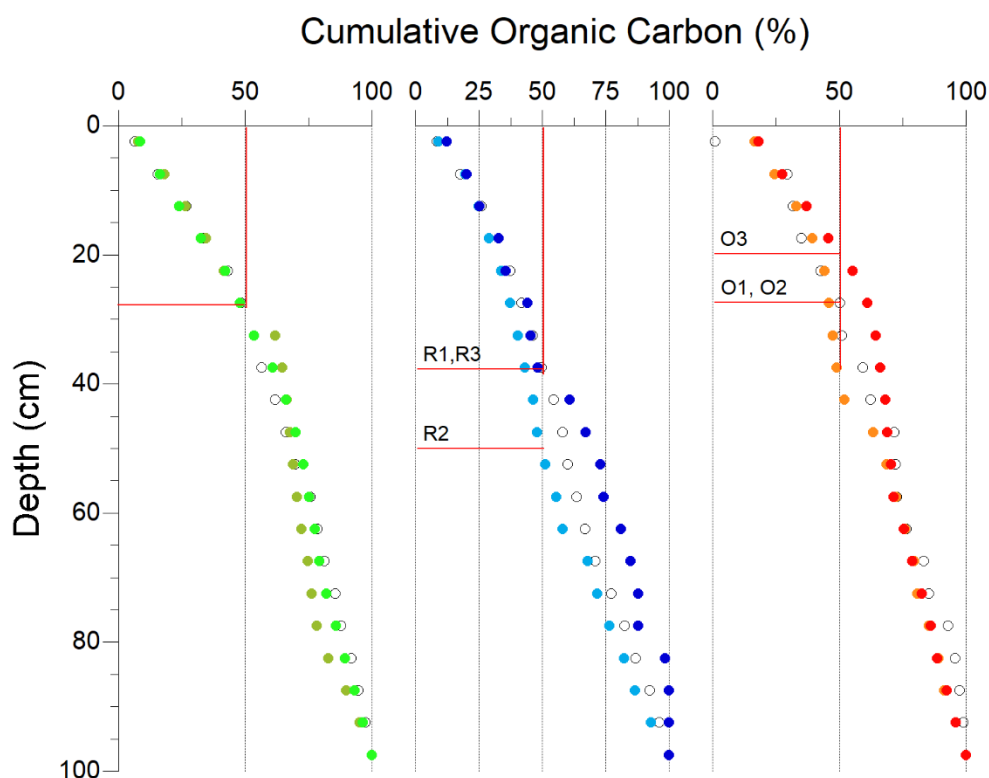


**Figure 3-23: Cumulative organic carbon (%) with depth from sediment surface.** Left to right: Katikati, Rereatukahia and Oikimoke Estuary core sites. The sediment depths at the 50<sup>th</sup> percentile carbon stock value indicated.

### 3.2.2 Organic carbon inventories and sequestration rates

Table 3-2 summarises organic carbon inventories ( $\text{MgC ha}^{-1}$ ) for the last 100 years ( $\sim 1923\text{--}2023$ ) and to the base of each core in each of the three salt marshes. Organic carbon inventories in the Katikati salt marsh are the largest and most uniform (100 yr inventory, mean: 58, range 57–60  $\text{MgC ha}^{-1}$ ) whereas the inventories for the Rereatukahia (mean: 28, range 20–41  $\text{MgC ha}^{-1}$ ) and Oikimoke (mean: 40, range 24–62  $\text{MgC ha}^{-1}$ ) salt marshes are smaller and more variable. Comparison of these 100-year inventories with the entire 100-cm core, spanning more than  $\sim 6,500$  years (e.g., Oikimoke  $^{14}\text{C}$  ages) enables the relative contribution of the modern era to be quantified. In the Katikati salt marsh, 46% of the organic carbon, on average, has been sequestered in the last 100 years. Organic carbon sequestration over the last 100 years in the Rereatukahia and Oikimoke salt marshes accounts for 24% and 39% respectively of the total inventory.

**Table 3-2: Organic carbon inventory in mega-grams per hectare (MgC ha<sup>-1</sup>) in salt marsh sediment cores.**  
Mg = 1 tonne. Calculation methods described in Section 2.5.

| Core                | To 100 cm depth<br>(MgC ha <sup>-1</sup> ) | Base of <sup>210</sup> Pb profile | <sup>210</sup> Pb year<br>at base | 100 years<br>(1920s – 1923) |
|---------------------|--|-----------------------------------|-----------------------------------|-----------------------------|
| <b>Katikati</b>     |  |                                   |                                   |                             |
| K1                  | 116.6                                      | 62.4                              | 1905                              | 56.7                        |
| K2                  | 119.4                                      | 73.7                              | 1901                              | 57.3                        |
| K3                  | 141.6                                      | 67.9                              | 1901                              | 59.7                        |
| Mean                | 125.9                                      | 68.0                              |                                   | 57.9                        |
| Median              | 119.4                                      | 67.9                              |                                   | 57.3                        |
| Std Dev             | 13.7                                       | 5.6                               |                                   | 1.6                         |
| <b>Rereatukahia</b> |  |                                   |                                   |                             |
| R1                  | 84.3                                       | 22.0                              | 1938                              | 22.0                        |
| R2                  | 102.2                                      | 25.5                              | 1885                              | 20.1                        |
| R3                  | 161.6                                      | 71.5                              | 1861                              | 40.6                        |
| Mean                | 116.0                                      | 39.7                              |                                   | 27.6                        |
| Median              | 102.2                                      | 25.5                              |                                   | 22.0                        |
| Std Dev             | 40.5                                       | 27.6                              |                                   | 11.4                        |
| <b>Oikimoke</b>     |  |                                   |                                   |                             |
| O1                  | 144.4                                      | 85.7                              | 1842                              | 61.6                        |
| O2                  | 76.4                                       | 37.4                              | 1875                              | 35.0                        |
| O3                  | 88.2                                       | 32.8                              | 1854                              | 24.2                        |
| Mean                | 103.0                                      | 51.9                              |                                   | 40.3                        |
| Median              | 88.2                                       | 37.4                              |                                   | 35.0                        |
| Std Dev             | 36.3                                       | 29.3                              |                                   | 19.3                        |

Table 3-3 summarises organic carbon sequestration rates ( $\text{MgC ha}^{-1} \text{ yr}^{-1}$ ) for the last 100 years (~1923–2023) based  $^{210}\text{Pb}$  dating of the cores analysed from each of the three salt marshes. The 100-year sequestration rates in the Katikati salt marsh are the largest and most uniform (mean: 53, range 51–55  $\text{MgC ha}^{-1} \text{ yr}^{-1}$ ) whereas the inventories for the Rereatukahia (mean: 0.25, range 0.16–0.41  $\text{MgC ha}^{-1} \text{ yr}^{-1}$ ) and Oikimoke (mean: 0.36, range 0.19–0.59  $\text{MgC ha}^{-1} \text{ yr}^{-1}$ ) salt marshes are smaller and more variable.

**Table 3-3: Salt marsh organic carbon sequestration rates, mega-grams per hectare per year ( $\text{MgC ha}^{-1} \text{ yr}^{-1}$ ) over the 100 years prior to 2023.** Estimates based on TOC% and dry bulk density profiles data and  $^{210}\text{Pb}$  dating. Averages with standard deviation values (in brackets).

| Core                | Base of $^{210}\text{Pb}$ profile | $^{210}\text{Pb}$ year at base | 100 years (1920s – 1923) |
|---------------------|-----------------------------------|--------------------------------|--------------------------|
| <b>Katikati</b>     |                                   |                                |                          |
| K1                  | 0.51 (0.15)                       | 1905                           | 0.54 (0.13)              |
| K2                  | 0.56 (0.16)                       | 1901                           | 0.51 (0.09)              |
| K3                  | 0.52 (0.09)                       | 1901                           | 0.55 (0.05)              |
| <b>Rereatukahia</b> |                                   |                                |                          |
| R1                  | 0.19 (0.01)                       | 1938                           | 0.18 (0.02)              |
| R2                  | 0.14 (0.04)                       | 1885                           | 0.16 (0.02)              |
| R3                  | 0.36 (0.16)                       | 1861                           | 0.41 (0.19)              |
| <b>Oikimoke</b>     |                                   |                                |                          |
| O1                  | 0.49 (0.54)                       | 1842                           | 0.59 (0.62)              |
| O2                  | 0.26 (0.23)                       | 1875                           | 0.30 (0.22)              |
| O3                  | 0.17 (0.07)                       | 1854                           | 0.19 (0.09)              |

## Background organic carbon sequestration rates

Background organic carbon sequestration rates were calculated for cores O1 and O3 for the ~6,300–6,700-year period prior to the mid-1800s (i.e., below excess  $^{210}\text{Pb}$  profile). Background sequestration rates were calculated using the time-averaged  $^{14}\text{C}$  SAR ( $0.04 \text{ mm yr}^{-1}$ , Table 3-1). These calculations yielded organic carbon sequestration rates of  $0.0061 \pm 0.0049$  (SD) and  $0.0013 \pm 0.0009$   $\text{MgC ha}^{-1} \text{ yr}^{-1}$  for cores O1 and O3 respectively. These background organic carbon sequestration rates represent 1% (O1) and 0.7% (O3) of the rates over the last 100 years (i.e., to 1923). These relatively low values

largely reflect the low background SAR that are typically less than 2% of modern values, and to a lesser extent, low background TOC values (i.e., < 1%) by comparison with the last 100 years.

It is also possible that these background sequestration rates are over-estimates. The x-radiographs indicate that fine salt marsh roots penetrating deeply into older sediment, to the base of the cores (i.e., 60 cm) (Figure 3-13, Figure 3-17). The salt marshes these Tauranga Harbour estuaries are also likely to have only developed following formation of upper-intertidal habitats during the historical period of catchment deforestation and elevated soil erosion (i.e., within last ~200 years). In that case, this historical-era salt marsh carbon may contribute a substantial fraction of the calculated background sequestration rate.

## 4 Discussion

### 4.1 Sediment accumulation rates

The apparent  $^{210}\text{Pb}$  SAR measured in the salt marsh sediment reflects differences in conditions and resulting sedimentation patterns in the Katikati, Rereatukahia and Oikimoke Estuaries. Key factors controlling local sediment accumulation rate include hydroperiod (i.e., duration of tidal submergence), sediment settling flux and resuspension (i.e., by tidal currents and wind waves) that controls net deposition. An earlier study commissioned by BoPRC quantified sediment accumulation rates on unvegetated intertidal flats in three other estuaries fringing the western shore of Tauranga Harbour: Taupiro, Waikareo and Waimapu (Huiarama et al., 2021) (Figure 4-1).

Comparison of these data show that  $^{210}\text{Pb}$  sediment accumulation rates have been substantially higher on the intertidal flats (averages: 4–9.7 mm yr<sup>-1</sup>) than in the salt marshes (1.1–2.6 mm yr<sup>-1</sup>) (Table 4-1).  $^{210}\text{Pb}$  record lengths on the intertidal flats have, however, been shorter (i.e., no earlier than 1940 to 1990s) in comparison to the salt marshes (i.e., 1840s to 1930s). These spatial differences in SAR between habitat types are consistent with increased hydroperiod on the intertidal flats relative to the saltmarshes growing in the upper intertidal zone. Typically, the salt marshes will be inundated for short periods during spring-hide tides and storm tides when the potential for suspended mineral sediment to be delivered to the marsh exists. However, sediment deposited in the salt marshes is unlikely to be remobilised by waves or tidal currents due to effective dampening by the salt marsh plants. Consequently, the salt marshes preserve a more complete and longer record of the systems' sedimentation history.

On the intertidal flats, wave-driven sediment resuspension, fine-sediment winnowing, and transport will regularly disturb the deposited sediment (Green and Coco, 2014) so that the sedimentation record is less complete. Once resuspended, these fine sediments are transported by wind-driven currents and ebb tides into channels. In turn these sediments are either exported to the sea or deposited in salt marsh and mangrove where quiescent conditions favour settling out of suspension and deposition. The low mud content of surficial sediment observed at the intertidal core sites is consistent with this fine sediment winnowing process (Huirama et al., 2021).

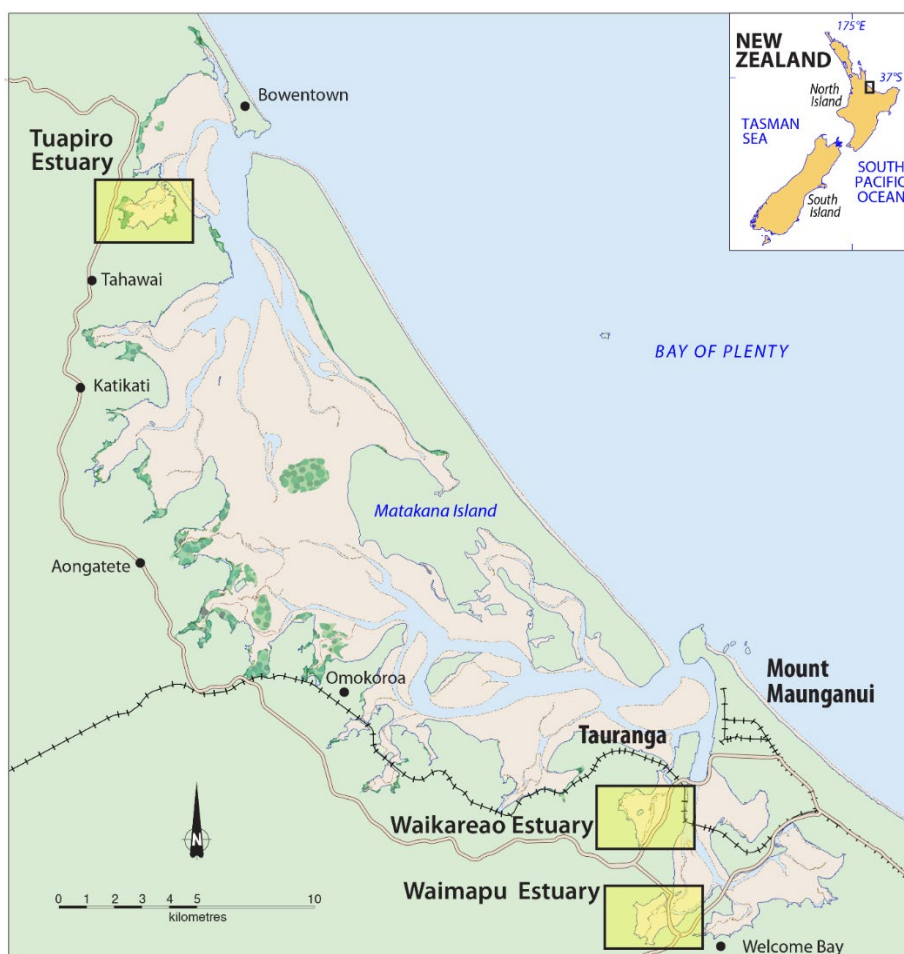


**Figure 4-1: Location of Tauranga Harbour estuaries in earlier study where sediment accumulation rates quantified (Huirama et al., 2021).**

$^{210}\text{Pb}$  SAR determined from intertidal sediment cores collected at three sites per estuary.

### Long-term changes in sediment accumulation rates

Radiocarbon and  $^{210}\text{Pb}$  dating of the Oikimoke salt marsh cores O1 and O3 show that sediment has accumulated extremely slowly in the estuary over most of its history. Background SAR averaged only  $0.04 \text{ mm yr}^{-1}$  from around 6,500 years before present (BP = 1950) until the mid-1800s when SAR substantially increased, averaging 20 to 50-fold over the last 130–170 years. These findings are consistent with temporal changes in SAR observed in the Tuapiro, Waikareo and Waimapu estuaries. Huirama et al., (2021) found that  $^{210}\text{Pb}$  SAR measured in these estuaries were at least fifty-fold higher than background SAR over the previous ~7,000 years (i.e.,  $0.05 \text{ mm yr}^{-1}$ ), calculated from radiocarbon dating of cockle shell. An order of magnitude (ten-fold) increase in SAR above background values is more typical of NZ estuaries (e.g., Thrush et al., 2004; Hunt, 2019 and references therein). Stokes (2010) obtained a similar  $^{14}\text{C}$  SAR of  $0.1 \text{ mm yr}^{-1}$  (cockle shell) for a core from Waikaraka Estuary (Tauranga Harbour). These background SAR values from Tauranga Harbour estuaries are some of the lowest measured to date in NZ estuaries (range:  $0.04\text{--}1.2 \text{ mm yr}^{-1}$ , Huirama et al., 2021).

In both studies, we identified a cockle shell layer that occurs at 60–70-cm depth in several estuaries, suggesting that cockle may have inhabited substantial areas of the harbour in the mid-intertidal zone, 6,600–7000 years ago.

In addition to what these cockle beds could tell us about the pre-historic ecology of these estuaries, they have proven to be an important resource for quantifying background sediment accumulation rates in Tauranga Harbour.

**Table 4-1: Summary of  $^{210}\text{Pb}$  SAR ( $\text{mm yr}^{-1}$ ) for Tauranga Harbour salt marshes and comparison with unvegetated intertidal flats.** Time period is the estimated year at the base of the regression relationship fitted to the excess  $^{210}\text{Pb}$  profile regression profile.

| Estuary  | $^{210}\text{Pb}$ SAR & Time Period | Estuary             | $^{210}\text{Pb}$ SAR & Time Period | Estuary         | $^{210}\text{Pb}$ SAR & Time Period |
|--|-------------------------------------|---------------------|-------------------------------------|-----------------|-------------------------------------|
| <b>Katikati</b>  |                                     | <b>Rereatukahia</b> |                                     | <b>Oikimoke</b> |                                     |
| K1   | 2.8 (1905)                          | R1                  | 1.3 (1938)                          | O1              | 2.2 (1842)                          |
| K2   | 2.7 (1901)                          | R2                  | 0.8 (1885)                          | O2              | 2.7 (1875)                          |
| K3   | 2.3 (1901)                          | R3                  | 1.3 (1861)                          | O3              | 0.8 (1885)                          |
| Mean   | 2.6                                 |                     | 1.1                                 |                 | 1.9                                 |
| Std Deviation  | 0.27                                |                     | 0.29                                |                 | 0.98                                |
| $^{210}\text{Pb}$ SAR data for intertidal flats, Tauranga Harbour estuaries (Huirama et al., 2021) |                                     |                     |                                     |                 |                                     |
| <b>Taupiro</b>   |                                     | <b>Waikareao</b>    |                                     | <b>Waimapu</b>  |                                     |
| P54  | 5.4 (1971)                          | P16                 | 6.4 (1972)                          | P12             | 2.6 (1911)                          |
| P55  | 4.5 (1940)                          | P17                 | 7.5 (1966)                          | P13             | 3.2 (1954)                          |
| P56  | 5.6 (1956)                          | P21                 | 15.1 (1993)                         | P14             | 6.2 (1994)                          |
| Mean   | 5.2                                 |                     | 9.7                                 |                 | 4                                   |
| Std Deviation  | 0.59                                |                     | 4.7                                 |                 | 1.9                                 |

## 4.2 Organic carbon sequestration

### 4.2.1 Combined LOI – TOC Methodology

Total organic carbon (%) was determined in the present study using a hybrid approach – direct measurement of a sub-set of samples (i.e., ~30%, Elemental Analyser) and LOI measurements of all samples. TOC was estimated for the remaining 70% of samples by linear regression ( $\text{TOC}\% = (0.36 * \text{LOI}\%) - 0.45$ ,  $r^2 = 0.87$ ). The measurement of LOI of relatively large sub-samples (i.e., 10-20 g) compensated for potential inaccuracy that could arise from direct TOC analysis of small sub-samples alone (i.e., 10-30 mg) taken from heterogenous sediment mixtures. The slope of our LOI-TOC relationship (0.36) is smaller but similar to TOC/LOI ratios (0.4–0.52) reported for young salt marshes and salt marshes with strong contributions of carbon from terrigenous and/or estuarine sources (e.g., Craft et al., 1991; Ouyang and Lee, 2020).

#### 4.2.2 Organic carbon sequestration in Tauranga Harbour salt marshes

Organic carbon inventories ( $\text{MgC ha}^{-1}$ ) in the Tauranga Harbour salt marshes were calculated for the 100 years prior to sediment core collection (i.e., 1923–2023) and for the entire core to 100-cm depth and spanning the last 6,500 years or more. Organic carbon inventories over the last 100 years (~1923–2023) were in the range 20 to 62  $\text{MgC ha}^{-1}$  and 76–162  $\text{MgC ha}^{-1}$ , for the entire sediment column to 100-cm depth. These Core-100-cm values are substantially higher than the organic carbon inventories for New Zealand salt marshes cited by Ross et al. (2023, 38–57  $\text{MgC ha}^{-1}$ ) from previous studies. In the present study, organic carbon sequestration rates over the last 100 years displayed substantial variability (range: 0.19–0.59  $\text{MgC ha}^{-1} \text{ yr}^{-1}$ ) that largely reflected local sediment accumulation rate. The organic carbon sequestration rate cited by Ross et al, (2023) of 0.46  $\text{MgC ha}^{-1} \text{ yr}^{-1}$  (i.e., their Table 1, converting from  $\text{CO}_2/3.67 = \text{C}$ ) is within the range of values calculated here for Tauranga Harbour salt marshes.

Background organic carbon sequestration rates were also calculated (Oikimoke cores O1, O3) for the ~6,300–6,700-year period prior to the mid-1800s (i.e., below excess  $^{210}\text{Pb}$  layer). A key finding is that background sequestration rates (0.0061, 0.0013  $\text{MgC ha}^{-1} \text{ yr}^{-1}$ ) represent no more than 1% of sequestration rates over the last 100 years. These relatively low values largely reflect the low background SAR that are typically less than 2% of modern values, and to a lesser extent, low background TOC values (i.e., < 1%) by comparison with the last 100 years. It is also possible that background sequestration rates are over-estimated due to salt marsh roots penetrating older sediment below the excess  $^{210}\text{Pb}$  layer.

The key objective of this study was to evaluate the carbon storage potential of intact salt marsh wetlands. Historical aerial photographs show that the salt marshes sampled in this study pre-date the 1940s. The Oikimoke salt marsh appears to be the most recent, with a 1943 image (Figure 1-8) indicating that this former farm paddock was in the process of being colonised by saltmarsh and thus the Katikati and Rereatukahia salt marshes pre-date Oikimoke. Organic carbon inventories and sequestration rates do not however reflect this. In particular, 100-year inventories and sequestration rates for Oikimoke ( $40 \pm 19 \text{ MgC ha}^{-1}$ , 0.19–0.59  $\text{MgC ha}^{-1} \text{ yr}^{-1}$ ) are within the range of values for Katikati ( $58 \pm 2(\text{SD}) \text{ MgC ha}^{-1}$ , 0.51–0.55  $\text{MgC ha}^{-1} \text{ yr}^{-1}$ ) and Rereatukahia ( $28 \pm 11 \text{ MgC ha}^{-1}$ , 0.16–0.41  $\text{MgC ha}^{-1} \text{ yr}^{-1}$ ).

## 5 Acknowledgements

We thank Shay Dean, Heather MacKenzie, Darryn Hitchcock, and Tom Harding (BOPRC Environmental Science Team) for supporting information and assistance in the field. Gamma spectrometry for  $^{210}\text{Pb}$  and  $^{137}\text{Cs}$  dating was undertaken by the ESR National Centre for Radiation Science (Drs Levi Bourke and Oksana Golovko). We thank Max Oulton Graphics for preparation of maps. Finally, we thank Dr Phoebe Stewart-Sinclair (NIWA Marine Ecology Group) for reviewing this report.

## 6 References

- BoPRC (2012) Te Rereatukahia Sub-catchment Action Plan: 8.  
<https://atlas.boprc.govt.nz/api/v1/edms/document/A3888899/content>
- Berthelsen, A., Walker, L., Skilton, J., Chamberose, D., Flewitt, S., Waters, S., Asquith, E., Butler, J., Kettles, H. (2023) Sediment organic carbon stocks in coastal blue carbon habitats: pilot study for Te Tau Ihu. Prepared for Tasman Environmental Trust. Cawthron Report. 3867: 19 plus appendices.
- Booker, D.J., Whitehead, A.L. (2017) NZ River Maps: An interactive tool for mapping predicted freshwater variables across New Zealand. [accessed 28 March 2018] <https://shiny.niwa.co.nz/nzrivermaps/>.
- Briggs, R.M., Hall, G.J., Harmsworth, G.R., Hollis, A.G., Houghton, B.F., Hughes, G.R., Morgan, M.D., Whitbread-Edwards, A.R. (1996) *Geology of the Tauranga area*. Hamilton, University of Waikato.
- Burggraaf, S., Langdon, A.G., Wilkins, A.L. (1994) Organochlorine contaminants in sediments of the Tauranga Harbour, New Zealand. *New Zealand Journal of Marine and Freshwater Research*, 28(3): 291-298.
- Bulmer, R.H., Stephenson, F., Jones, H.F., Townsend, M., Hillman, J.R., Schwendenmann, L., Lundquist, C.J. (2020) Blue carbon stocks and cross habitat subsidies. *Frontiers in Marine Science* 7: 380, doi: 10.3389/fmars.2020.00380
- Chappell, P.R. (2013) The climate and weather of Bay of Plenty. *NIWA Science and Technology Series* 62: 40.
- Clark, K., Howarth, J., Litchfield, N., Cochran, U., Turnbull, J., Dowling, L., Howell, A., Berryman, K., Wolfe, F. (2019) Geological evidence for past large earthquakes and tsunamis along the Hikurangi subduction margin, New Zealand. *Marine Geology*, 412: 139-172.
- Craft, C., Seneca, E.D., Broome, S.W. (1991) Loss on ignition and Kjeldahl digestion for estimating organic carbon and total nitrogen in estuarine marsh soils: calibration with dry combustion. *Estuaries*, 14:175–179.
- Duarte, C.M., Losada, I.J., Hendriks, I.E., Mazarrasa, I., Marba, N. (2013) The role of coastal plant communities for climate change mitigation and adaptation. *Nature Climate Change*, 3: 961–968, doi:10.1038/nclimate1970
- Hancock, N., Hume, T.M., Swales, A. (2009) Tauranga harbour sediment study: harbour bed sediments. *NIWA Client Report* HAM2008-123.
- Hicks, D.M., Hume, T.M. (1997) Determining sand volumes and bathymetric change on an ebb-tidal delta. *Journal of Coastal Research*: 407-416.

- Hicks, D.M., Shankar, U., Mc Kerchar, A.I., Basher, L., Jessen, M., Lynn, I., Page, M. (2011) Suspended sediment yields from New Zealand rivers. *Journal of Hydrology (New Zealand)* 50(1): 81–142.
- Hogg, A.G., Higham, T.F., Dahm, J. (1998)  $^{14}\text{C}$  dating of modern marine and estuarine shellfish. *Radiocarbon*, 40(2): 975-984.
- Howard, J., Hoyt, S., Isensee, K., Pidgeon, E., Telszewski, M. (eds.) (2014) Coastal Blue Carbon: Methods for assessing carbon stocks and emissions factors in mangroves, tidal salt marshes, and seagrass meadows. Conservation International, Intergovernmental Oceanographic Commission of UNESCO, International Union for Conservation of Nature. Arlington, Virginia, USA.
- Huirama, M., Swales A., Olsen G., Ovenden R. (2021) Sediment accumulation rates in Waimapu, Waikareao and Tuapiro Estuaries, Tauranga Harbour. *NIWA Client Report 2021255HN*: 75.
- Johnson, B.J., Moore, K.A., Lehmann, C., Bohlen, C. & Brown, T.A. (2007) Middle to late Holocene fluctuations of C3 and C4 vegetation in a Northern New England Salt Marsh, Sprague Marsh, Phippsburg Maine. *Organic Geochemistry*, 38, 394–403.
- Lawton, R., Conroy, E. (2019) *Tauranga Moana: State of the environment report 2019*. Bay of Plenty Regional Council.
- Lo Iacono, C., Mateo, M.A., Gràcia, E., Guasch, L., Carbonell, R., Serrano, L. et al. (2008) Very high-resolution seismo-acoustic imaging of seagrass meadows (Mediterranean Sea): Implications for carbon sink estimates. *Geophysical Research Letters*, 35.
- Lovelock, C.E., Duarte, C.M. (2019) Dimensions of Blue Carbon and emerging perspectives. *Biology Letters*, 15: 20180781, <http://dx.doi.org/10.1098/rsbl.2018.0781>
- MacPherson, D., Fox, B.R., de Lange, W.P. (2017) Holocene evolution of the southern Tauranga Harbour. *New Zealand Journal of Geology and Geophysics*, 60(4): 392-409.
- Matthews, K.M. (1989) Radioactive fallout in the South Pacific: a history. Part 1: Deposition in New Zealand. *Report NRL1989/2*, National Radiation Laboratory, Christchurch, New Zealand.
- Miller, A.J., Kuehl, S.A. (2010) Shelf sedimentation on a tectonically active margin: a modern sediment budget for Poverty continental shelf, New Zealand. *Marine Geology*, 270(1-4): 175–187.
- McKee, K.L., Cahoon, D.R. & Feller, I.C. (2007) Caribbean mangroves adjust to rising sea level through biotic controls on change in soil elevation. *Global Ecology and Biogeography*, 16: 545–556.
- Ministry for the Environment (2022) New Zealand’s greenhouse gas inventory 1990 – 2020. Wellington: Ministry for the Environment.

- Ministry for the Environment, Carbon tables for post-1989 forest land. [accessed 2023 Mar 10]. [https://legislation.govt.nz/regulation/public/2008/0355/latest/DLM1633733.html?search=ts\\_act%40bill%40regulation%40deemedreg\\_climate+change\\_resel\\_25\\_a&p=1](https://legislation.govt.nz/regulation/public/2008/0355/latest/DLM1633733.html?search=ts_act%40bill%40regulation%40deemedreg_climate+change_resel_25_a&p=1).
- Mook, D.H., Hoskin, C.M. (1982) Organic determinations by ignition: caution advised. *Estuarine, Coastal and Shelf Science*, 15: 697–699.
- Morrisey, D.J., Swales, A., Dittmann, S., Morrison, M.A., Lovelock, C.E., Beard, C.M. (2010) Ecology and Management of Temperate Mangroves. *Oceanography and Marine Biology: An Annual Review* 48: 43–160.
- Ouyang X., Lee S.Y. (2020) Improved estimates on global carbon stock and carbon pools in tidal wetlands. *Nature Communications* 11: 317, doi.org/10.1038/s41467-019-14120-2
- Petchey, F., Anderson, A., Zondervan, A., Ulm, S., Hogg, A. (2008) New marine  $\Delta R$  values for the South Pacific subtropical gyre region. *Radiocarbon*, 50(3): 373-397.
- Ritchie, J.C., McHenry, J.R. (1990) Application of radioactive fallout cesium-137 for measuring soil erosion and sediment accumulation rates and patterns: A review. *Journal of Environmental Quality*, 19(2): 215-233.
- Robbins, J.A., Edgington, D.N. (1975) Determination of recent sedimentation rates in Lake Michigan using Pb-210 and Cs-137. *Geochimica et Cosmochimica Acta*, 39(3): 285-304.
- Ross, F.W.R., Clark, D.E., Albot, O., Berthelsen, A., Bulmer, R., Crawshaw, J., Macreadie, P.I. (2023) A preliminary estimate of the contribution of coastal blue carbon to climate change mitigation in New Zealand. *New Zealand Journal of Marine and Freshwater Research*, doi:10.1080/00288330.2023.2245770
- TNLET (1994). Manual of Analytical Methods Vol 1, Method 01-1090, Ver. 1, 1994. The National Laboratory for Environmental Testing, Burlington, Ontario, Canada.
- Serrano, O., Lavery, P.S., Rozaimi, M. & Mateo, M.Á. (2014) Influence of water depth on the carbon sequestration capacity of seagrasses. *Global Biogeochemical Cycles*. DOI: 10.1002/2014GB004872
- Smith, J.N. (2001). Why should we believe  $^{210}\text{Pb}$  geochronologies. *Journal of Environmental Radioactivity*, 55: 121–123.
- Sommerfield, C., Nittrouer, C., Alexander, C. (1999)  $^7\text{Be}$  as a tracer of flood sedimentation on the northern California continental margin. *Continental Shelf Research*, 19(3): 335-361.
- Stokes, D. (2010) *The physical and ecological impacts of mangrove expansion and mangrove removal: Tauranga Harbour, New Zealand*. Doctoral thesis, University of Waikato.
- Swales A., Bentley S.J., Lovelock C.E. (2015) Mangrove-forest evolution in a sediment-rich estuarine system: Opportunists or agents of geomorphic change? *Earth Surface Processes and Landforms*, 40: 1672–1687. doi: 10.1002/esp.3759.

TNLET (1994). Manual of Analytical Methods Vol 1, Method 01-1090, Ver. 1,1994. The National Laboratory for Environmental Testing, Burlington, Ontario, Canada.

Wise, S. (1977) The use of radionuclides  $^{210}\text{Pb}$  and  $^{137}\text{Cs}$  in estimating denudation rates and in soil e/rosion measurement. *Occasional Paper* (7).

## Appendix A Sediment core sites

### Katikati Estuary

| Core Site | Date      | Time (NZST) | NZTM-East | NZTM-North | Comments   |
|-----------|-----------|-------------|-----------|------------|--|
| K1        | 15/5/2023 | 0915        | 1857985   | 5841196    | <b>Vegetation cover dominated by Sea Rush</b> ( <i>Juncus kraussii</i> subsp. <i>australiensis</i> ) with some Oioi ( <i>Apodasmia similis</i> ). Difficulties collecting X-ray core. Thick root mass to penetrate. Repeated twice. Bottom section not good. GPS (Heather) 1857984, 5841197. Site is approx. 125m from tidal channel.                          |
| K2        | 15/5/23   | 1125        | 1858009   | 5841129    | <b>Vegetation cover dominated by Oioi</b> ( <i>A. similis</i> ) with some Sea Rush ( <i>J. kraussii</i> subsp. <i>australiensis</i> ). Difficulties collecting X-ray core. Thick root mass to penetrate. Cores retrieved easily. Site approx. 55m from tidal channel.  |
| K3        | 15/5/23   | 1225        | 1860851   | 5846587    | <b>Vegetation cover dominated by Oioi</b> ( <i>A. similis</i> ) with some Sea Rush ( <i>J. kraussii</i> subsp. <i>australiensis</i> ). Difficulties collecting X-ray core. Thick root mass to penetrate. x-ray core bottom section was poor. <b>Another x-ray core was collected from this site on 16-5-2023 @ 3:15pm.</b> Site approx 15m from tidal channel. |

## Rereatukahia Estuary

| Core Site | Date    | Time (NZST) | NZTM-East | NZTM-North | Comments   |
|-----------|---------|-------------|-----------|------------|--|
| R1        | 16/5/23 | 0930        | 1858332   | 5836730    | <b>Vegetation cover dominated by Sea Rush (<i>J. kraussii</i>)</b> with some Oioi ( <i>A. similis</i> ). Difficulties collecting X-ray core. Thick root mass to penetrate. Used s/s device to slice through profile before inserting Perspex slide. Lost a little of sloppy surface sediment from slide on retrieval. GPS (Heather) 1858331, 5836730. Site approx. 140m from kiwifruit cropping on land.                             |
| R2        | 16/5/23 | 1120        | 1858268   | 5836728    | <b>Vegetation cover dominated by Sea Rush (<i>J. kraussii</i>)</b> with a little Oioi ( <i>A. similis</i> ). Difficulties collecting X-ray core. Thick root mass to penetrate. Lots of overlying water at site. Used stainless steel (s/s) insertion tool to penetrate the substrate before inserting Perspex slide. Lost some of sloppy surface sediment from slide on retrieval. Site approx. 80m from kiwifruit cropping on land. |
| R3        | 16/5/23 | 1300        | 1858204   | 5836721    | <b>Vegetation cover dominated by Sea Rush (<i>J. kraussii</i>)</b> with a little Oioi ( <i>A. similis</i> ). X-ray core was collected from this site using the s/s insertion tool to penetrate the substrate before inserting Perspex slide. Site approx. 20m from kiwifruit cropping on land.   |

## Oikimoke Estuary

| Core Site | Date    | Time (NZST) | NZTM-East | NZTM-North | Comments   |
|-----------|---------|-------------|-----------|------------|--|
| O1        | 17/5/23 | 1315        | 1872889   | 5826168    | <b>Vegetation cover dominated by Oioi</b> ( <i>A. similis</i> ) with some Sea Rush ( <i>J. kraussii</i> ). Thick root mass to penetrate. Used s/s device to slice through profile before inserting Perspex slide. X-ray slide bowed at the bottom. Obtained section 93-97cm from a second Blue Carbon core. Site approx. 15m from mangroves and drain on landward side.  |
| O2        | 17/5/23 | 1145        | 1872924   | 5826175    | <b>Vegetation cover dominated by Sea Rush</b> ( <i>J. kraussii</i> ) with a little Oioi ( <i>A. similis</i> ). Difficulties collecting X-ray core. Thick root mass to penetrate. Lots of overlying water at site. Used s/s insertion tool to penetrate the substrate and slice through profile before inserting Perspex slide. Lost a little of sloppy surface sediment from slide on retrieval. Site approx. 80m from kiwifruit cropping on land. |
| O3        | 17/5/23 | 1030        | 1872959   | 5826180    | <b>Vegetation cover dominated by Sea Rush</b> ( <i>J. kraussii</i> ) with a little Oioi ( <i>A. similis</i> ). X-ray core was collected from this site using the s/s insertion tool to penetrate the substrate and slice through profile before inserting Perspex slide. Site approx. 20m from kiwifruit cropping on land.   |

## Appendix B Sediment dating

### Radionuclides as geological clocks

Radionuclides are unstable atoms that release excess energy in the form of radiation (i.e., gamma rays, alpha particles) in the process of radioactive decay. The radioactive-decay rate can be considered fixed for each type of radionuclide, and it is this property that makes them very useful as geological clocks. The half-life ( $t_{1/2}$ ) of a radionuclide is one measure of the radioactive decay rate and is defined as the time period taken for the quantity of a substance to reduce by exactly half. Therefore, after two half-lives only 25% of the original quantity remains.

The  $t_{1/2}$  value of radionuclides also defines the timescale over which they are useful for dating. For example,  $^{210}\text{Pb}$  (naturally occurring radionuclide) has a half-life of 22 years and can be used to date sediments up to seven half-lives old or about 150 years. Dating by  $^{210}\text{Pb}$  is based on the rate of decrease in unsupported or excess  $^{210}\text{Pb}$  activity with depth in the sediment. Excess  $^{210}\text{Pb}$  is produced in the atmosphere and is deposited continuously on the earth's surface, where it falls directly into the sea or on land. Like other radionuclides,  $^{210}\text{Pb}$  is strongly attracted to fine sediment particles (e.g., clay and silt), which settle out of the water column and are deposited on the seabed.  $^{210}\text{Pb}$  also falls directly on land and is attached to soil particles. When soils are eroded, they may eventually be carried into estuaries and the sea and provide another source of excess  $^{210}\text{Pb}$ . As these fine sediments accumulate on the seabed and bury older sediments over time, the excess  $^{210}\text{Pb}$  decays at a constant rate (i.e., the half-life). The rate of decline in excess  $^{210}\text{Pb}$  activity with depth also depends on the local SAR. Slow declines in  $^{210}\text{Pb}$  activity with depth indicate rapid sedimentation whereas rapid declines indicate that sedimentation is occurring more slowly. More details of  $^{210}\text{Pb}$  dating are described below.

Although radionuclides can occur naturally, others are manufactured. Caesium-137 ( $t_{1/2} = 30$  yr) is an artificial radionuclide that is produced by the detonation of nuclear weapon or by nuclear reactors. In New Zealand, the fallout of caesium-137 associated with atmospheric nuclear weapons tests was first detected in 1953, with peak deposition occurring during the mid-1960s. Therefore, caesium-137 occurs in sediments deposited since the early 1950s. The feeding and burrowing activities of benthic animals (e.g., worms and shellfish) can complicate matters due to downward mixing of younger sediments into older sediments. Repeated reworking of seabed sediments by waves also mixes younger sediment down into older sediments. X-radiographs and short-lived radionuclides such as  $^7\text{Be}$  ( $t_{1/2} = 53$  days) can provide information on sediment mixing processes.

### $^{210}\text{Pb}$ profiling and dating

$^{210}\text{Pb}$  ( $t_{1/2} = 22.3$  yr) is a naturally occurring radionuclide that has been widely applied to dating recent sedimentation (last 150 years) in lakes, estuaries, and the sea (Figure H-1).  $^{210}\text{Pb}$  is an intermediate decay product in the uranium-238 ( $^{238}\text{U}$ ) decay series and has a radioactive decay constant ( $k$ ) of  $0.03114 \text{ yr}^{-1}$ . The intermediate parent radionuclide radium-226 ( $^{226}\text{Ra}$ , half-life 1622 years) yields the inert gas radon-222 ( $^{222}\text{Rn}$ , half-life 3.83 days), which decays through several short-lived radionuclides to produce  $^{210}\text{Pb}$ . A proportion of the  $^{222}\text{Rn}$  gas formed by  $^{226}\text{Ra}$  decay in catchment soils diffuses into the atmosphere where it decays to form  $^{210}\text{Pb}$ . This atmospheric  $^{210}\text{Pb}$  is deposited at the earth surface by dry deposition or rainfall. The  $^{210}\text{Pb}$  in estuarine sediments has two components: supported  $^{210}\text{Pb}$  derived from *in situ*  $^{222}\text{Rn}$  decay (i.e., within the sediment column) and an unsupported  $^{210}\text{Pb}$  component derived from atmospheric fallout.

This unsupported  $^{210}\text{Pb}$  component of the total  $^{210}\text{Pb}$  concentration in excess of the supported  $^{210}\text{Pb}$  value is estimated from the  $^{226}\text{Ra}$  assay (see below). Some of this atmospheric unsupported  $^{210}\text{Pb}$  component is also incorporated into catchment soils and is subsequently eroded and deposited in estuaries. Both the direct and indirect (i.e., soil inputs) atmospheric  $^{210}\text{Pb}$  input to receiving environments, such as estuaries, is termed the unsupported or excess  $^{210}\text{Pb}$ .

The activity profile of unsupported  $^{210}\text{Pb}$  in sediment is the basis for  $^{210}\text{Pb}$  dating. In the absence of atmospheric (unsupported)  $^{210}\text{Pb}$  fallout, the  $^{226}\text{Ra}$  and  $^{210}\text{Pb}$  in estuary sediment would be in radioactive equilibrium, which results from the substantially longer  $^{226}\text{Ra}$  half-life. Thus, the  $^{210}\text{Pb}$  activity profile would be uniform with depth. However, what is typically observed is a reduction in  $^{210}\text{Pb}$  activity with depth in the sediment column. This is due to the addition of unsupported  $^{210}\text{Pb}$  directly or indirectly from the atmosphere that is deposited with sediment particles on the bed. This unsupported  $^{210}\text{Pb}$  component decays with age ( $k = 0.03114 \text{ yr}^{-1}$ ) as it is buried through sedimentation. In the absence of sediment mixing, the unsupported  $^{210}\text{Pb}$  activity decays exponentially with depth and time in the sediment column. The validity of  $^{210}\text{Pb}$  dating rests on how accurately the  $^{210}\text{Pb}$  delivery processes to the estuary are modelled, and in particular the rates of  $^{210}\text{Pb}$  and sediment inputs (i.e., constant versus time variable).

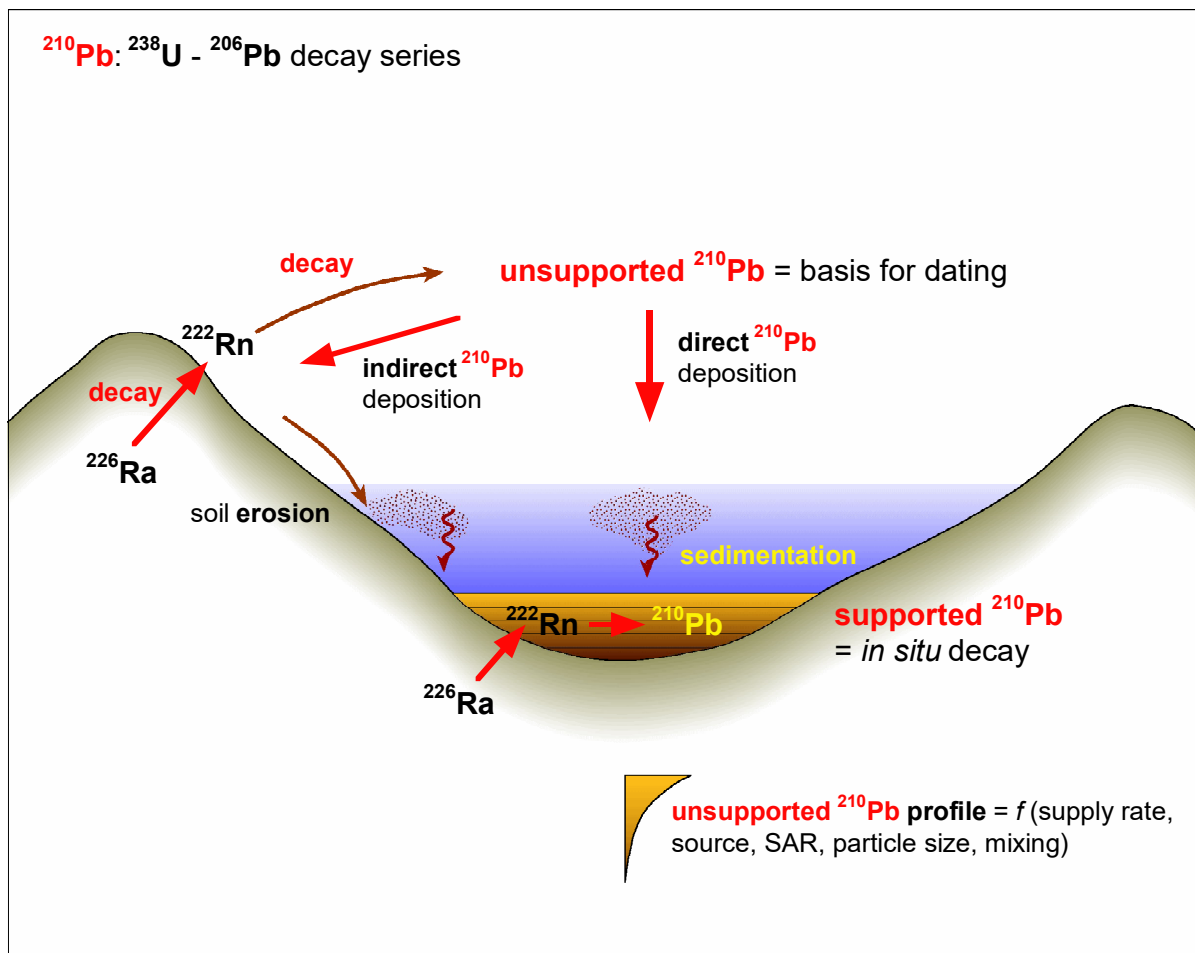


**Figure B-1:**  $^{210}\text{Pb}$  pathways to estuarine sediments.

## Sediment accumulation rates

Time-averaged SAR were calculated from the excess lead-210 ( $^{210}\text{Pb}_{\text{ex}}$ ) activity vertical profiles. This assumes that the  $^{210}\text{Pb}_{\text{ex}}$  profile is primarily a product of radioactive decay and sediment accumulation rate, rather than sediment mixing. The  $^{210}\text{Pb}_{\text{ex}}$  activity at time zero ( $A_0$ ,  $\text{Bq kg}^{-2}$ ), declines exponentially with age ( $t$ ):

$$A_t = A_0 e^{-kt} \quad (1)$$

Assuming that within a finite time period, sedimentation ( $S$ ) is constant then  $t = z/S$  can be substituted into Eq. 2 and by re-arrangement:

$$\frac{\ln\left[\frac{A}{A_0}\right]}{z} = -k/S \quad (2)$$

Because  $^{210}\text{Pb}_{\text{ex}}$  activity decays exponentially and assuming that sediment age increases with depth, a vertical profile of natural log( $A$ ) should yield a straight line of slope  $b = -k/S$ . Fitting a linear regression model to natural-log transformed  $^{210}\text{Pb}_{\text{ex}}$  activity profile to calculate  $b$ . The SAR over the depth of the fitted data is given by:

$$S = -(k)/b \quad (3)$$

An advantage of the  $^{210}\text{Pb}$ -dating method is that the SAR is based on the entire  $^{210}\text{Pb}_{\text{ex}}$  profile rather than a single layer, as is the case for  $^{137}\text{Cs}$  deposition peak or maximum penetration depth, or  $^{14}\text{C}$  dating of a shell layer.

The uncertainty ( $U_{2\sigma}$ ) of the  $^{210}\text{Pb}_{\text{ex}}$  activities was calculated as:

$$U_{2\sigma} = \sqrt{({}^{210}\text{Pb}_{2\sigma})^2 + ({}^{226}\text{Ra}_{2\sigma})^2} \quad (4)$$

where  ${}^{210}\text{Pb}_{2\sigma}$  and  ${}^{226}\text{Ra}_{2\sigma}$  are the two standard deviation uncertainties in the total  $^{210}\text{Pb}$  and  ${}^{226}\text{Ra}$  concentrations at the 95% confidence level. The main source of uncertainty in the measurement of radionuclide activities relates to the counting statistics (i.e., variability in the rate of radioactive decay). This source of uncertainty is reduced by increasing the sample size and the counting time.

Pre 20<sup>th</sup> century time-average SAR, over time scales of several hundred years, were estimated from the radiocarbon dates ( $^{14}\text{C}$ ) obtained from pairs of shell samples collected below the maximum depth of excess  $^{210}\text{Pb}$  in each core. The time averaged  $^{14}\text{C}$  SAR ( $\text{mm yr}^{-1}$ ) was calculated as:

$$S_B = (D_{\text{Pb}} - D_{\text{C}}) / (T_{\text{Pb}210} - T_{\text{C}14}) \quad (5)$$

Where  $D_{\text{Pb}}$  and  $D_{\text{C}}$  are respectively the depths (mm) below the top of each core of the maximum penetration of the  $^{210}\text{Pb}_{\text{ex}}$  profile and mean AMS  $^{14}\text{C}$  age of the dated shell samples. The matching ages of these layers ( $T_{\text{Pb}210}$ ,  $T_{\text{C}14}$ ) are estimates as years A.D., with the AMS  $^{14}\text{C}$  age (before present [BP = 1950]), adjusted to the year of core collection (2015). The  $S_B$  estimate integrate the effects of land disturbance and soil erosion by Māori and early Europeans over several hundred years as well as background SAR prior to human arrival.

## Radiocarbon dating – sample details and results

**Table B-1: Summary of cockle shell samples submitted for AMS radiocarbon dating.** The Wk number is the sample identification for the University of Waikato Radiocarbon Dating Laboratory. Whether or not the cockle was preserved in an articulated state is indicated, however, only a single valve was prepared and submitted for analysis.

| Core/shell | Depth increment (cm) | Sample type  | Articulated | Wk number |
|------------|----------------------|--|-------------|-----------|
| O-1/A      | 65–66 (Sample A)     | Cockle shell valve ( <i>Austrovenus stutchburyi</i> )            | Yes         | Wk-57779  |
| O-1/B      | 64–65 cm (Sample B)  | Cockle shell valve ( <i>Austrovenus stutchburyi</i> )            | Yes         | Wk-57780  |
| O-1/D      | 65–66 (Sample D)     | Cockle shell valve ( <i>Austrovenus stutchburyi</i> )            | No          | Wk-57781  |
| O-3/B      | 64–65 cm (Sample B)  | Cockle shell valve ( <i>Austrovenus stutchburyi</i> )            | No          | Wk- 57782 |
| O-3/D      | 67–68 (Sample D)     | Cockle shell valve ( <i>Austrovenus stutchburyi</i> )            | Yes         | Wk- 57783 |
| O-3/E      | 60–61 (Sample E)     | Cockle shell valve (juvenile) ( <i>Austrovenus stutchburyi</i> ) | Yes         | Wk-57784  |

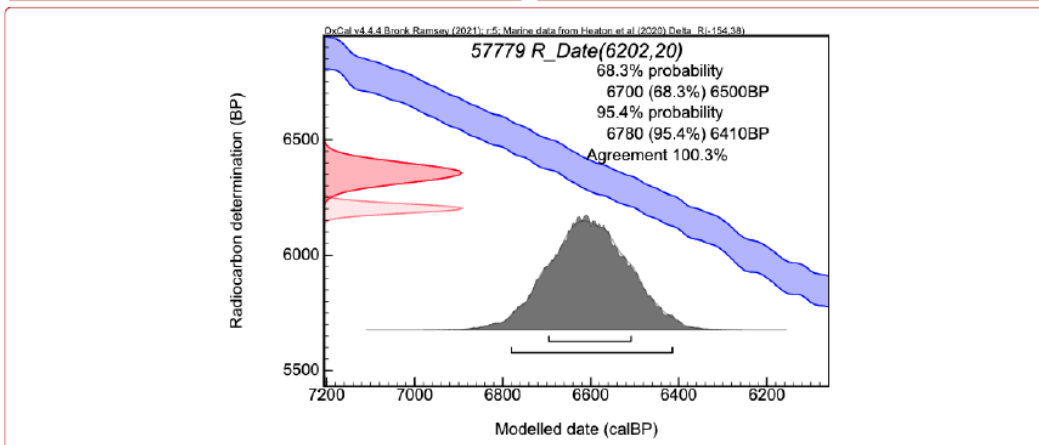
Shell samples were acid-washed in 0.1 N hydrochloric acid, rinsed and dried prior to AMS analysis. The AMS dating results are expressed as calibrated radiocarbon ages in years before present (B.P., 1950 AD, Stuiver and Polach, 1977). Duplicate samples were analysed from the same depth interval in several cores to evaluate the likelihood of shell material being reworked from its original stratigraphic position. The UoW Radiocarbon Dating reports for the cockle shell samples are appended below.

Report on Radiocarbon Age Determination for 57779

Tuesday, 23 April 2024

|                       |  |
|-----------------------|--|
| Submitter             | Andrew Swales  |
| Submitter's Code      | BOP23203_Saltmarsh_Oikimoke_O1-A   |
| Site & Location       | O1 Oikimoke, Tauranga  |
| Sample Material       | Estuarine Shell Cockle   |
| Physical Pretreatment | Surfaces cleaned. Washed in an ultrasonic bath. Tested for recrystallization: aragonite. |
| Chemical Pretreatment | Sample acid washed using 0.1N HCl, rinsed and dried.                                     |

|                     |                     |  |
|---------------------|---------------------|--|
| D <sup>14</sup> C   | -537.96 ± 1.05 ‰    | Comments<br>NZ DeltaR values: Petchey, F., & Schmid, M. 2020.<br>Nature – Scientific Reports. Available:<br>www.nature.com/articles/s41598-020-70227-3 |
| F <sup>14</sup> C ‰ | 46.2 ± 0.1 ‰        |  |
| Result              | <b>6202 ± 20 BP</b> |  |



- Explanation of the calibrated OxCal plots is now found at URL <https://c14.arch.ox.ac.uk/explanation.php>
- Conventional Age or F<sup>14</sup>C ‰ (also known as Percent Modern Carbon [pMC]) is following Stuiver and Polach, 1977, Radiocarbon, 19:355-363. This is based on the Libby half-life of 5568 yr with correction for isotopic fractionation applied. This age is normally quoted in publications and must include the appropriate error term and WkA number.
- Quoted errors are 1 standard deviation due to counting statistics with additional uncertainty added in quadrature to account for sample-to-sample variability.

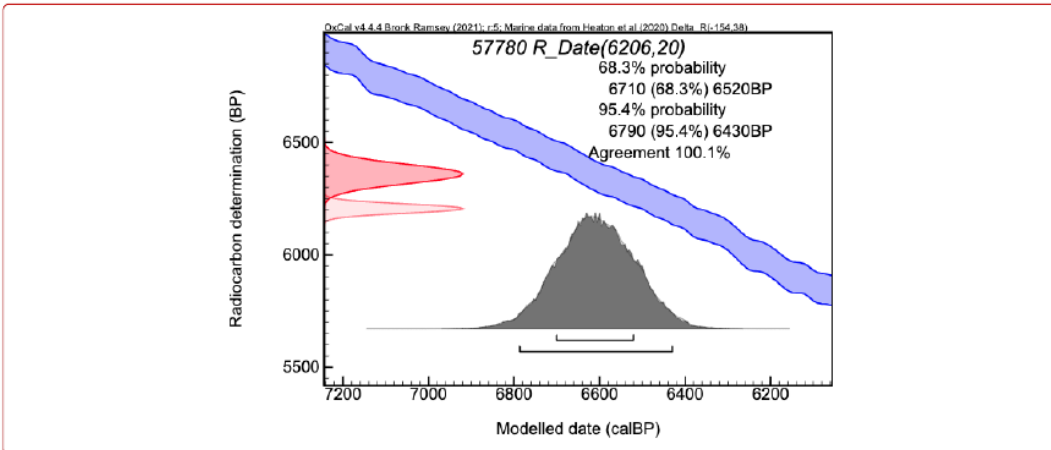


Report on Radiocarbon Age Determination for 57780

Tuesday, 23 April 2024

|                       |  |
|-----------------------|--|
| Submitter             | Andrew Swales  |
| Submitter's Code      | BOP23203_Saltmarsh_Oikimoke_O1-B   |
| Site & Location       | O1 Oikimoke, Tauranga  |
| Sample Material       | Estuarine Shell Cockle   |
| Physical Pretreatment | Surfaces cleaned. Washed in an ultrasonic bath. Tested for recrystallization: aragonite. |
| Chemical Pretreatment | Sample acid washed using 0.1N HCl, rinsed and dried.                                     |

|                     |                     |  |
|---------------------|---------------------|--|
| D <sup>14</sup> C   | -538.17 ± 1.08 ‰    | Comments<br>NZ DeltaR values: Petchey, F., & Schmid, M. 2020.<br>Nature – Scientific Reports. Available:<br><a href="http://www.nature.com/articles/s41598-020-70227-3">www.nature.com/articles/s41598-020-70227-3</a> |
| F <sup>14</sup> C ‰ | 46.18 ± 0.11 ‰      |  |
| Result              | <b>6206 ± 20 BP</b> |  |



- Explanation of the calibrated OxCal plots is now found at URL <https://c14.arch.ox.ac.uk/explanation.php>
- Conventional Age or F<sup>14</sup>C ‰ (also known as Percent Modern Carbon [pMC]) is following Stuiver and Polach, 1977, Radiocarbon, 19:355-363. This is based on the Libby half-life of 5568 yr with correction for isotopic fractionation applied. This age is normally quoted in publications and must include the appropriate error term and WkA number.
- Quoted errors are 1 standard deviation due to counting statistics with additional uncertainty added in quadrature to account for sample-to-sample variability.

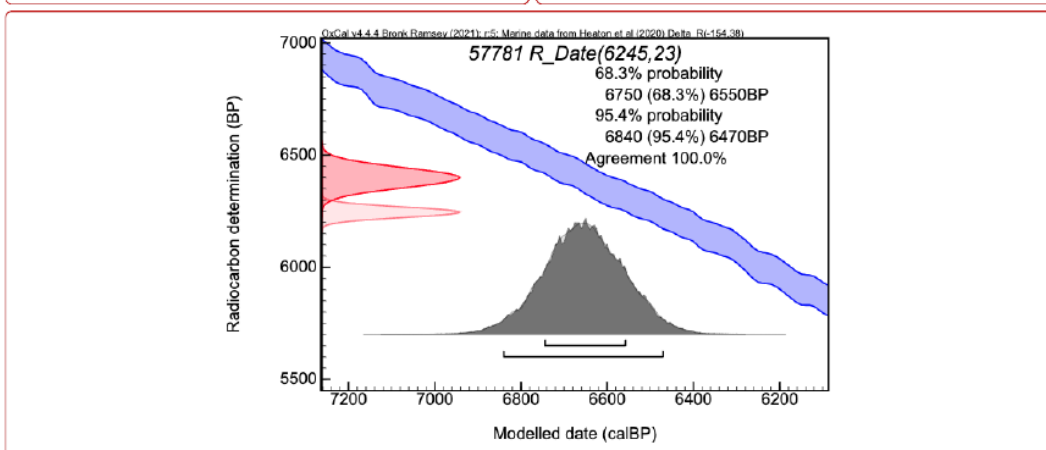
*M. Atkinson*

Report on Radiocarbon Age Determination for 57781

Tuesday, 23 April 2024

|                       |  |
|-----------------------|--|
| Submitter             | Andrew Swales  |
| Submitter's Code      | BOP23203_Saltmarsh_Oikimoke_O1-D   |
| Site & Location       | O1 Oikimoke, Tauranga  |
| Sample Material       | Estuarine Shell Cockle   |
| Physical Pretreatment | Surfaces cleaned. Washed in an ultrasonic bath. Tested for recrystallization: aragonite. |
| Chemical Pretreatment | Sample acid washed using 0.1N HCl, rinsed and dried.                                     |

|                     |                     |  |
|---------------------|---------------------|--|
| D <sup>14</sup> C   | -540.4 ± 1.24 ‰     | Comments<br>NZ DeltaR values: Petchey, F., & Schmid, M. 2020.<br>Nature – Scientific Reports. Available:<br><a href="http://www.nature.com/articles/s41598-020-70227-3">www.nature.com/articles/s41598-020-70227-3</a> |
| F <sup>14</sup> C ‰ | 45.96 ± 0.12 ‰      |  |
| Result              | <b>6245 ± 23 BP</b> |  |



- Explanation of the calibrated OxCal plots is now found at URL <https://c14.arch.ox.ac.uk/explanation.php>
- Conventional Age or F<sup>14</sup>C ‰ (also known as Percent Modern Carbon [pMC]) is following Stuiver and Polach, 1977, Radiocarbon, 19:355-363. This is based on the Libby half-life of 5568 yr with correction for isotopic fractionation applied. This age is normally quoted in publications and must include the appropriate error term and WkA number.
- Quoted errors are 1 standard deviation due to counting statistics with additional uncertainty added in quadrature to account for sample-to-sample variability.

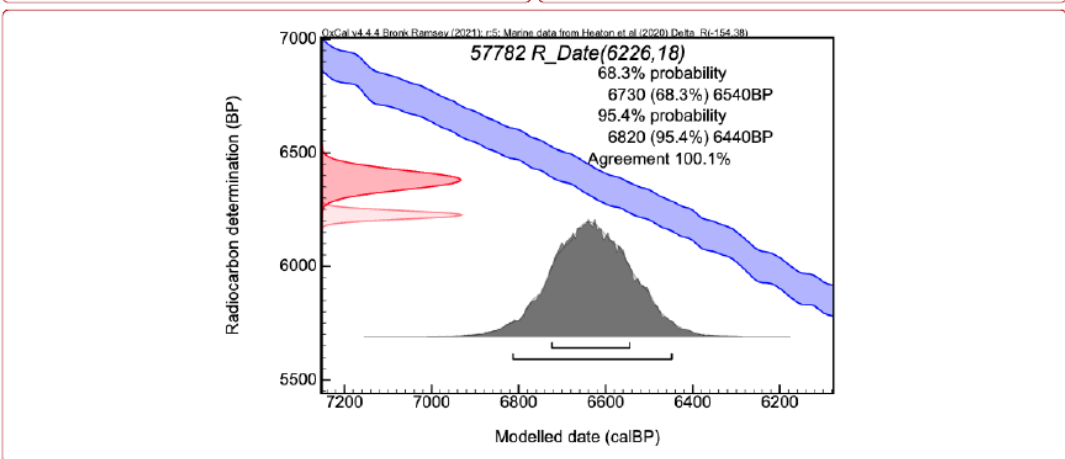
*M. H. L.*

Report on Radiocarbon Age Determination for 57782

Tuesday, 23 April 2024

|                       |  |
|-----------------------|--|
| Submitter             | Andrew Swales  |
| Submitter's Code      | BOP23203_Saltmarsh_Oikimoke_O3-B   |
| Site & Location       | O3 Oikimoke, Tauranga  |
| Sample Material       | Estuarine Shell Cockle   |
| Physical Pretreatment | Surfaces cleaned. Washed in an ultrasonic bath. Tested for recrystallization: aragonite. |
| Chemical Pretreatment | Sample acid washed using 0.1N HCl, rinsed and dried.                                     |

|                     |                     |  |
|---------------------|---------------------|--|
| D <sup>14</sup> C   | -539.31 ± 0.94 ‰    | Comments<br>NZ DeltaR values: Petchey, F., & Schmid, M. 2020.<br>Nature – Scientific Reports. Available:<br><a href="http://www.nature.com/articles/s41598-020-70227-3">www.nature.com/articles/s41598-020-70227-3</a> |
| F <sup>14</sup> C % | 46.07 ± 0.09 %      |  |
| Result              | <b>6226 ± 18 BP</b> |  |



- Explanation of the calibrated OxCal plots is now found at URL <https://c14.arch.ox.ac.uk/explanation.php>
- Conventional Age or F<sup>14</sup>C% (also known as Percent Modern Carbon [pMC]) is following Stuiver and Polach, 1977, Radiocarbon, 19:355-363. This is based on the Libby half-life of 5568 yr with correction for isotopic fractionation applied. This age is normally quoted in publications and must include the appropriate error term and WkA number.
- Quoted errors are 1 standard deviation due to counting statistics with additional uncertainty added in quadrature to account for sample-to-sample variability.

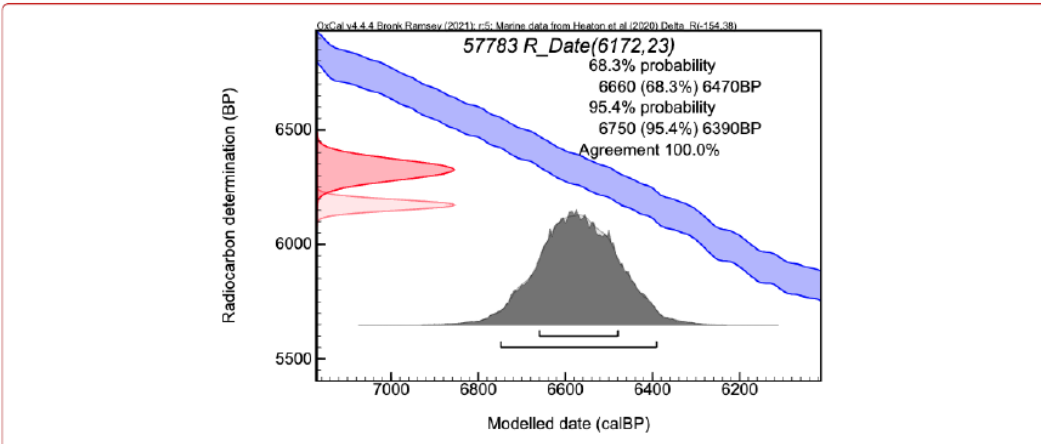


Report on Radiocarbon Age Determination for 57783

Tuesday, 23 April 2024

|                       |  |
|-----------------------|--|
| Submitter             | Andrew Swales  |
| Submitter's Code      | BOP23203_Saltmarsh_Oikimoke_O3-D   |
| Site & Location       | O3 Oikimoke, Tauranga  |
| Sample Material       | Estuarine Shell Cockle   |
| Physical Pretreatment | Surfaces cleaned. Washed in an ultrasonic bath. Tested for recrystallization: aragonite. |
| Chemical Pretreatment | Sample acid washed using 0.1N HCl, rinsed and dried.                                     |

|                     |                     |  |
|---------------------|---------------------|--|
| D <sup>14</sup> C   | -536.2 ± 1.27 ‰     | Comments<br>NZ DeltaR values: Petchey, F., & Schmid, M. 2020.<br>Nature – Scientific Reports. Available:<br><a href="http://www.nature.com/articles/s41598-020-70227-3">www.nature.com/articles/s41598-020-70227-3</a> |
| F <sup>14</sup> C % | 46.38 ± 0.13 %      |  |
| Result              | <b>6172 ± 23 BP</b> |  |



- Explanation of the calibrated OxCal plots is now found at URL <https://c14.arch.ox.ac.uk/explanation.php>
- Conventional Age or F<sup>14</sup>C% (also known as Percent Modern Carbon [pMC] is following Stuiver and Polach, 1977, Radiocarbon, 19:355-363. This is based on the Libby half-life of 5568 yr with correction for isotopic fractionation applied. This age is normally quoted in publications and must include the appropriate error term and WkA number.
- Quoted errors are 1 standard deviation due to counting statistics with additional uncertainty added in quadrature to account for sample-to-sample variability.



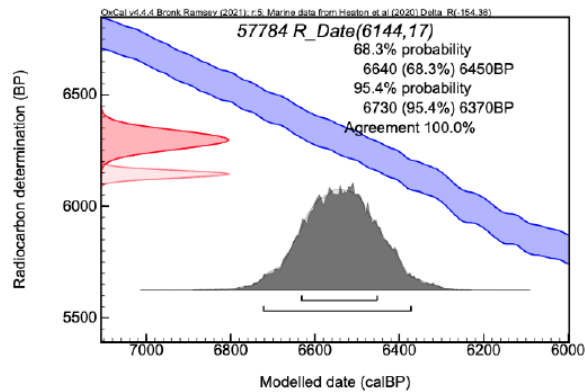
Report on Radiocarbon Age Determination for 57784

Tuesday, 23 April 2024

|                       |  |
|-----------------------|--|
| Submitter             | Andrew Swales  |
| Submitter's Code      | BOP23203_Saltmarsh_Oikimoke_O3-E   |
| Site & Location       | O3 Oikimoke, Tauranga  |
| Sample Material       | Estuarine Shell Cockle   |
| Physical Pretreatment | Surfaces cleaned. Washed in an ultrasonic bath. Tested for recrystallization: aragonite. |
| Chemical Pretreatment | Sample acid washed using 0.1N HCl, rinsed and dried.                                     |

|                     |                     |
|---------------------|---------------------|
| D <sup>14</sup> C   | -534.57 ± 0.87 ‰    |
| F <sup>14</sup> C ‰ | 46.54 ± 0.09 ‰      |
| Result              | <b>6144 ± 17 BP</b> |

Comments  
NZ DeltaR values: Petchey, F., & Schmid, M. 2020.  
Nature – Scientific Reports. Available:  
[www.nature.com/articles/s41598-020-70227-3](http://www.nature.com/articles/s41598-020-70227-3)



- Explanation of the calibrated OxCal plots is now found at URL <https://c14.arch.ox.ac.uk/explanation.php>
- Conventional Age or F<sup>14</sup>C ‰ (also known as Percent Modern Carbon [pMC]) is following Stuiver and Polach, 1977, Radiocarbon, 19:355-363. This is based on the Libby half-life of 5568 yr with correction for isotopic fractionation applied. This age is normally quoted in publications and must include the appropriate error term and WkA number.
- Quoted errors are 1 standard deviation due to counting statistics with additional uncertainty added in quadrature to account for sample-to-sample variability.

